

2012

# Regulation of Tuberin in Cell Fate Acquisition within Developing Neural Tissues

Gordon Omar Davis  
*University of Windsor*

Follow this and additional works at: <https://scholar.uwindsor.ca/etd>

---

## Recommended Citation

Davis, Gordon Omar, "Regulation of Tuberin in Cell Fate Acquisition within Developing Neural Tissues" (2012). *Electronic Theses and Dissertations*. 5424.  
<https://scholar.uwindsor.ca/etd/5424>

This online database contains the full-text of PhD dissertations and Masters' theses of University of Windsor students from 1954 forward. These documents are made available for personal study and research purposes only, in accordance with the Canadian Copyright Act and the Creative Commons license—CC BY-NC-ND (Attribution, Non-Commercial, No Derivative Works). Under this license, works must always be attributed to the copyright holder (original author), cannot be used for any commercial purposes, and may not be altered. Any other use would require the permission of the copyright holder. Students may inquire about withdrawing their dissertation and/or thesis from this database. For additional inquiries, please contact the repository administrator via email ([scholarship@uwindsor.ca](mailto:scholarship@uwindsor.ca)) or by telephone at 519-253-3000ext. 3208.

Regulation of Tuberin in Cell Fate Acquisition within Developing Neural Tissues

By

Gordon Omar Davis

A Thesis

Submitted to the Faculty of Graduate Studies  
through the Department of Biological Sciences  
In Partial Fulfilment of the Requirements for  
the Degree of Master of Science at the  
University of Windsor

Windsor, Ontario, Canada

2011

© 2011 Gordon Davis

Regulation of Tuberin in Cell Fate Acquisition within Developing Neural Tissues

by

Gordon Omar Davis

APPROVED BY:

---

Dr. Panayiotis O. Vacratsis  
Biochemistry

---

Dr. Andrew Swan  
Biological Sciences

---

Dr. Lisa A. Porter, Advisor  
Biological Sciences

---

Dr. Elizabeth Fidalgo da Silva, Advisor  
Biological Sciences

---

Dr. Oliver Love, Chair of Defense  
Biological Sciences

October 19, 2011

**Author's Declaration of Originality**

I hereby certify that I am the sole author of this thesis and that no part of this thesis has been published or submitted for publication.

I certify that, to the best of my knowledge, my thesis does not infringe upon anyone's copyright nor violate any proprietary rights and that any ideas, techniques, quotations, or any other material from the work of other people included in my thesis, published or otherwise, are fully acknowledged in accordance with the standard referencing practices. Furthermore, to the extent that I have included copyrighted material that surpasses the bounds of fair dealing within the meaning of the Canada Copyright Act, I certify that I have obtained a written permission from the copyright owner(s) to include such material(s) in my thesis and have included copies of such copyright clearances to my appendix.

I declare that this is a true copy of my thesis, including any final revisions, as approved by my thesis committee and the Graduate Studies office, and that this thesis has not been submitted for a higher degree to any other University or Institution.

## **Abstract**

Inhibition or misregulation of the tumour suppressor protein Tuberin is known to cause the benign tumour disorder Tuberous Sclerosis, involving developmental defects in many organ systems including the central nervous system. Data supports that appropriate control of Tuberin levels may play an essential role in the regulation of neural fate decisions. Hence, this work investigates the regulation of Tuberin through neural development both *in vitro*, using SH-SY5Y and RN33B neuronal precursor cells, and *in vivo* using murine neural tissues. We demonstrate that Tuberin expression and activity are significantly down-regulated during neuronal differentiation *in vitro*, and during aging *in vivo*, in a cell and tissue specific manner. We have developed tools needed to address the essentiality of Tuberin in neural differentiation *in vitro* and to begin to dissect the molecular pathways affected. Understanding how Tuberin is regulated through neural development is necessary in understanding the developmental defects and pathologies associated with Tuberous Sclerosis.

**Dedication**

To Those who stood in my corner and Those who will follow when I am gone,

*Always Remember:*

*The Cake is a Lie and there is No Spoon*

## Acknowledgements

Before anyone else, I must first thank God, the source of my blessings and strength.

Next, I want to thank everyone who helped me make it this far in life. My most sincere thanks go to my mother Joan, father Eustace, sister Jasmine and aunt Martha, for guiding me through life and giving me all the support and encouragement I needed to complete this achievement. My deepest thanks and love go to Ayda, for being my heart, my support and my shelter through the long years of this journey. Also, many thanks go to Amir, Tina, Ava, Arman, Heather, Zeba, Jeff and Ahmed for keeping me alive, fed and in good spirits, in both the high and low times. I owe all of you above more than you'll know and more than I can ever repay.

Finally, I want to thank the people who helped me earn this degree and taught me so much in the process. First of all, thank you to Lisa, for sharing your knowledge and patience, in addition to your time, resources, and beer, as I went my 12 rounds with Tuberin. I am truly grateful to have been given this opportunity. Thank you Elizabeth, for giving me the benefit of your skills and always providing a clear and level perspective when mine was clouded. Thank you both for always challenging me and pushing me to do and learn more. Thank you Agnes. You know exactly why. Thank you Dorota (Dorito) and Espanta for being two of the smartest ladies and best teachers I could have ever hoped to meet. I owe you both so much and I promise I won't ask either of you any more questions. Thank you Jiamila, for giving me plenty of opportunities to practice my "man's touch" and for being awesome. Thanks "Big" Mo and Martin for the shawarma lunches and for generating some much needed testosterone in the lab. Thanks to "Little" Mo, Breanne, Rosa, Janice, David, Miranda, Nick, Rebecca, Dorothy and Jenna, for the good times. It was great working with you. Special thanks go to: Mallika, for all of the editing and preparation help; Dr. Weiss, for all your help with the statistics; Drs. Swan and Vaccratsis, for being a great committee; and Dr. Fackrell, for the good advice. AS SUCH, I wish, for you all, every success in the years to come.

## **Table of Contents**

Author's Declaration of Originality	iii
Abstract	iv
Dedication	v
Acknowledgments	vi
List of Tables	x
List of Figures	xi
List of Abbreviations	xiii
<b><u>Chapter</u></b>	
<b><u>1: Introduction</u></b>	<b><u>1</u></b>
1.1: Tuberous Sclerosis (TS): Pathology & Diagnosis	1
1.2: Neurological Phenotype of TS	3
1.3: The TS Gene Family: History & Genetics	6
1.4: The TSC Gene Products: Hamartin & Tuberin	9
1.5: TSC Signalling: mTOR Regulation	17
1.6: TSC Signaling: Cell Cycle Regulation, Differentiation & Fate	25
1.7: TSC1 & TSC2 Gene Mutations: Consequences for TSC Function	27
1.8: Neurogenesis and the Regulation of Neural Cell Fate	28
1.9: Misregulation of TSC Gene Function: Effects on Cell Differentiation, Development and Fate	32
1.10: Hypothesis and Objectives	35
<b><u>2: Design and Methodology</u></b>	<b><u>36</u></b>
2.1: Cell Culture and Neuronal Lineage Differentiation	36
2.2: Whole Cell and Cellular Fraction Protein Extraction	38
2.3: Immunoblotting	40



2.4: Antibodies	41
2.5: Neurosphere Formation Assay	41
2.6: Quantitative Real-Time Polymerase Chain Reaction (qRT-PCR) mRNA Analysis	42
2.7: BALB/c Neural Tissue Extraction	43
2.8: Cloning of Plasmid DNA Constructs	44
2.9: Testing and Expression of shRNA Vectors	47
2.10: Analytical Methods	51
3: <u>Results and Analysis</u>	<u>53</u>
3.1: Tuberin expression levels are regulated during neuronal cell differentiation	53
3.2: Tuberin levels do not change significantly based on cellular localization during neuronal cell differentiation	59
3.3: Regulation of TSC2 mRNA levels during neuronal differentiation	64
3.4: TSC2 mRNA levels show a slight variation between partially committed and stem-like neuronal cell populations	69
3.5: Tuberin expression and activity levels remain relatively consistent during late embryonic and post-natal development	75
3.6: Design and construction of shRNA plasmid vectors for in vitro knockdown of TSC2	86
3.7: Testing of constructed TSC2 shRNA plasmid vectors	96
4: <u>Discussion</u>	<u>100</u>
4.1: Regulation of Tuberin Occurs Through the Course of Neuronal Cell Differentiation in vitro, but Does Not Appear to Directly Result in Significant Modulation of p70S6K phosphorylation	101
4.2: Cellular Localization of Tuberin May be Implicated in Cell-Specific Downregulation During Differentiation.	105
4.3: Tuberin Protein Levels Do Not Appear to be Transcriptionally Regulated During the Course of Neuronal Differentiation	106
4.4: Tuberin Levels and p70S6K Phosphorylation Are Regulated within Sub-sets of Neural Tissues During Late Embryonic and Postnatal Development	109

4.5: Conclusions and Future Directions -----111

References -----114

Vita Auctoris -----130

## **List of Tables**

1) Table 1: Diagnostic Criteria for Tuberous Sclerosis	3
2) Table 2: Oligonucleotide Primers for Use in qRT-PCR	43
3) Table 3: pLKO.1 Vectors: TSC2 shRNA Oligonucleotide Sequences	46
4) Table 4: pLB Vector: TSC2 shRNA Oligonucleotide Sequences	47
5) Table 5: Plasmid Vectors Used in Transfection/Infection Trials	49

## List of Figures

1) <b>Figure 1:</b> TSC1 & TSC2 Gene Mutations	10
2) <b>Figure 2:</b> Schematic Diagrams: Tuberin and Hamartin	13
3) <b>Figure 3:</b> The TSC integrates intracellular signaling cues, such as growth and energy signals, to influence numerous cellular processes within the CNS	18
4) <b>Figure 4:</b> Endogenous levels of Tuberin demonstrate steady down-regulation during induced in vitro neuronal differentiation in human SH-SY5Y cells, but not in rat RN33B cells.	55
5) <b>Figure 5:</b> Regulation of Tuberin activity levels occurs during the first 24 hours of induced in vitro neuronal differentiation in human SH-SY5Y cells.	57
6) <b>Figure 6:</b> Reduced levels of Tuberin protein occur in the nuclear compartment of SH-SY5Y cells.	60
7) <b>Figure 7:</b> Tuberin protein levels are ubiquitous in cellular fractions of RN33B cells during neuronal differentiation.	62
8) <b>Figure 8:</b> TSC2 mRNA levels are not regulated across full neuronal differentiation in SH-SY5Y cells	65
9) <b>Figure 9:</b> TSC2 mRNA levels do not undergo regulation during neuronal differentiation in RN33B cells	67
10) <b>Figure 10:</b> TSC2 mRNA levels follow those of Oct4 in neurosphere-cultured SH-SY5Y cells	71
11) <b>Figure 11:</b> TSC2 mRNA levels follow those of Nestin in neurosphere-cultured RN33B cells	73
12) <b>Figure 12:</b> Tuberin levels and activity are reduced during post-natal development in the hippocampus	78

13) <b>Figure 13:</b> Tuberin levels and activity are constant within the olfactory bulb during late embryonic and postnatal development	80
14) <b>Figure 14:</b> Tuberin levels and activity are ubiquitous within the cerebral cortex during late embryonic and postnatal development	82
15) <b>Figure 15:</b> Tuberin levels and activity are reduced during post-natal development in the cerebellum	84
16) <b>Figure 16:</b> Design and cloning of shRNA vectors for knockdown of rat TSC2 in vitro	88
17) <b>Figure 17:</b> Design and cloning of shRNA vectors for in vitro knockdown of human TSC2	93
18) <b>Figure 18:</b> Testing and troubleshooting of pLB and PLKO.1 TSC2 shRNA plasmid vectors	98

## **List of Abbreviations**

TS – Tuberos Sclerosis

TSC – Tuberos Sclerosis Complex

TSC1 – Tuberos Sclerosis 1 (Gene)

TSC2 – Tuberos Sclerosis 2 (Gene)

mTOR – Mammalian Target of Rapamycin

mTORC1 – Mammalian Target of Rapamycin Complex 1

mTORC2 – Mammalian Target of Rapamycin Complex 2

mRNA – Messenger RNA

cDNA – Complementary DNA

SDS-PAGE – Sodium Dodecyl Sulphate Polyacrylamide Gel Electrophoresis

PCR – Polymerase Chain Reaction

shRNA – Short Hairpin RNA

TBS – Tris-buffered Saline

TBST – Tris-buffered Saline + Tween-20

MAP2 – Microtubule-associated Protein 2

Oct-4 – Octamer-binding Transcription Factor 4

PBS – Phosphate Buffered Saline

TU – Transfection Units

## **CHAPTER 1**

### **1. Introduction**

#### **1.1: Tuberous Sclerosis (TS): Pathology & Diagnosis**

Tuberous sclerosis (TS) was first fully documented, in 1880, by the French neurologist and paediatrician Désiré-Magloire Bourneville, who described the condition as a disorder of distinctive cerebral pathology which was closely linked to incidence of seizures, mental deficiency and CNS abnormalities (Bourneville 1880; Curatolo & Bombardieri 2003). Following these initial observations, Tuberous Sclerosis (TS) was later characterized, by van der Hoeve in 1933, as a multisystem phakomatosis, identifiable by the widespread and unpredictable development of benign, tumour-like lesions, which would later be known as hamartomas (van der Hoeve 1933; Grajkowska et al. 2010). Today, among the worldwide population, TS affects nearly 1 in 6000 live births (Nellist et al. 1993).

Pathologically, TS is a disorder of cell migration, proliferation and differentiation (Crino & Henske 1999). Hamartomas, which are broadly non-metastatic and non-malignant focal malformations, bear strong resemblance to neoplasms and have, in certain manifestations, been indicated to possess the potential for metastasis (Henske 2003, Barnes et al. 2010). Known to localize to numerous sites throughout the body, TS hamartomas are commonly observed to develop within the brain, heart, skin, liver and kidneys. Development of TS lesions has been observed, through immunohistochemical and radiological study, to occur as early as 19 weeks of gestation, indicating formation of TS-related abnormalities begins during embryonic development (Wei et al. 2002, Park et al. 1997). Due to the range of organ systems affected, TS presents with a diverse phenotypic spectrum. Although most organs are susceptible, dermatological, renal, pulmonary and neurological manifestations are most prevalent among TS patients (Curatolo et al. 2008). Dermatological presentations are commonly quite evident within

the paediatric population and can include hypomelanotic macules, found in over 90% of TS patients, and facial angiofibromas, seen in 75% of patients. Other dermatological abnormalities can include fibrous forehead plaques, periungual fibromas and shagreen patches. Renal lesions, including angiomyolipomas, renal cysts, renal cell carcinomas and oncocytomas, can occur in 50-80% of TS patients. In fact, despite being most commonly seen in adult TS patients, multiple bilateral angiomyolipomas represent a leading cause of mortality within the TS patient population, across all age categories, secondary only to spontaneous haemorrhage (Shepherd et al. 1991). Furthermore, renal angiomyolipomas have also been implicated in the metastatic model of TS, as cells originating from these lesions are believed in some cases to spur the development of pulmonary lymphangiomyomatosis, a form of TS known to develop exclusively in females (Astrinidis and Henske 2005). The most common manifestation of pulmonary TS lesion, lymphangiomyomatosis lesions have been observed to demonstrate the capacity for migration, invasion and metastasis, despite being found to be histologically benign (Henske 2003). Other frequently observed clinical manifestations of TS include: cardiac rhabdomyomas, commonly seen to affect 50-70% of infant patients, and retinal astrocytic hamartomas, which are believed to arise from glial precursors during retinal embryogenesis (Mennel et al. 2007).

Diagnosis of TS remains centred around clinical assessment, primarily through histopathological observation. Recently revised diagnostic criteria for this disorder now classify TS manifestations into one of two categories: major features and minor features (Table 1, Curatolo et al., 2002). Major features are indicated by their high degree of specificity for TS, occurring quite frequently within the TS patient population, while minor features show a less specific association with TS. Furthermore, by comparison to major features, minor features occur with a much lower frequency, but can affect as broad a range of tissues as major features.



Definitive diagnosis of TS is typically predicated on the presentation of two or more major features or one major feature and two minor features. Additionally, recent advances have led to an increasing popularity of neurogenetic testing to support clinical diagnoses. However, clinical observation remains the diagnostic standard (Orlova & Crino 2010).

**Table 1: Diagnostic Criteria for Tuberous Sclerosis**

<b>Major Features</b>	
1. Facial angiofibromas or forehead plaques	6. Cortical Tubers
2. Non-traumatic ungula or periungual fibromas	7. Subependymal nodules
3. Hypomelanotic macules (3 or more)	8. Subependymal giant cell astrocytomas
4. Shagreen patches (connective tissue naevus)	9. Cardiac rhabdomyomas (single or multiple)
5. Multiple retinal nodular hamartomas	10. Lymphangiomyomatosis and/or renal angiomyolipoma
<b>Minor Features</b>	
1. Multiple, randomly distributed pits in dental enamel	6. Non-renal hamartomas
2. Hamartomatous rectal polyps	7. Retinal achromic patches
3. Bone cysts	8. 'Confetti' skin lesions
4. Cerebral white matter radial migration lines	9. Multiple renal cysts
5. Gingival fibromas	

### 1.2: Neurological Phenotype of TS

Presenting with the highest morbidity, second highest mortality, behind renal manifestations, and a collective occurrence of over 80% in TS all patients, the neurological abnormalities associated with TS have been called some of the most devastating and therapeutically challenging manifestations of the disorder (Marcotte & Crino 2006). Present evidence suggests TS-associated lesions, which appear in the central nervous system, arise due to developmental aberrations during neurogenesis and neuronal migration. It has been observed, in TS patients, that two populations of neuroepithelial cells are typically generated by the germinal matrix during neurogenesis. The first is a population of neuroblasts that produce normal neurons and astroglia which ultimately give rise to histologically normal cerebral cortex.

The second is an abnormal cell population which produces cells that demonstrate a defect in cellular differentiation, failing to clearly exhibit the characteristics of either neuronal or glial differentiation. Commonly referred to as “neuroastrocytes”, these cells remain in the germinal matrix zone and give rise to subependymal nodules (SENs), and subependymal giant cell astrocytomas (SEGAs). Some of these neuroastrocytes demonstrate partial migration, forming heterotopias in the subcortical white matter. Frequently, some of the less primitive neuroastrocytes migrate to the cortical plate where they form the aggregates of dysplastic cortex commonly known as cortical and subcortical tubers (Crino & Henske 1999; Curatolo et al. 2002).

Found within the cerebral and cerebellar cortex, in addition to the subcortical white matter, cortical/subcortical tubers are focal abnormalities of cortical architecture found within more than 80% of TS patients. These lesions represent the hallmark of the disease and are strongly indicative of cerebral TS (Curatolo et al. 2002). Macroscopically, tubers are circumscribed, firm pale flat regions of cerebral cortex that tend to be focused to a single gyrus. These tubers have a variable appearance with mushroom shaped gyri and loss of the cortex white matter junction. Often these tubers can extend from the cortical surface deep into the subcortical white matter and can range from one to several centimetres. Additionally, they may also calcify or undergo cystic degeneration. Microscopically, they are often characterized by a marked disorganization of cortical lamination with aggregates of abnormal glial and dysplastic neuronal elements. Glial elements commonly consist of gemistocytic astrocytes with abundant eosinophilic cytoplasm. The neuronal component of the tubers contains a heterogeneous population of morphologically dysplastic neurons, exhibiting a disrupted radial orientation within the cortex and abnormal dendritic arborisation, in addition to phenotypically normal cortical neurons. Furthermore, neuroastrocytes are also present, in addition to the key

histopathological feature of tubers, giant cells. As the name implies, giant cells are abnormally enlarged cells with diameters ranging from 80 to 150  $\mu\text{m}$ . Ovoid or polygonal in shape, giant cells appear to be defective with respect to regulation of growth and cellular development as they commonly possess abnormal dendritic arborisation, as well as frequently display multiple and laterally displaced nuclei (Crino et al. 1996; Crino & Henske 1999; Mizuguchi et al. 2002).

Located near the wall of the lateral and third ventricles, SENS are present in approximately 80% of TS patients. Developing early in fetal life, SENS are nodular lesions, less than 1 cm in size, that form either singly or in rows and often degenerate or calcify during later life. Microscopically, SENS consists of large cells, somewhat similar to giant cells, and elongated glial cells. Usually benign and asymptomatic, SENS are quite proliferative and have the potential to develop into SEGAs over time. Although the exact molecular mechanism governing the conversion of SENS to SEGAs is unknown, SEGAs are the most common brain tumours occurring in 5-10% of TS patients (Vinters & Miyata 2006). The appearance of SEGAs typically occurs within the first 20 years of life among TS sufferers, developing into tumours 1 cm in diameter or larger. These tumours usually extend into the lateral ventricle, often leading to obstructions of the foramen of Monro and blocking the flow of cerebrospinal fluid, leading to hydrocephalus or even death. Macroscopically, SEGAs form grey to pinkish-red tumours that can in some cases develop into large haemorrhages or calcifications. Microscopically, SEGAs are comprised of a heterogeneous population of cells containing dysmorphic astrocytes, similar to those seen in cortical tubers, and giant cells. Typically, SEGAs are highly vascular, but exhibit a low mitotic index. Additionally, foci of necrosis and inflammatory cell components, such as mast cells and T-lymphocytes, are interspersed within the tumour mass (Boer et al. 2008).

Beyond the risk of mortality and hydrocephalus, severe neurological abnormalities, such as epilepsy, neurocognitive dysfunction and pervasive developmental disorders (PDD), such as autism, are also strongly associated with the neurological manifestations of TS (Orlova & Crino 2010). Occurring within 60-90% of TS patients demonstrating neurological manifestations of TS, epilepsy usually manifests within the first year of life in TS patients and is the most common neurological disorder observed. Documented seizure types include infantile spasms, simple partial, complex partial and generalized tonic-clonic seizures (Thiele 2004). TS associated tubers are commonly regarded as the epileptogenic foci within sufferers and surgical intervention, via tubectomy, has, in most cases, been demonstrated to alleviate these seizures. Conversely though, as many as 10% of TS patients have been found to demonstrate seizures in the absence of cortical tubers (Thiele 2004). The exact mechanisms surrounding epileptogenesis in TS patients has never fully been identified, however aberrant glutamate receptor expression, observed within dysmorphic astrocytes, has been implicated as a contributing factor (White et al. 2001). In addition to epilepsy, the neurocognitive disorders associated with TS can affect between 30 to 80% of TS patients. Ranging widely in terms of severity, these disturbances are also highly variable in terms of expression, including behavioural problems, sleep disorders, hyperactivity, attention deficit, aggressiveness, and autism (Curatolo et al. 1991). In addition to these disorders, TS patients often present with altered cognitive function, with 14% of patients exhibiting mild to severe impairment and 30.5% of patients exhibiting severe mental retardation (Joinson et al. 2003).

### **1.3: The TS Gene Family: History & Genetics**

Investigation into the genetics underlying TS have spanned the last 130 years and are still ongoing today. Studies conducted by van der Hoeve, in 1933, and Gunther and Penrose, in

1935, identified TS as an autosomal dominant mutational disorder; these studies have formed the basis of our understanding of TS (van der Hoeve 1933; Gunther & Penrose 1935). However, it wasn't until the late 1980's that significant strides were made towards understanding and identifying the genes at the core of this disorder.

The first advances in this respect came in the form of genetic linkage studies, conducted in 1987, which served to identify and localize the genes implicated in the causation of this disorder. Targeted to chromosomal locus 9q34, the first of these genes was designated TSC1 (Fryer et al. 1987; van Slechtenhorst et al. 1997). A group of researchers, operating under the banner of the European Chromosome 16 Tuberous Sclerosis Consortium, conducted several experiments to localize the second TS gene family member to chromosomal locus 16p13.3, identifying it as TSC2 (Kandt et al. 1992; Nellist et al. 1993). These studies made it clear that mutation in either the TSC1 or TSC2 genes were fundamental to the development of TS. These studies lead to the discovery that there is frequent loss of heterozygosity within alleles at the 16p and 9q chromosomal regions in hamartomatous tissues taken from TS patients (Green & Yates 1993; Smith et al. 1993; Green et al. 1994). This evidence, coupled with *a priori* observation of growth aberrations in hamartoma tissues, provided credence for the theory that, much like genes misregulated in other phakomatoses, like neurofibromatosis (types 1 & 2) and von Hippel-Lindau disease, the TS genes acted as tumour suppressor genes (Leguis et al. 1993; Latif et al. 1993; Nellist et al. 1993; Huang & Manning 2008). When analyzed collectively, these findings allowed researchers to clearly characterize the genetic mechanism by which mutations in TSC1 or TSC2 lead to the development of TS.

The acquisition of TSC1 or TSC2 gene mutations is now known to occur via two principle methods. The first is genetic inheritance, being passed to patients during conception from

parents harbouring established germ cell mutations. The second method is through sporadic, *de novo* mutations, which occur during embryonic development. While both can occur, *de novo* mutations are more prevalent, with approximately 60-70% of TS cases showing no genetic inheritance (Jones et al. 1997; Jones et al. 1999). However, heterozygous inactivation of one of these genes is not sufficient to produce a disease phenotype. Disease pathogenesis and lesion formation have been found to result from the acquisition of a second somatic mutation, leading to homozygous inactivation of either of the TSC genes (Green et al. 1993). This loss of heterozygosity occurs in a manner consistent with Knudson's second-hit model, depending on secondary mutations, in this case commonly leading to large deletions involving the loss of surrounding loci (Knudson 1971; Green et al. 1994; Crino et al. 2006). Linkage analysis studies, examining familial TS, have suggested that distribution of TS-associated mutations is approximately split, with half of patients presenting TSC1 mutations and half presenting with TSC2 mutations (Jones et al. 1997; Jones et al. 1999). In the sporadic TS population however, this is not the case, as TSC2 mutations are observed to be nearly five times more common than mutation in TSC1 (Sanack et al. 2005; Jones et al. 1999). Furthermore, while the range of associated conditions is similar for patients harbouring TSC1 or TSC2 mutations, patients presenting with TSC2 mutations appear to be more severely afflicted than patients presenting with TSC1 mutations (Astrinidis & Henske 2005). The increased frequency of patients presenting with TSC2 mutations is thought to result from a higher incidence of second hit mutation events occurring when TSC2 is mutated; this however remains speculative and has yet to be fully elucidated (Rosner et al. 2008).

Extensive mutational studies have been conducted to investigate the spectrum of mutations observed in TS cases. TSC1 mutations have been found to predominantly represent nonsense or frame shift mutations, which lead to premature protein truncation upon translation

(Figure 1a). TSC2 mutations, however have demonstrated a broader spectrum, presenting as frameshift, missense, nonsense, in-frame deletions and splice mutations (Jones et al. 1999) (Figure 1b). Through these studies more than 200 TSC1 and 700 TSC2 allelic variants have been identified (Niida et al. 1999; Jones et al. 1999; van Slegtenhorst et al. 1999; Kwiatkowska et al. 1998). Certain TSC2 missense mutations, within exons 16 and 38, and an 18-bp in frame deletion, in exon 40, appear at an elevated frequency among several TS patients (Sancak et al. 2005). Further studies comparing the frequency of TSC1 mutations to that of TSC2 mutations have observed that missense and large genomic deletions occur much more frequently on the TSC2 gene (Crino & Henske 2006).

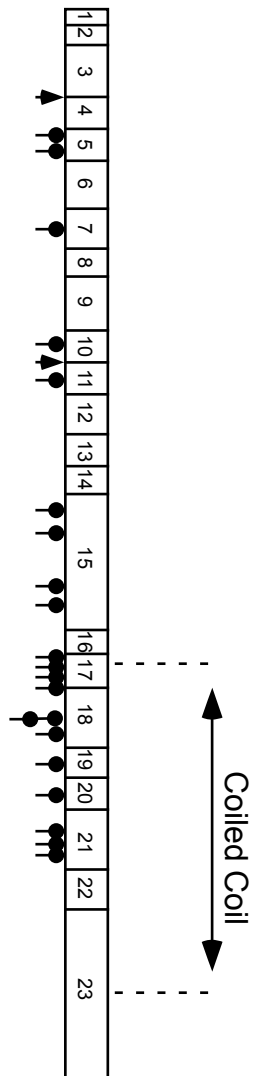
#### **1.4: The TSC Gene Products: Hamartin & Tuberin**

As part of the studies conducted in 1993 and 1997 investigating the chromosomal loci of the TSC genes the unique protein products of TSC1 and TSC2, known as Hamartin and Tuberin respectively, were also uncovered (Nellist et al. 1993; van Slegtenhorst et al. 1997). Research in subsequent years has elucidated the structural organization of these two proteins and has also yielded several insights into their function, interactions and the nature of their association to TS.

Hamartin, the 130 kDa protein encoded by the 23 exons of the TSC1 gene, was observed to be ubiquitously expressed within all eukaryotic cells existing as one of two isoforms, derived from the alternative splicing of the transcript at exon 2 (van Slegtenhorst et al. 1997). Structural domains identified on Hamartin include an N-terminal transmembrane domain and a C-terminal coiled coil domain. In addition to these structural motifs, Hamartin also contains several functional domains distributed across the length of the protein which serve to mediate its interaction with a broad range of other proteins including: NADE (aa 671-1084), FIP200 (aa 403-787), ezrin-radixin-moesin (ERM) actin binding proteins (aa 881-1084), NF-L (aa 674-1164), Plk1

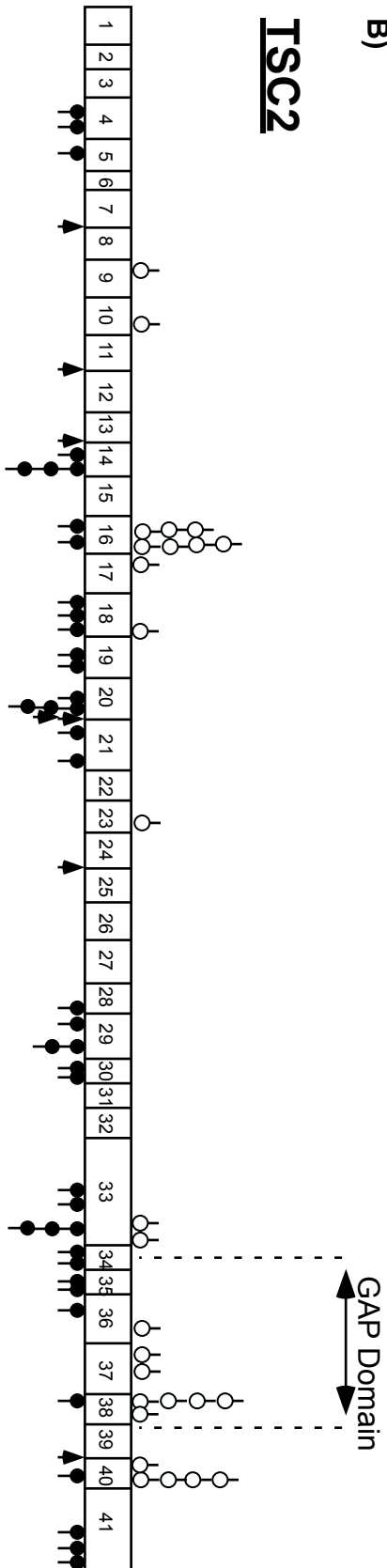
A)

### TSC1



B)

### TSC2



- Nonsense / Frameshift
- Missense / In-frame Deletion
- ▲ Splice



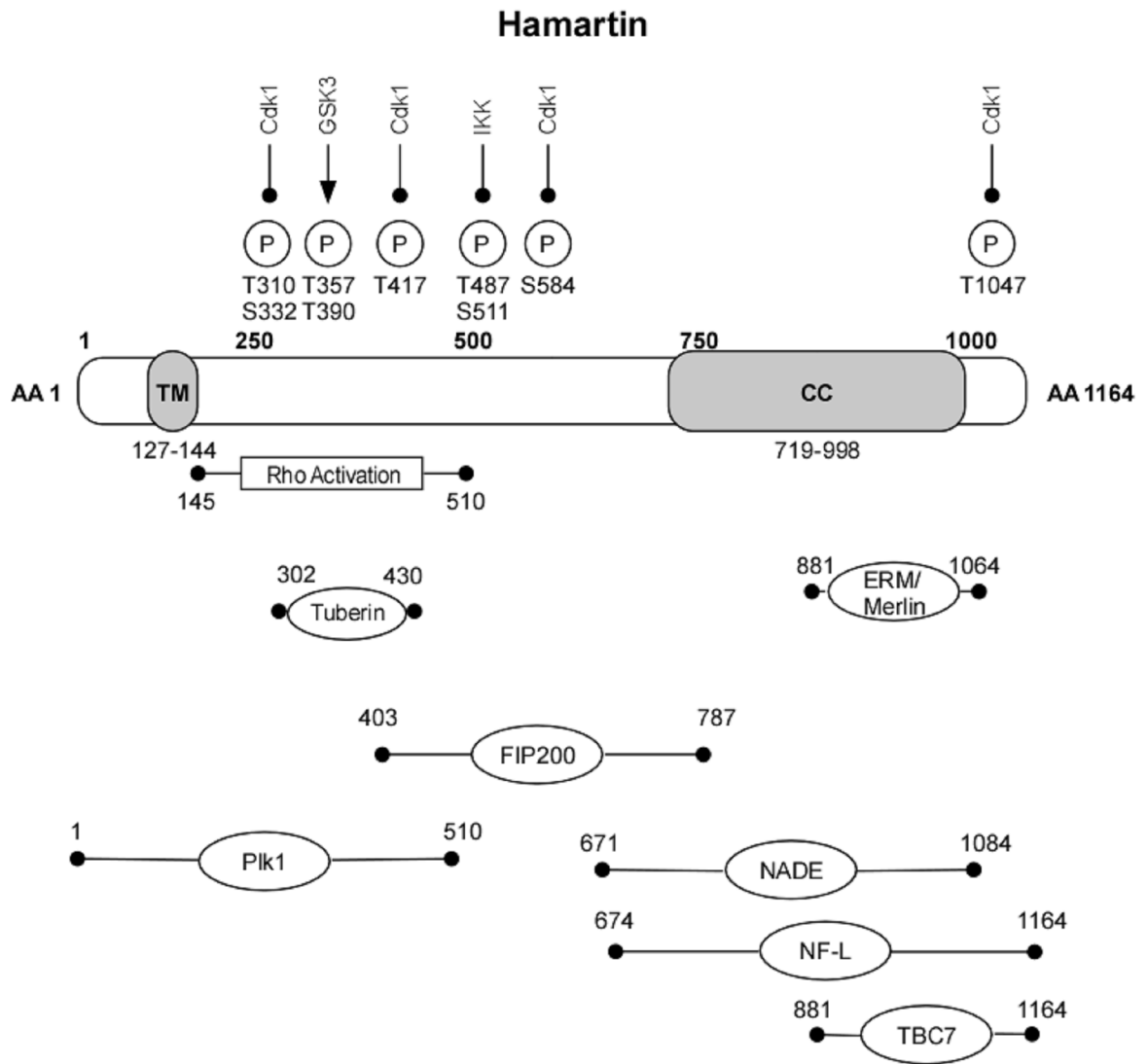
**Figure 1** *TSC1 & TSC2 Gene Mutations*

Schematic representation indicating the distribution of mutations along the **A)** TSC1 and **B)** TSC2 genes. Indicated here are all identified point mutation, small deletions and insertions. Numbered boxes denote individual exons. Adapted from: Jones et al. 1999.

(aa 1-510) and TBC7 (aa 881-1164) (Nakashima et al. 2007; Murthy et al. 2000; Lamb et al. 2000; Shillingford et al. 2006; Surpili et al. 2003; Gao et al. 2002) (Figure 2a). The N-terminal region of Hamartin has also been identified to be the most critical region of the protein, as it contains domains which mediate Hamartin's most characterized interactions: activation of the small GTP-binding protein Rho (aa 145-510); and binding to, and stabilization of Tuberin (aa 302-430) (Krymskaya 2003; Chong-Kopera 2006). Furthermore, both the N and C-terminal regions of Hamartin have been suggested to be vital for the maintenance of Hamartin's protein-protein interactions, as truncation of the protein, in either of these regions, has been found to result in significantly decreased binding to Tuberin (Hoogeveen-Westerveld et al. 2010). Additionally, Hamartin also contains several phosphorylation sites, which allow for regulatory phosphorylations by various kinases, including GSK3 $\beta$ , Cdk1 and IKK $\beta$  (Mak et al. 2003; Lee et al. 2007; Catania et al. 2007).

Product of TSC2's 5.4 kb mRNA transcript, the second TSC gene product Tuberin is a protein comprised of 1807 amino acid at full length (Nellist et al. 1993) (Figure 2b). Comprised of 41 exons, the transcript is alternatively spliced at exons 25, 26 and 31 to produce the six isoforms that have, to date, been identified (Sampson 2003). Among these isoforms, isoform 5, the 1784 bp product which results from the excision of exon 25 and 31, is observed to be the most commonly expressed isoform within the cell (Martin et al. 2004; Krymskaya 2003). Across its length, Tuberin contains several important structural and functional domains including two small coiled coil domains (aa 346-371; aa 1008-1021), a leucine zipper motive (aa 81-98), and a small c-terminal region (aa 1517-1674) that harbours similarity with the GTPase-activating protein (GAP) GAP3 (Rap1) (Rubinfeld et al. 1991; Rubinfeld et al. 1992). Further investigation subsequently identified this region as Tuberin's primary functional domain, with observations

A)



B)

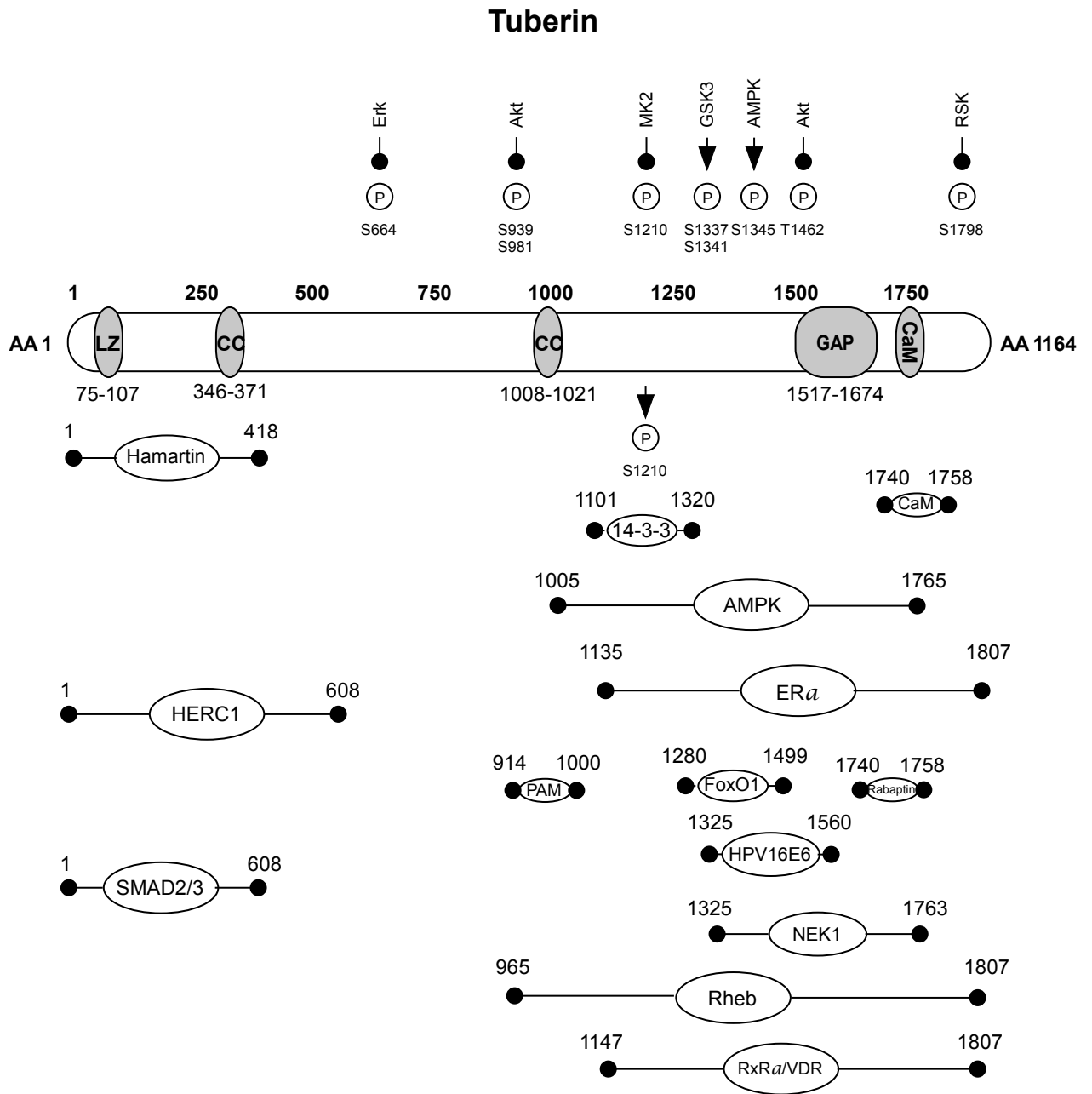


Figure 2 - 14

**Figure 2 Schematic Diagrams: Tuberin and Hamartin**

Schematic representation of the TSC proteins, Hamartin and Tuberin. **A) Hamartin** (130 kDa protein, 23 exons, 1164 aa). Domains (Structural and Functional): N-terminal transmembrane domain (TM) (127-144), C-terminal coiled coil domain (CC) (719-998), NADE (aa 671-1084), FIP200 (aa 403-787), ezrin-radixin-moesin (ERM) actin binding proteins (aa 881-1084), NF-L (aa 674-1164), Plk1 (aa 1-510), TBC7 (aa 881-1164), Rho (aa 145-510), Tuberin (aa 302-430). Phosphorylation Sites: GSK3 $\beta$  (T357, T390), Cdk1 (T310, S332, T417, S584, T1047), IKK $\beta$  (T487, S511). **B) Tuberin** (200 kDa protein, 41 exons, 1807 aa). Domains (Structural and Functional): coiled coil domains (CC) (aa 346-371; aa 1008-1021), luciferase zipper motive (aa 81-98), C-terminal GAP region (aa 1517-1674), Hamartin (aa 1-418), HERC1 (aa 1-608), SMAD2/3 (aa 1-440), Pam (aa 914-100), 14-3-3 (aa 1101-1320), AMPK (aa1005-1765), ER $\alpha$  (aa 1135-1807), FOXO1 (aa 1280-1499), HPV16 E6 (aa 1315-1560), NEK1 (aa 1325-1763), PATJ (aa 1538-1763), Rabaptin (aa 1668-1726), ROR $\alpha$ /VDR (aa 1147-1807), Rheb (aa 965-1807). Phosphorylation Sites: Akt (Ser939, Thr993, Ser11309, Ser1132, Thr1162, Thr1462), Erk (Ser540, Ser664), MK2 (Ser1210), GSK3 (Ser1337, S1341), AMPK (Ser1345), RSK (Ser1798) and 14-3-3 (Ser1210). Adapted from: Rosner et al. 2008.

demonstrating GAP activity, mediated through this region, towards several members of the Ras family of small GTPases, including Ras homolog enriched in brain (Rheb), Rap1A and Rab5 (Wienecke et al. 1995; Maheshwar 1997; Xiao et al. 1997). Additionally, a number of activating and inhibitory phosphorylation sites exist along the length of Tuberin, allowing for regulation of its activity by a number of kinases. Some of these kinases include: the serine threonine/kinases Akt (Ser939, Thr993, Ser1309, Ser1132, Thr1162, Thr1462), Erk (Ser540, Ser664), MK2 (Ser1210), GSK3 (Ser1337, S1341), AMPK (Ser1345), RSK (Ser1798) (Dan et al. 2002; Ma et al. 2005; Roux et al. 2004; Mak et al. 2003; Nellist et al. 2002). Tuberin also possesses a number of functional domains which mediate direct interaction with various other proteins, such as: Hamartin (aa 1-418), HERC1 (aa 1-608), SMAD2/3 (aa 1-440), Pam (aa 914-100), 14-3-3 (aa 1101-1320), AMPK (aa1005-1765), ER $\alpha$  (aa 1135-1807), FOXO1 (aa 1280-1499), HPV16 E6 (aa 1315-1560), NEK1 (aa 1325-1763), PATJ (aa 1538-1763), Rabaptin (aa 1668-1726), RxR $\alpha$ /VDR (aa 1147-1807), Cyclin B1 (aa 600-746) and finally, Rheb (aa 965-1807), the target through which Tuberin mediates its primary function (Chong-Kopera et al. 2006; Lu et al. 2004; Birchenall-Roberts et al. 2004; Castro et al. 2003; Yasui et al. 2007; Finlay et al. 2004; Henry et al 1998; Cao et al. 2006; Rosner & Hengstschlager 2004; Fidalgo da Silva et al. 2011).

*In vivo*, Tuberin and Hamartin physically interact to form a protein complex, known as the Tuberous Sclerosis Complex (TSC). This complex, observed to have a molecular weight of approximately 450 kDa, is larger than a heterodimeric complex composed of individual Tuberin and Hamartin peptides and is predominantly believed to be a heterotrimeric complex, composed of Tuberin and Hamartin peptides organized in a 2:1 or 1:2 ratio (Nellist et al. 1999). Within the TSC, Tuberin has been found to behave as a chaperone protein for Hamartin, preventing the self-aggregation of Hamartin, while Hamartin has been observed to stabilize Tuberin, preventing its HERC1 ubiquitin ligase mediated degradation and allowing for its

functional activity towards Rheb (Benvenuto et al. 2000; Chong-Kopera et al. 2006; Nellist et al. 1999). Formation of this heteromeric complex has been observed to be regulated primarily through the tyrosine kinase phosphorylation of Tuberin and as mutational studies have identified several amino acid residues, such as R611, A614, F615, C696, V769, Y1571 and P1675, as necessary for Tuberin binding to Hamartin (Aicher et al. 2001; Nellist et al. 2001; Nellist et al. 2005). These, and other studies, have concluded the interaction between Tuberin and Hamartin, and the subsequent formation of the TSC, are important to the appropriate regulation of a number of cellular processes, due to its involvement in a several signaling cascades, most notable among them, its downstream effector the mTOR signaling cascade (Young & Povey 1998; Jones et al. 1999; Nellist et al. 1999; Tee et al. 2002).

### **1.5: TSC Signalling: mTOR Regulation**

Investigations into the mechanisms governing Tuberin and Hamartin function have observed that, when associated within the TSC, these proteins function as an important central hub of signal transduction, receiving signals from several upstream signal transduction pathways, such as the PI3K/Akt, MAPK, and AMPK signalling pathways, and distributing them in turn to downstream effectors for the regulation of cell growth, metabolism, cellular proliferation and cell cycle progression (Potter et al. 2002, Inoki et al. 2003a, Ma et al. 2007, Mieulet & Lamb 2010). Within this role, the TSC effectively behaves as a nutrient sensor, integrating upstream signalling events, which indicate important changes in the energy status of the cell, nutrient and growth factor availability, and conditions of cellular stress (Wullschleger et al. 2006; Rosner et al. 2008). Following receipt of these signals, the TSC then distributes these signals to downstream effectors, acting primarily through the mammalian target of rapamycin (mTOR) signalling cascade (Young & Povey 1998; Tee et al. 2002) (Figure 3).

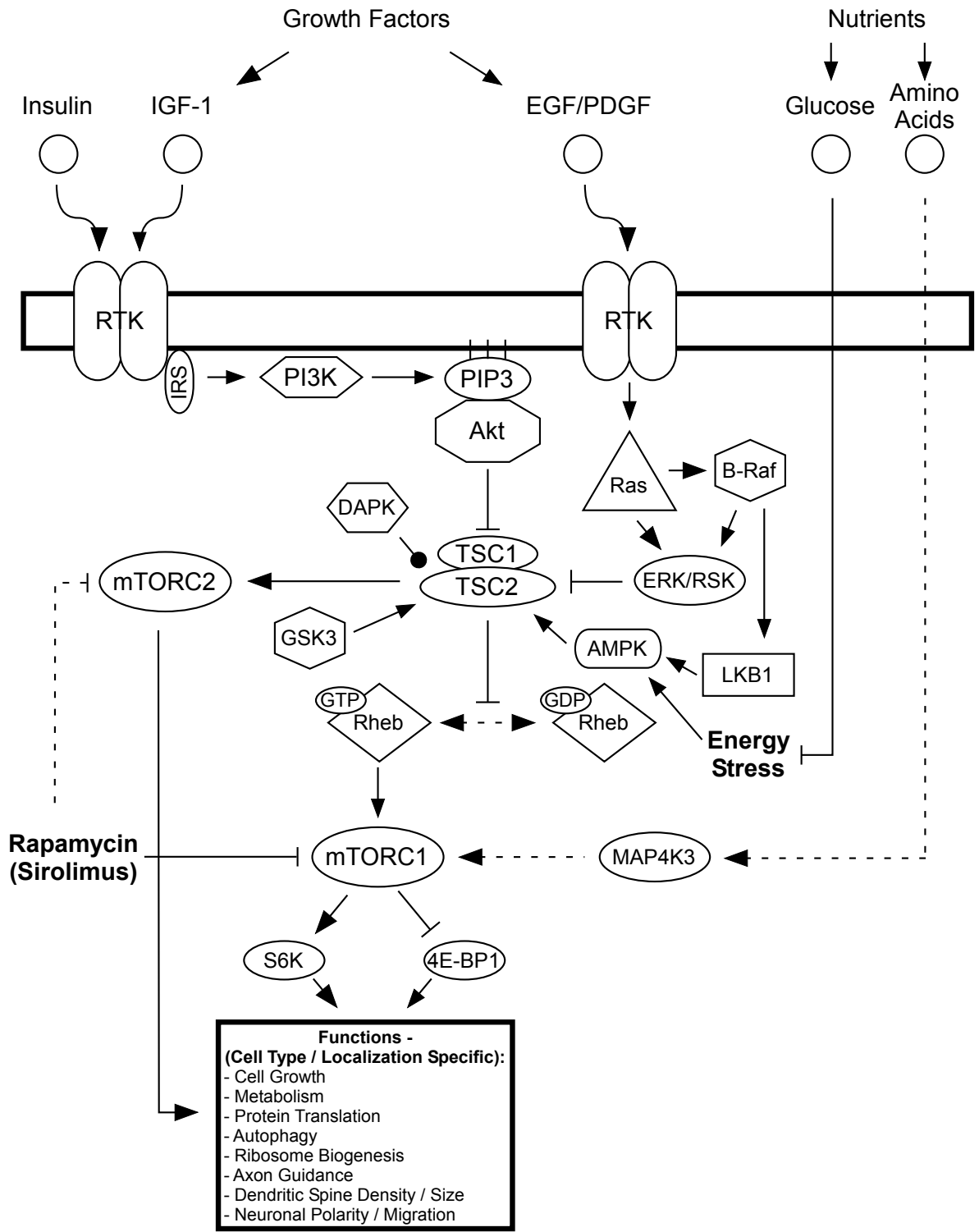


Figure 3 - 18



**Figure 3** *The TSC integrates intracellular signaling cues, such as growth and energy signals, to influence numerous cellular processes within the CNS*

This schematic representation provides a simplified view of the multiple signaling pathways in which the TSC participates in, both directly and indirectly. Well known immediate regulators of TSC activity include: Akt, GSK3, AMPK, ERK/RSK and DAPK. Primary function of the TSC is mediated through its GTPase activating protein function towards Rheb (Ras homolog enriched in brain), which served to regulate the activity of Tuberin's most studied downstream effector the mTOR complex (mTORC1 & mTORC2). Through mTOR, the TSC is able to influence a number of cellular processes, ranging from protein translation to autophagy. Adapted from: Han & Sahin 2011.

Belonging to the phosphatidylinositol kinase-related kinase (PIKK) superfamily, mTOR is a serine/threonine kinase with a molecular weight of 289 kDa (Sabatini et al. 1994; Chiang & Abraham 2005). Discovered in 1994, TOR proteins were first identified through studies focused at investigating the mechanism of action for the macrolide antibiotic Rapamycin (Sirolimus) and identification of the intracellular target of the functional complex it forms with the immunophilin FK binding protein-12 (FKBP12) (Brown et al. 1994; Sabatini et al. 1994; Sehgal 2003). Structurally conserved among species as diverse as yeasts, flies and mammals, TOR proteins have been found to be heavily involved in the regulation of a number of cellular and metabolic processes which control cell growth, proliferation, survival, protein translation and differentiation (Fingar & Blenis 2004; Wullschleger et al. 2006). In mammals, TOR proteins are known to exist as members of at least two distinct ternary complexes, mTOR complex 1 (mTORC1) and mTOR complex 2 (mTORC2), and primarily function through a C-terminal catalytic kinase domain, which displays a high degree of homology to the catalytic domain of phosphatidylinositol 3-kinase (PI3K) (Sehgal 2003). Additionally, mTOR also contains several well characterized functional domains which include: an FKBP12-Rapamycin Binding (FRB) domain; an auto-inhibitory repressor domain, near the C-terminus; up to 20 tandemly repeated HEAT motifs at its N-terminal end; a FRAP-ATM-TRAP (FAT) domain; and a c-terminal FATC domain (Wullschleger et al. 2006). Functionally, mTOR serves as a central component of a signalling pathway which acts to regulate cell growth and proliferation.

Controlled by a wide variety of intracellular and extracellular signals, ranging from growth factors to cellular energy levels, mTOR has most clearly been characterized as a downstream target of the PI3K/Akt signalling pathway. Known to be highly involved in the regulation of an array of cellular processes, stimulation of the PI3K/Akt signalling pathway is typically initiated through the binding of various ligands, such as mitogens, cytokines and

hormones, to receptor tyrosine kinases at the cellular membrane. These receptors include the insulin-like growth factor receptor (IGFR), the platelet-derived growth factor receptor (PDGFR), the epidermal growth factor receptor (EGFR) and the receptors that comprise the Her family of membrane bound receptors (Jozwiak et al. 2005). Upon binding of the appropriate ligand, receptor activation leads to autophosphorylation of the receptor and to activation of the PI3K, causing it to catalyze the conversion of membrane bound phosphatidylinositol (4,5)-bisphosphate (PIP<sub>2</sub>) to phosphatidylinositol (3,4,5)-triphosphate (PIP<sub>3</sub>). PI3K can also be activated through growth factor receptor activation of the oncogenic small GTPase, Ras or by insulin, which causes the phosphorylation of insulin receptor substrates 1 or 2 (IRS 1/2), leading them to bind PI3K (Alberts et al. 2002; Freilinger et al. 2007). Following its activation, PIP<sub>3</sub> binds to the pleckstrin homology domain of Akt, resulting in the activation of Akt through dimerization and exposure of its catalytic site or phosphorylation by phospholipid-dependent kinase-1 (PDK-1). Once active, Akt then signals to mTOR via regulation of its activity in one of two ways. The first is via direct phosphorylation, as Akt bears the ability to activate mTOR through phosphorylation at Ser2448, while the second is via indirect activation, working through phosphorylation of the TSC protein Tuberin (Chiang & Abraham 2005; Jozwiak et al. 2005).

In its active state, the TSC functions as a negative regulator of mTOR, mediating its function through the activity of the GAP domain found on the C-terminal end Tuberin. This GAP domain acts to inactivate mTOR signalling by stimulating auto-hydrolysis of Rheb-GTP, converting it to Rheb-GDP (Inoki et al. 2003b). Phosphorylation of TSC2 by Akt, at Ser939, Ser981 and Thr1462, serves to functionally inactivate the TSC, leading to retention of Rheb's GTP bound form (Cai et al. 2006). In addition to Akt, several other proteins and kinases have demonstrated the ability to inhibit TSC activity. Among these are Erk and RSK1, which demonstrate the ability to inhibit TSC activity via phosphorylation of Tuberin at Ser664 and

Ser1798 respectively; DAPK, which binds to Tuberin and subsequently phosphorylates it leading to dissociation of the TSC; and FOXO1, which can bind to Tuberin leading to inhibition of TSC complex formation (Ma et al. 2005; Roux et al. 2004; Cao et al. 2006; Stevens et al. 2009). Inhibition of mTOR is also facilitated through phosphorylation by kinases such as AMPK, which activates TSC through phosphorylation of Tuberin at Ser1345; and GSK3, which also activates TSC via phosphorylation of Tuberin at Ser1337 and Ser1341 (Inoki et al. 2003a; Shaw et al. 2004).

Activation of mTOR can subsequently lead to the phosphorylation of several downstream targets as it propagates the signals initiated by the PI3K/ Akt pathway. However, in order for mTOR to disseminate these signals downstream it acts through its two distinct ternary complexes, mTORC1 and mTORC2 (Sabatini 2007). While structurally similar, these complexes exemplify the diversity of mTOR's regulatory involvement and their functions are quite divergent. The first of these complexes, mTORC1, functions primarily to regulate the size of the cell, accomplishing this through regulation of gene transcription. Composed of three subunits including mTOR, the regulatory associated protein of mTOR (RAPTOR), and G-protein Beta-subunit-like protein (G-BetaL), mTORC1 acts to control mRNA translation through parallel regulation of its downstream effectors, eukaryotic translation initiation factor-4E-binding protein 1 (eIF4EBP1 or 4EBP1) and the ribosomal protein p70S6K (Loweith et al. 2002). An important regulator of translation, 4EBP1 binds strongly to the eukaryotic translation initiation factor-4E (eIF4E) in its unphosphorylated state, repressing its association with the eukaryotic initiation factor-4F (eIF4F) complex. As a component of the eIF4F, eIF4E recognizes and binds to the 5' end of mRNA prior to translation (Gingras et al. 1998). Phosphorylation of 4EBP1 by mTOR, as part of a series of consecutive phosphorylation events beginning of on Thr37/Thr46 and proceeding to Ser65/Thr70, results in release of eIF4E from 4EBP1 repression and permits the initiation of the cap-dependent translation of a subset of mRNA's that encode for proteins which regulate the

proliferative response and cell cycle progression, like c-Myc, Cyclin D1 and Ornithine Decarboxylase (Gingras et al. 2001). Regulation of the activity of mTORC1's second major downstream effector, the serine/threonine kinase p70S6K, is also carried out through a series of phosphorylation events, including mTORC1-dependent phosphorylations at Thr371 and Thr389 (Dufner et al. 1999). Phosphorylation at these two residues stimulates the catalytic activity of p70S6K, leading to its phosphorylation and activation of the ribosomal proteins S6K1 and S6K2 on Ser235/Ser236 (Ruvinsky et al. 2005; Ruvinsky & Meyuhas 2006). This activation of S6K1/S6K2 subsequently stimulates recruitment of the 40S ribosomal subunit to actively translating polysomes, resulting in translation of mRNA's, such as those encoding ribosomal proteins, elongation factors and IGF-II, which bear 5'-TOP (5'-Terminal Oligopyrimidine) sequences. In addition, S6K1 activation establishes a negative feedback loop towards PI3K/Akt and mTOR signalling by negative regulation of insulin receptor substrate-1 (IRS-1) (Lang & Frost 2005). mTORC1 also plays a pivotal role in the regulation of angiogenesis acting as a negative regulator of the vascular endothelial growth factor (VEGF), as mTORC1 inhibition has been demonstrated to result in the accumulation of the transcription factor hypoxia-inducible factor 1 $\alpha$  (HIF1 $\alpha$ ) and increased expression of HIF responsive genes like VEGF (Brugarolas et al. 2003).

Though less understood than mTORC1, the second mTOR complex, mTORC2 is structurally quite similar to mTORC1. Composed of mTOR, G-BetaL, the rapamycin insensitive companion of mTOR (Rictor), and the mitogen-activated-protein-kinase-associated protein 1 (mSin1), mTORC2 displays a key difference from mTORC1 in that does not demonstrate a susceptibility to Rapamycin treatment. Specifically, the Rapamycin-FKBP12 inhibitory complex has demonstrated an inability to bind directly to mTOR2, indicating that the effects of rapamycin on cellular signalling are due to inhibition of mTORC1 (Sarbasov et al. 2006). Additionally, mTORC2 also differs from mTORC1 in that while mTORC1 appears to be primarily involved in

regulation of signalling and the subsequent expression of genes which primarily influence the size of the cell, mTORC2 appears to be primarily involved in influencing the shape of the cell. Through regulatory mechanisms involved in controlling mTORC2 function are poorly understood, mTORC2 is believed to be under the regulatory control of the TSC in a manner similar to that of mTORC1 (Huang & Manning 2009). However, the exact components regulating their interaction have not been clearly identified. Functionally, mTORC2 has been demonstrated to play a role in the formation of the actin cytoskeleton, as it has been observed to signal through small Rho GTPases and protein kinase C alpha (PKC) to regulate the formation of F-actin. Additionally, mTORC2 has also been observed to control the formation of GTP-bound Rac1 which also plays a role in F-actin formation (Jacinto et al. 2004). However, the exact mechanism which by which mTORC2 influences these proposed partners is still currently being investigated. Furthermore, mTORC2 has also demonstrated the ability to phosphorylate Akt at Ser473 to activate its function, suggesting mTORC2 may serve to mediate a positive feedback mechanism between mTOR and Akt signalling to control their function (Jacinto et al. 2006).

Observation of the inter-connectedness of mTOR to its signalling partners strongly suggests that TOR kinases participate in critical events that integrate external signals with internal signals to co-ordinate cellular growth, survival and proliferation. mTOR effectively receives signalling input which indicate whether the transcriptional and translational machinery should be upregulated, then efficiently transmits them to the appropriate downstream targets. In recent decades, significant evidence has accumulated to suggest that dysregulation of mTOR and many of its associated signalling partners often occurs in many type of cancers and neoplasia disorders, from breast cancer to tuberous sclerosis (Choo & Blenis 2006; Crino et al. 2006).

## 1.6: TSC Signaling: Cell Cycle Regulation, Differentiation & Fate

While classical observations of the functional significance of the TSC proteins have most closely associated them with the regulation of the mTOR signaling cascade, a growing body of research has found that they participate in the regulation of various cellular processes, through mTOR-independent means. These studies primarily highlight Tuberin, as the active component of the TSC, in these functions, suggesting a significant role for the protein as a key regulator of cellular signaling.

Notwithstanding its mTOR-mediated effects on cell cycle progression, Tuberin has been further implicated as a regulator of the cell cycle, through its influence on a number of cell cycle regulatory proteins. Recent studies conducted by Rosner et al. (2007a) have found that Tuberin bears the ability to regulate the localization of the Cyclin-dependent kinase inhibitor, p27, through inhibition of its 14-3-3 mediated cytoplasmic retention (Rosner & Hengstschlager 2004; Rosner et al. 2007a). They observed that in G0 cells, Tuberin binds to p27, sequestering it from 14-3-3 and preventing the Akt-mediated phosphorylation of p27 within its nuclear localization signal (NLS) at T157 (Sekimoto et al. 2004). This interaction with Tuberin subsequently allows p27 to undergo NLS-importin-dependent nuclear localization, where it inhibits the catalytic activity of Cyclin E/CDK2 and Cyclin D/CDK4 complexes and restricts progression through the G1/S phase checkpoint (Alberts et al. 2002). In addition to its effects on p27 localization, Tuberin has also been observed to interact directly with Cyclin B1, Cyclin A, and CDK1 (Catania et al. 2001). Fidalgo da Silva et al. (2011) also went on to find that upon binding to Cyclin B1, Tuberin was capable of retaining it within the cytoplasm, restricting progression through the G2/M phase checkpoint (Fidalgo da Silva et al. 2011).

Tuberin has also been demonstrated to interact with various signaling cascades involved in regulating cell differentiation and cell fate choice. The first among these is the Wnt signaling pathway. In their 2003 study, Mak et al. demonstrated that the TSC interacted with the canonical Wnt signaling pathway, as it was able to regulate  $\beta$ -catenin stability and protein expression, inhibited Wnt-induced  $\beta$ -catenin-dependent transcriptional activity and interacted with the GSK3 $\beta$ -degradation complex (Mak et al. 2003). Follow up studies also found that Tuberin was also able to bind directly to the Wnt signaling component Dishevelled (Dsh) (Mak et al. 2005). Inoki et al. (2006) later observed that Tuberin served as a direct physiological substrate for GSK3 $\beta$ , an important component of the canonical Wnt pathway, being phosphorylated by it at S1341, S1337, S1333, and T1329 (Inoki et al. 2006). They went on to conclude that Wnt functioned as a positive regulator of mTOR activity, through inhibition of GSK3 phosphorylation/activation of Tuberin.

Tuberin has also been implicated as an upstream regulator of the Notch signaling pathway. Ma et al. (2010) observed that the TSC acts as a negative regulator of Notch activation, in an mTOR-dependent manner, wherein inactivation of the TSC resulted in constitutive activity in Rheb, which in turn led to sequential activation of mTORC1 and STAT3. STAT3 activation, in turn, lead to p63-mediated upregulation of Jagged1 and subsequent Notch1 activation (Ma et al. 2010). A similar role for Tuberin was also suggested by Karbowniczek et al. (2010), but while still dependent on the TSC-Rheb interaction, Notch regulation was suggested to occur through an as yet determined mTOR-independent mechanism (Karbowniczek et al. 2010).

Additionally, Tuberin has also been functionally linked to the MAPK signaling pathway in a regulatory capacity. Expression of Rheb has been demonstrated to negatively regulate B-Raf kinase activity, and subsequent phosphorylation and activation of p42/44 MAPK, through a



direct binding interaction with B-Raf (Im et al. 2002; Karbowniczek et al. 2004). This implicates Tuberin as a positive regulator of p42/44 MAPK signaling, via regulation of Rheb activation. Furthermore, studies focusing on medulloblastoma pathogenesis have indicated that Tuberin serves as an indirect downstream effector of Sonic Hedgehog (SHH) signaling, wherein SHH activity functions cooperatively with PI3K/Akt activation, to negatively regulate Tuberin activity (Bhatia et al. 2009). However, the exact mechanism by which this cooperative interaction occurs is still under investigation.

### **1.7: TSC1 & TSC2 Gene Mutations: Consequences for TSC Function**

Mutations in either of the TSC1 or TSC2 genes have been noted to disrupt the formation of the TSC, leading to abrogation of the TSCs characteristic functions. In terms of effect, mutations in either gene lead to the same phenotypic outcome, the consequent pathogenesis of TS. However, the mechanisms by which the mutations can prevent TSC function are believed to be different. Mutations in TSC1 are believed to result primarily in the truncation of Hamartin, removing regions of the protein that are required to mediate its interaction with Tuberin (Hodges et al. 2001). This in turn prevents TSC formation and leads to the subsequent ubiquitin mediated degradation of Tuberin (Benvenuto et al. 2000; Jones et al. 1997; Hoogeveen-Westerveld et al.2010). Mutations in TSC2, on the other hand, can potentially have a more subtle effect, as they often do not always lead to truncation of the resultant protein (Maheshwar et al. 1997; Mayer et al. 2003). TSC2 mutations can lead to formation of a non-functional TSC, in cases when mutations occurs within Tuberin's GAP domain, functionally inactivating the TSC, while Tuberin-Hamartin binding, though weakened, can still occur (Mayer et al. 2003). Additionally, they can also prevent the binding to Hamartin, via disruption of regions that mediate the Tuberin-Hamartin interaction, such as the phosphorylation sites residing C-terminal

to the Hamartin binding domain (Nellist et al. 2001). These mutations, frequently observed in TS patients, support the importance of specific residues outside of the Hamartin binding domain to maintaining the proper protein conformation necessary for mediation of the Tuberin-Hamartin interaction (Aicher et al. 2001). Furthermore, in conditions of TS, patients have commonly been observed to acquire multiple mutations, leading to disruptions in Tuberin's functional control of its downstream signalling partners and subsequent abrogation of appropriate differentiation and fate choices within TS afflicted cell types, and notably, during neural fate decisions within the CNS (Jones et al. 1999).

### **1.8: Neurogenesis and the Regulation of Neural Cell Fate**

Neural development can be characterised as a process which is comprised of a series of events and interactions which guide pluripotent stem and progenitor cells to take on a neural cell fate and begin programs of differentiation that ultimately give rise to some of the most specialized and unique cell types found within the mammalian body. Integrating a range of cellular mechanisms which modify patterns of gene expression and cell cycle progression, neural development is effected primarily through the processes of neurogenesis and gliogenesis. Serving as the point of initiation for neural development, neural induction is the process by which the stem cells of the embryonic ectoderm are stimulated to adopt neural cell fates, consequently leading to the development of the cell types which compose the nervous system. During gastrulation, the phase of early embryonic development which leads to formation of the ectodermal, mesodermal and endodermal germ cell layers from the single layered blastula, epiblast cells of the mesodermal germ cell layer form together, giving rise to the rod-like structure known as the notochord (Alberts et al. 2002). The key 'organizer' of neural induction, the notochord regulates the expression and activation of various morphogenic factors and

signalling cascades to promote neural organization and patterning, as well as neural fate decisions in the cells of the adjacent ectodermal progenitors. Among the factors regulated by the notochord are Bone Morphogenetic Proteins (BMPs), specialized members of the Transforming Growth Factor Beta (TGF $\beta$ ) superfamily of proteins (Gaulden and Reiter 2008). Observed to be potent regulators of patterning and polarity within developing embryos, where precise concentration gradients of BMP signalling has been observed to be crucial significance, BMPs bind to TGF $\beta$  receptors and initiate alterations in gene expression through downstream activation of SMAD (*Small and Mothers Against Dpp*) proteins (Marchant et al. 1998; Yew et al. 2005). During induction, the notochord acts to negatively regulate BMP activity by secreting inhibitory compounds such as Noggin, Chordin and Follistatin, which bind to BMPs, inhibiting their activity (Zimmerman et al. 1996; Hemmati-Brivanlou et al. 1994; Sasai et al. 1994). In addition, the notochord also regulates the activity of the Wnt signalling cascade, which in recent years, has been implicated as a significant regulator of neural patterning (Alvarez-Medina et al. 2008; Robertson et al. 2004). Commonly observed to be an important signalling pathway in the regulation of cell polarity and carcinogenesis, the Wnt signalling pathway is known to effect changes in gene transcription through binding of the Wnt ligand to the Frizzled receptor, leading to stabilization of the intracellular signalling molecule  $\beta$ -catenin through inhibition of the GSK-3/Axin/APC destruction complex. Following inhibition of this complex,  $\beta$ -catenin is subsequently allowed to translocate to the nucleus and interact with members of the TCF/LEF transcription factor family to alter gene transcription (Cadigan and Nusse 1997). During induction, the notochord acts to inhibit Wnt signaling by secreting the Wnt signalling inhibitors Dickkopf1 (Dkk1) and Secreted frizzled-related protein 2 (SFRP2) (De Robertis and Kuroda 2004). As a result of its regulation of the activity of morphogens like BMP and Wnt, the notochord induces the adjacent ectodermal epiblast cells to become more differentiated, producing a layer of cells,

known as the neural plate, composed of progenitor cells, known as neuroepithelial cells, which display typical epithelial cell features and are highly polarized along their apical-basal axis (Gotz and Huttner 2005). With formation of the neural plate, vertebrate neurogenesis and gliogenesis effectively begin, spurred on by changes in gene expression, such as the upregulation of the transcription factor genes CUX1, CUX2 and TBR2 or the astroglial markers glial fibrillary acidic protein (GFAP) or brain-lipid-binding protein (BLBP), and the downregulation of epithelial features like tight junctions (Nieto et al 2004; Englund et al. 2005; Campbell & Gotz 2002; Aaku-Saraste et al. 1996). These changes in gene expression lead many of the neuroepithelial cells to differentiate further, giving rise to more fate-restricted progenitor cells known as radial glial cells and basal progenitors (Gotz & Huttner 2005).

Following formation of the neural plate, progression of neural development and differentiation is promoted through attachment of mesodermal notochord cells to the basal surface of the overlying neural plate. This initiates a process known as neurulation, which is characterized by the curling up and fusion of the bilateral halves of the neural plate, resulting in the formation of a structure known as the neural tube (Alberts et al. 2002; Crane and Trainor 2006). Composed of a now thickened, layer of pseudostratified neuroepithelial cells, radial glial cells and basal progenitors, the neural tube serves as the rudimentary structure from which the entire nervous system will be formed. Structural re-organization of the neural tube proceeds as development progresses inducing proliferative progenitor cell populations to undergo rounds of neurogenic symmetrical or asymmetrical cell divisions (Iacopetti et al. 1999). Underlying the transition of neural progenitor cells from programs of proliferative cell divisions to neurogenic cell divisions is regulation of cell cycle progression, as it has been observed that the length of the cell cycle within particular regions of the neural tube correlates strongly to the proportion of neuroepithelial and radial glial cells within these regions (Takahashi et al. 1995). This increase in

cell cycle length has been attributed to a lengthening of the G1 phase, with all other phases of the cycle remaining constant, and has been observed to occur exclusively within neurogenic progenitor cell populations and not within proliferative populations (Durand & Raff 2000; Calegari et al. 2005). Effected through the action of G1-S phase cell cycle regulators, such as Tis21 and p27, this lengthening of the cell cycle suggests a method for the temporal regulation of cell fate decisions, as increased G1 length may potentially allow more time for various intrinsic or extrinsic cell fate determinants to stimulate successive rounds of neurogenic cell divisions (Calegari et al. 2005; Ohunuma et al. 2001; Calegari & Huttner 2003). Among these cell fate determinants, BMP and Wnt signalling play heavily in this re-organization process, regulating neural patterning along the dorsoventral axis of the neural tube, subsequently leading to region specific differentiation of the neuroepithelium (Temple 2001). Additionally, the notochord also produces the morphogen Sonic Hedgehog (SHH). A secretory product of the notochord, SHH acts to regulate gene expression through activation of GLI transcription factor responsive genes, via activation of the membrane bound G-protein receptor Smoothed. Activation of Smoothed results as SHH binds to its repressor Patched, releasing inhibition of Smoothed and leading to the activation and translocation of GLI transcription factors to the nucleus (Ruiz i Altaba et al 2002). Secretion of SHH by the notochord produces a concentration gradient of the morphogen within the neural tube which acts synergistically with BMP signalling and antagonistically against Wnt mitogen gradients to initiate formation of domains of specified cell differentiation across the neural tube (Wilson and Maden 2005; Robertson et al. 2004) In addition, patterning across the rostrocaudal axis of the neural tube is also occurs concurrently with patterning along the dorsoventral axis to create similar domains of specialized cell differentiation controlled largely through the influence of mitogens, like the MAPK signalling agonist Fibroblast Growth Factor (FGF) and retinoids like Tretinoin (Retinoic Acid - RA) (Duester

2008; Iwata and Henver 2009). Furthermore, working synergistically with morphogen signalling, neurotrophic factors, such as Brain-derived Neurotrophic Factor (BDNF) and Nerve Growth Factor (NGF) also facilitate neural differentiation and development. Released by the cells of the developing ectoderm and neural tube, these factors support neural organization and neural cell morphological development through promotion of neural cell proliferation, survival and migration via regulation of gene transcription through activation of signalling pathways such as the PI3K/Akt and MAPK signalling pathways (Bibel & Barde 2000). Working in unison, these factors act to promote neural cell fate and developmental decisions that ultimately lead the neural progenitor cells of the neural tube to become the fully differentiated cells that compose the adult nervous system.

In recent decades, observations of severe disturbances in neural cell differentiation, cell cycle progression and appropriate cellular organization of the brain, across a multitude of disorders, including TS, has provided strong support for assertions that such disorders may be caused in part by a misregulation of the aforementioned processes that govern neural development and cell fate decisions, ultimately resulting in the disease's unique pathology.

### **1.9: Misregulation of TSC Gene Function: Effects on Cell Differentiation, Development and Fate**

In addition to the clinical and histopathological evidence indicating an impairment of appropriate cellular differentiation in the cells of TS associated lesions (described in section 1.2), an array of studies conducted over the past two decades have found significant molecular evidence supportive of these findings. Several of these studies have observed a distinct alteration in appropriate cell development and differentiation both *in vitro* and *in vivo* (Rennebeck et al.1998), suggesting an essential role for TSC in the regulation of these processes.

Abnormalities in neural cell morphology have been acutely observed on a number of occasions, indicating an essentiality for TSC involvement in the events that govern neural cell development. Most notable among such experiments were studies conducted by Tavazoie and colleagues, who demonstrated that knockdown of either the TSC1 or TSC2 genes within a population of cultured post-mitotic hippocampal pyramidal neurons could lead to an increase in cell size. Additionally, they also observed that suppression of either of these genes could lead to a subsequent decrease in dendritic branching or arborisation (Tavazoie et al. 2005). They also noted the development of morphological abnormalities within the dendrites among the population of examined neurons, including aberrations in dendritic spine length and head shape, which could result in perturbations in synaptic signalling *in vivo*. Studies conducted by Floricel and colleagues further supported these findings, as *in vivo* suppression of TSC2 was found to result in a significant inhibition of neurite outgrowth in PC12h cells (Floricel et al 2007). In a seemingly contradictory manner to the observations of Floricel et al., Choi and colleagues observed disorganized or mislocalized axon formation upon TSC1/2 knockdown and suppression of axon formation when the genes were overexpressed, withinin developing cortical neurons (Choi et al. 2008). Studies conducted by Willdonger and colleagues supported the observations of Choi et al., demonstrating that overexpression of TSC1 or TSC2 could suppress axon formation, and knockdown could promote axon formation, within mouse and rat hippocampal neurons (Willdonger et al. 2008). While the mechanism underlying this effect is still under investigation, it has been reported that promotion of axonal growth due to TSC1/TSC2 inactivation is, at least in part, a result of upregulation of SAD (Synapse of the Amphid Defective) kinases (Willdonger et al. 2008). Recently, SAD kinase and its activator LKB1, itself an activator of the positive TSC regulator AMPK, have been implicated in regulation of neuronal polarity (Barnes et al. 2008). Importantly, it has also been observed that SAD kinases and LKB1 levels are

elevated in cortical tuber tissue samples taken from TS patients (Willdonger et al. 2008). The defects in cell size and axon/dendrite formation upon manipulation of TSC1/TSC2 may represent key physiological events regulating the formation of the CNS lesions found in TS. Therefore, elucidating the molecular pathways underlying these events is of utmost importance.

Beyond altering cellular morphology, mutation of the TS genes has also been implicated in altering cellular differentiation. McNeill and colleagues observed through the generation of TSC2 loss of function mutants in *Drosophila* that the subsequent preclusion of mTOR control results in precocious differentiation within photoreceptor neurons (McNeill et al. 2008). *In vivo* studies examining the consequence of TSC2 mutation have observed that within the Eker rat, a naturally occurring model organism possessing a germline TSC2 mutation that results in the loss of the carboxyl terminus of Tuberin, TSC2 homozygous mutants (-/-) suffer embryonic lethality at approximately day 10.5 of gestation and display dysraphia and papillary overgrowth of the embryonic neuroepithelium (Kobayashi et al. 1999; Rennebeck et al. 1998). Additionally, cortical neuron progenitor cells from embryonic day 14/15 mouse embryos induced to express a TSC2 shRNA, and subsequently organotypically cultured within cortical tissue sections, demonstrated disorganized axon orientation and exhibited the retarded axon/dendrite migration described by Shelley and associates as characteristic of neurons with ectopic axon formation (Choi et al. 2008; Shelley et al. 2007). Furthermore, *in vitro* studies investigating the involvement of mTOR in regulation of human embryonic stem cell (hESC) differentiation have observed that TSC1/2 levels are significantly elevated within hESCs, by comparison to differentiated cells. Additionally, these studies also observed elevated expression of mTORC2 by comparison to differentiated cells, as well as increased neuronal differentiation of hESCs following siRNA knockdown of TSC2 (Easley et al. 2010). These results, when examined together, suggest that the TSC and specifically Tuberin, as the primary functional component of the complex, may significantly influence neural



cell fate decisions and appropriate succession of developmental events that give rise to a normal neural phenotype.

### **1.10: Hypothesis and Objectives**

Given the demonstrated involvement of Tuberin with various regulators of cell fate and differentiation, and the apparent perturbations in appropriate neural cell fate decisions which result from Tuberin mutation or inactivation, I propose that Tuberin plays an important role in neural fate decisions at key points throughout development. I hypothesize that strict maintenance of appropriate levels and activity of Tuberin are essential for normal cell fate decisions to occur. To investigate this proposal, experimental focus was directed towards three primary objectives:

- 1) *To characterize the levels of Tuberin protein and mRNA, and activation of the mTOR pathway, during neural differentiation in vitro.*
- 2) *To characterize the levels of Tuberin protein and activation of the mTOR pathway, during neural development in vivo.*
- 3) *To develop tools to examine the effects of disruption of Tuberin expression on neural differentiation.*

Collectively, the objectives of this study are aimed at clarifying the relationship between Tuberin function/expression and the regulation of cell fate determination. This will provide a more comprehensive understanding of Tuberin's role in development, proliferation, and pathological processes.

## **CHAPTER 2**

### **2. Design and Methodology**

#### **2.1: Cell Culture and Neuronal Lineage Differentiation**

##### **SH-SY5Y Human Neuroblastoma Cells**

SH-SY5Y human neuroblastoma cells were obtained from the American Type Culture Collection (ATCC – Product #: CRL-2266). Cells (at or below passage 25) were propagated in Dulbecco's Modified Eagle's Medium (Sigma-Aldrich Co. – Product #: D5796) supplemented with Fetal Bovine Serum, to a 10% concentration (Sigma-Aldrich Co. – Product #: F1055), and a penicillin/streptomycin antibiotic solution, to a concentration of 0.25 µg/mL (GIBCO – Product #: 15140). Culture and differentiation of these cells was carried out on 60mm SUREGrip cell culture dishes (Sarstedt AG & Co. – Product #: 83.1801). Cells were maintained at 37°C in a 5% CO<sub>2</sub> environment. For passaging, as cells of this line may periodically remain in suspension during culture, all used growth media was collected to allow harvesting of all non-adherent cells. For cells growing adherently, trypsinization was used. 1X PBS was used to wash the cells prior to trypsinization to remove any residual traces of growth media. After washing, the entire culture was rinsed with 1-2 mL of a 10X Trypsin-EDTA solution (SH-SY5Y) (Sigma-Aldrich Co. - Product #: T4174), which was immediately removed via vacuum aspiration. Treated cells were then incubated at 37°C for 6 minutes to allow detachment of the adherent cells. Trypsin neutralization was conducted by washing with complete growth media following incubation. All trypsinized cells were then collected, in combination with the aforementioned non-adherent cells, pelleted via centrifugation at 1000 r.p.m and split at a 1:6 ratio for reseeding.

Neuronal differentiation of the SH-SY5Y cells was induced via the administration of a 1 mM solution of 13-cis retinoic acid (RA) (Sigma-Aldrich Co. – Product #: R3255), diluted in 100% ethanol and dimethyl sulfoxide to achieve the desired 1 mM concentration from the 1mg/mL

stock. Prior to neuronal differentiation, cells were allowed grow to approximately 60 - 70% confluence to allow for primary neurite development. A differentiation time course was constructed, with time points reflecting 0 (undifferentiated), 1, 2, and 3 (full differentiation) days of differentiation. A 2  $\mu$ M final concentration of RA was maintained within the media during the course of the experiment, with supplementary addition of RA at 48 hours following the initial administration. Full neuronal differentiation was confirmed by the development of extended neurite processes measuring at least 2x the diameter of the cell soma (Wright et al. 1997; Soucek et al. 1998; Simpson et al. 2001).

### **RN33B Rat Neuronal Precursor Cells**

RN33B neuronal cells were obtained from the American Type Culture Collection (ATCC - Product #: CRL-2825). Cells were cultured in a 1:1 mixture of Dulbecco's Modified Eagle's Medium and Ham's Nutrient Mixture F12 (Sigma-Aldrich Co. – Product #: D6421), supplemented with Fetal Bovine Serum to a 10% concentration (Sigma-Aldrich) and a penicillin/streptomycin antibiotic solution to a 0.25  $\mu$ g/mL concentration (GIBCO). Culture and differentiation of these cells was performed in a manner similar to SH-SY5Y protocols using 60mm SUREGrip cell culture dishes (Sarstedt AG & Co.). Cells were maintained at a culture temperature of 33°C in a 5% CO<sub>2</sub> environment. For passaging, cultured cells were rinsed 2-3 times with 1X PBS to remove residual growth media. Adherent cells were removed using a 0.25% Trypsin-EDTA solution (RN33B) (Thermo – Product #: SH30042.01) rinsed over the entire culture and removed immediately via aspiration. Cells were then incubated at 37°C for 5 minutes to allow detachment of adherent cells. Neutralization was completed using complete growth media following incubation. All trypsinized cells were collected via centrifugation at 1000 r.p.m and split at a ratio of 1:10 for reseeded.

Neuronal differentiation in the RN33B cells was induced via inactivation of the temperature sensitive mutant SV40 large T antigen gene via long-term incubation at 37°C. Cells were allowed to grow to approximately 60% confluence prior to differentiation to allow sufficient room for cell spreading during differentiation. During differentiation, complete growth media was exchanged for serum-free DMEM-F12 media (Sigma-Aldrich), supplemented with mixture of supportive factors modified from Bottenstein and Sato's N2 neuronal growth supplement, formulated to support neuronal progenitor survival (10 µg/mL Putrescine, 5 mM HEPES, 5 µg/mL Insulin, 5 µg/mL Transferrin, 0.012% Glucose, 0.125 µg/mL Sodium Selenite, 6.3 ng/mL Progesterone) (Bottenstein and Sato 1979, Pacey et al. 2006). Differentiation was conducted over a course of 6-8 days. Full neuronal differentiation was confirmed by separation and spreading of the cells, from their characteristic "clustered" growth pattern, in addition to the formation of extended neurite processes (Wright et al. 1997; Soucek et al. 1998; Simpson et al. 2001).

## **2.2: Whole Cell and Cellular Fraction Protein Extraction**

For analyses of total cell protein, cultured cells were first harvested utilizing trypsinization, collected via centrifugation and flash frozen or lysed immediately. Total protein was subsequently extracted by subjecting collected cells to a 0.1% NP40 lysis buffer (0.1% NP40; 0.05mM EDTA; 0.1 M NaCl; 0.02 M Tris (pH 7.5)) for 40 minutes on ice. This buffer was also supplemented with protease inhibitors at the following concentrations: 0.005 mg/mL aprotinin, 0.1 mg/mL leupeptin, and 0.005 mg/mL phenylmethylsulfonyl fluoride. Following incubation, the crude cell lysate was centrifuged at 10,000 rpm for 10 minutes at 4°C to separate the protein containing supernatant from the any extraneous non-proteinaceous cellular debris. Protein concentrations of the obtained lysates were measured via Bradford protein assay, in accordance

with the reagent manufacturers specifications (Sigma-Aldrich – Product #: B6916), using a BioMate 5 uv/vis spectrophotometer (Thermo – Product #: 9423BIO1202E).

For cell fractionation analyses, cultured cells were collected and pelleted via high speed centrifugation. Collected cells were subsequently washed with ice cold 1X PBS buffer and pelleted two times via centrifugation at 5000 r.p.m for 7 minutes. Following collection, cell pellets were treated with a sufficient volume of cell lysis buffer (Composition: 10 mM Tris (pH 7.5), 0.05% NP-40, 3 mM MgCl<sub>2</sub>, 1 mM EGTA, 10 uL/mL of 10 mg/mL PMSF, 1 uL/mL of 5 mg/mL leupeptin, 0.5 uL/mL of 10 mg/mL aprotinin, 10 uL/mL of 0.1 mM Dithiothrietol (DTT)), typically 5 times the volume of the packed cell pellet, on ice for 10 minutes. After incubation, re-suspended cells were aspirated through a 21-guage-needle 3 times and then collected via centrifugation at 5000rpm for 7 minutes at 4°C. Following centrifugation, the supernatant was stored as the cytoplasmic protein fraction, while the pellet was stored as the nuclear fraction. The collected supernatant was then centrifuged at 13000 rpm for 15 minutes, to remove any extraneous nuclear material, and subsequently stored at -80°C until required for immunoblotting. The collected nuclear pellet was then immersed within a wash buffer (Composition: 10mM PIPES (pH 6.8) buffer, 300mM Sucrose, 3mM MgCl<sub>2</sub>, 25mM NaCl, 1mM EGTA), upon which an equal volume of a 1M sucrose solution was gently layered. This was followed by two successive centrifugations at 5000rpm. The obtained pellet was then re-suspended in a digestion buffer (Composition: 10mM PIPES (pH 6.8), 250 unit/mL DNase, 300mM Sucrose, 50mM NaCl, 3mM MgCl<sub>2</sub>) and incubated on ice for 1 hour to obtain the nuclear protein fraction. Following incubation, DNA and associated proteins were eluted from the lysate via slow addition of a 2M NaCl buffer (Composition: 10mM PIPES (pH 6.8) buffer, 2M NaCl, 1mM EGTA) with gentle mixing to a final concentration of 1.6M NaCl. The resultant crude lysate was then centrifuged at 8000rpm and 4°C for 20 minutes to pellet any remaining debris. Following

centrifugation, the supernatant containing all soluble nuclear proteins was then collected and stored at - 80°C until required for immunoblotting.

### **2.3: Immunoblotting**

SDS-PAGE immunoblotting assays were conducted using equal amounts of protein for all loaded samples, measured and aliquoted from extracted lysates. Total protein used for these samples, however, was variable based on the individual experiment, with either 150 or 200ug of protein loaded. Following mixture with 4X sample buffer (40% Glycerol; 240mM Tris HCl, pH 6.8; 8% SDS; 0.04% Bromphenol Blue; 5% Beta-mercaptoethanol), prepared lysate samples were boiled for 5-10 minutes and subsequently centrifuged to collect any vapour condensates from the sides of the container. Samples were then run for protein separation on 7.5 or 10% denaturing polyacrylamide gels at 80 to 110 volts for 3 hours. At the conclusion of the run, the proteins were then transferred from the gel to a PVDF membrane (Fisher Scientific - Product #: PV4HYB0010), utilizing a wet transfer system, for 3.5 hours. Following transfer, PVDF membranes were incubated for 1 hour in a blocking solution containing powdered non-fat dry milk or bovine serum albumin (BSA), used at concentrations of 1, 2 or 5 % w/v, in TBST (TBS and 0.05% Tween 20). After blocking, membranes were incubated at 4°C overnight with antibodies directed against the target protein of interest (Antibody Dilutions: TSC2 (XP) - 1/1000; TSC2 (C20) - 1/500; p70S6K – 1/500; p70S6K (T389) – 1/250; Nestin – 1/250; MAP2 – 1/1000; Actin – 1/1000; Topoisomerase II $\beta$  – 1/1000;  $\alpha$ -Tubulin – 1/1000). Following incubation, membranes were washed in TBST for 30 minutes, in three 10 minute intervals, and were then incubated for 1 hour in a solution containing secondary antibody, prepared at a 1:10000 v/v dilution with the blocking solution. For developing and exposure following incubation, the membranes were washed a second time for 15 minutes, in three 5 minute intervals, and imaged using the Pierce

ECL Substrate (Thermo – Product #: 32106), in accordance with the manufacturer’s guidelines, and a FluorChem 9000 Imaging System (Alpha Innotech).

#### **2.4: Antibodies**

Antibodies used in these studies included: Tuberin (XP) (Cell Signaling – Product #: 4308), Tuberin (C20) (Santa Cruz – Product #: sc-893), Actin (Millipore – Product #: MAB1501R), Nestin (Santa Cruz – Product #: sc-21248), MAP2 (Santa Cruz – Product #: sc-56561), p-p70 S6 Kinase (T389) (Cell Signaling – Product #: 9234), p70 S6 Kinase (Abcam – Product #: ab9366), Topoisomerase II $\beta$  (Santa Cruz – Product #: sc-13059),  $\alpha$ -Tubulin (Santa Cruz – Product #: sc-8035), Donkey anti-goat IgG-HRP (Santa Cruz – Product #: sc-2020), anti-mouse IgG-peroxidase (Sigma-Aldrich Co. – Product #: A9917), and anti-rabbit IgG-peroxidase (Santa Cruz - Product #: sc-2020).

#### **2.5: Neurosphere Formation Assay**

Neurosphere formation assays were conducted, in a manner based on protocols established by Pacey et al. (2006), as an attempt to isolate and enrich the most stem-like cells within cultured SH-SY5Y and RN33B cell populations. Cells were initially grown in monolayer culture, to an approximate confluence of 70–80% on 60mm SUREGrip cell culture dishes (Sarstedt AG & Co. – Product #: 83.1801). Upon reaching the appropriate confluence, cells were trypsinized, using previously discussed methods, and collected via centrifugation at 1500 r.p.m, re-suspended in clean complete growth media and counted. If a sufficient concentration of cells was present, they were then seeded at a density of 25000 cells/mL in 2 mL of serum-free DMEM-F12 media (Sigma-Aldrich), supplemented with 10 ug/mL Putrescine, 5 mM HEPES, 5 ug/mL Insulin, 5 ug/mL Transferrin, 0.012% Glucose, 0.125 ug/mL Sodium Selenite, 6.3 ng/mL Progesterone (Pacey et al. 2006). Additionally, the cells were seeded onto ultra-low adherence

6-well culture plates (Corning – Product #: 3471) to promote sphere formation. Following seeding, the cells were returned to their normal culture temperatures (37°C for SH-SY5Ys, 33°C for RN33Bs) for 2 to 7 days to incubate and allow for sphere formation.

## **2.6: Quantitative Real-Time Polymerase Chain Reaction (qRT-PCR) mRNA Analysis**

Total mRNA was extracted from SH-SY5Y cells, RN33B cells and BALB/c neural tissues using the RNeasy Plus Mini Kit (Qiagen - Product #: 74134), as per manufacturers guidelines. Following extraction, cDNA synthesis was conducted using Superscript II Reverse Transcriptase (Invitrogen - Product #: 18064-014) to synthesize the antisense cDNA strand from the RNA template. mRNA and cDNA concentration and quality were subsequently measured using a NanoDrop Spectrophotometer (Thermo Scientific). Gene expression levels were assessed using the SYBR-Green qPCR method. PCR reactions were carried out in a final volume of 20 uL and were organized as follows: 10ul of SYBR-Green Master Mix (SA Biosciences Inc. - Product #: PA-012-24) was combined with 2 uL of the previously synthesized cDNA, 7 uL of nuclease-free water, and 1 uL of a 10 uM gene specific primer mixture containing forward and reverse primers designed against one of 5 gene targets. The primers designed for these assays were constructed using the NCBI Primer-Blast primer design tool (National Center for Biotechnology Information) and Primer Express 3.0 (Applied Biosystems) and were designed for human and rat variants of the following genes: TSC2, Nestin, GAP43, Oct 4 and GAPDH (Table 2). All primers were synthesized by a third party facility (Eurofins MWG Operon) and designed to span an exon-exon junction within each gene to prevent spurious amplification of genomic DNA. PCRs were conducted using an ABI 7300 Real Time PCR System (Applied Biosystems – Product #: 4345240). PCR cycling conditions for the 2-step PCR included: an initial, one repetition, 10 minute polymerase activation stage at 95°C; and a second 2-step, 60 repetition,



melting/annealing/extension stage, held first at 95°C for 15 seconds and then at 60°C for one minute. All reactions were conducted on 96-Well Clear Half-Skirt PCR Microplates (Axygen - Product #: PCR-96M2-HS-C). mRNA levels were analyzed through relative quantification study using the ABI 7300 System Sequence Detection Software v1.3 (Applied Biosystems) . Analysis of obtained C<sub>T</sub> values and mRNA quantification were conducted using the comparative C<sub>T</sub> method, with values represented as the mean log<sub>10</sub> RQ ± standard error (S.E.). Data analysis was conducted using Microsoft Excel (Microsoft).

**Table 2: Oligonucleotide Primers for Use in qRT-PCR**

qRT-PCR Primers: Human TSC2	For: 5' – GAGAGGAGCCGTGTTTTTGTG - 3' Rev: 5' – GACATGCCATGGCCTGGTA - 3'
qRT-PCR Primers: Human Nestin	For: 5' – AGAGGGGAATTCCTGGAG – 3' Rev: 5' – CTGAGGACCAGGACTCTCTA – 3'
qRT-PCR Primers: Human Oct 4	For: 5' – CTTGCTGCAGAAGTGGGTGGAGGAA – 5' Rev: 5' – CTGCAGTGTGGTTTCGGGCA – 3'
qRT-PCR Primers: Human GAPDH	For: 5' – GCACCGTCAAGGCTGAGAAC - 3' Rev: 5' – GGATCTCGCTCCTGGAAGATG - 3'
qRT-PCR Primers: Rat TSC2	For: 5' – CCGTGCTGGAAGCTGATGCGAA - 3' Rev: 5' – CCCAGAGCGCCATCCCAACAAA - 3'
qRT-PCR Primers: Rat Nestin	For: 5' – AAGCAGGGTCTACAGAGTCAGATCG - 3' Rev: 5' – GCTGTACAGGAGTCTCAAGGGTAT - 3'
qRT-PCR Primers: Rat Oct 4	For: 5' – TTGGGCTGGAGAGGGATGTGGT - 3' Rev: 5' – TTCCC CGGCCTCATACTCT - 3'
qRT-PCR Primers: Rat GAPDH	For: 5' – TGATGACATCAAGAAGGTGGTGAAG – 3' Rev: 5' – TCCTTGGAGGCCATGTGGGCCAT – 3'

## 2.7: BALB/c Neural Tissue Extraction

BALB/c (BALB/cAnNCrI) mice used in this study were purchased from Charles River Laboratories (Strain Code: 028) and were housed in the University of Windsor Animal Care facility prior to use, as per University of Windsor Animal Care Guidelines. Subjects selected for this study were chosen at specific dates, following conception, as they fit along a specified developmental time course comprised of the following dates: embryonic days 12, 14, 16 (16.5),

18 and post-natal days 2, 4, 7, 21 and 90. Prior to tissue harvesting selected subjects were euthanized using CO<sub>2</sub> gas asphyxiation administered at a 60% concentration within an isolation chamber, as mandated under the University of Windsor ethical research guidelines.

Tissue samples from the hippocampus, cerebral cortex, olfactory bulbs and cerebellum, as well as whole brain tissue samples, were harvested from the subject mice. These tissue samples were extracted from subjects surgically by making an initial incision through the skull, beginning at the base of the skull, at the occipital bone, continuing anterior along the superior sagittal sinus to the nasal bones. Additionally, two further lateral incisions were made in the skull, beginning from the initial midline incision, along the left and right transverse sinuses. All overlying dermal and bone tissue was subsequently removed and the brain was extracted by severing spinal attachment at the medulla. Hippocampal tissue samples were obtained by isolation of a portion of the hippocampal formation within a coronal section roughly 2 mm in thickness, approximately 1-2 mm anterior from the transverse sinus. Within the coronal section, the hippocampal formation was located inferior to the cerebral cortex and corpus callosum, adjacent to the lateral ventricles. Cerebral cortex tissues were also harvested from the same coronal section via isolating the portion of tissue superior to the corpus callosum. Olfactory bulb tissues were harvested by simply removing the olfactory bulbs from the anterior portion of the brain. Cerebellar tissue samples were collected by making a shallow oblique slice across the dorsal aspect of the cerebellum, avoiding the pons. All collected tissues were flash frozen via immersion in liquid nitrogen and subsequently stored at -80°C.

## **2.8: Cloning of Plasmid DNA Constructs**

TSC2 shRNA constructs directed against human TSC2 were synthesized utilizing the pLKO.1-TSC2 mammalian expression vector (Addgene – Product #: 15478). This vector is

designed to express shRNA oligonucleotide sequences under the control of the human U6 promoter and contains a Puromycin resistance gene for selection and screening within eukaryotic cells. The design of these vectors was based upon shRNA sequences originally designed and validated as part of the RNAi consortium (TRC) library, wherein oligonucleotide sequences identical to these would be inserted into a pLKO.1-puro backbone, which could be excised from the pLKO.1-TSC2 vector. Isolation of the pLKO.1-puro backbone was conducted using restriction enzyme digestion with the enzymes *AgeI* (Fermentas – Product #: FD1464) and *EcoRI* (Fermentas – Product #: ER0271) to remove the originally inserted TSC2 shRNA sequence from pLKO.1-TSC2. Following this, shRNA oligonucleotide sequences, synthesized by Eurofins (Eurofins MWG Operon), modeled on the TRC clone sequences (TRC Clone ID: TRCN0000040179, TRCN0000010455), and modified slightly to allow insertion between the unique *AgeI* and *EcoRI* restriction enzyme sites, were inserted (Table 3).

Prior to insertion, annealing of the lyophilized single stranded oligonucleotides, to form complementary double-stranded fragments, was done by diluting each oligonucleotide to a 200uM concentration in filter-sterilized DNase/RNase free water. Annealing reactions were then prepared using 5 uL of each oligonucleotide solution mixed with 2 uL of 10X Annealing Buffer (Composition: 100 mM Tris-HCl, pH 8.0; 10 mM EDTA, pH 8.0; 1M NaCl) and 8 uL of DNase/RNase free water. The reactions were then heated to 95°C for 4 min and allowed to cool slowly to room temperature. Insertion of the double stranded fragments into the pLKO.1 backbone was conducted through incubation of the vector backbone and double-stranded oligonucleotide insert with T4 DNA ligase (Fermentas – Product #: EL0011) and 10X T4 DNA Ligase Buffer (Fermentas – Product #: B69) for 16 hours at 4°C. Volumetric ratios employed for all ligations were calculated utilizing the equations outlined in (Cranenburgh 2004). Verification

of vector construction, for all pLKO.1 based vectors, was done through sequencing of each plasmid by a third-party sequencing facility (Robarts Research Laboratories).

**Table 3: pLKO.1 Vectors: TSC2 shRNA Oligonucleotide Sequences**

<p>pLKO.1-TSC2shRNA v.1</p> <ul style="list-style-type: none"> <li>• shRNA Oligonucleotide #1</li> <li>• TRCN0000010455</li> </ul>	<p>5'-CCGGTGCTCATCAACAGGCAGTTCTACTCGAGTAGAACTGCCTGTTGATGAGCG-3'</p>
<p>pLKO.1-TSC2shRNA v.2</p> <ul style="list-style-type: none"> <li>• shRNA Oligonucleotide #2</li> <li>• TRCN0000040179</li> </ul>	<p>5'-CCGGTCAATGAGTCACAGTCCTTTGACTCGAGTCAAAGGACTGTGACTCATTGG-3'</p>

Murine TSC2 shRNA plasmids directed against rat TSC2 were constructed utilizing the pLB mammalian expression vector backbone (Addgene – Product #: 11619). This vector is designed to express shRNA oligonucleotides under the control of the mouse U6 promoter and also contains an eGFP marker gene, under the control of the CMV promoter, for screening and selection purposes. Constructs were produced by inserting one of two oligonucleotide sequences designed against the NCBI catalogued sequence of rat TSC2 between the HpaI and XhoI restriction enzyme sites of the GFP-tagged pLB backbone, following excision of the native DNA fragment in this region via restriction enzyme digest with the enzymes HpaI (Fermentas – Product #: ER1051) and XhoI (Fermentas – Product #: ER0691) (Table 4). Annealing of single stranded oligonucleotides to produce double-stranded fragments and ligation of double-stranded fragments to the pLB vector back bone was conducted as outlined above. Polyethylene glycol (PEG 4000) (Bio Basic Inc. – Product #: pb0431-500G) was also used here to increase ligation efficacy. In addition to the shRNA vectors, a control vector was also produced, using an identical methodology, containing a scrambled oligonucleotide sequence (Table 3) for use as a negative control in further experiments.

**Table 4: pLB Vector: TSC2 shRNA Oligonucleotide Sequences**

pLB-TSC2shRNA v.1 • shRNA Oligonucleotide # 1	5'-AACGCTCCATTACAAGCATGGCTATTCAAGAGATAGCCATGCTTGAATGGAGCC-3'
pLB-TSC2shRNA v.2 • shRNA Oligonucleotide # 2	5'-AACGGTGAATGCGGCCTCAACAATTTCAAGAGAATTGTTGAGGCCGCATTACCCC-3'
pLB-shRNA Control • shRNA Oligonucleotide #3	5'-AACGTCTGGAGATGGCCAACATATTCAAGAGATATGTTGGCCATCTCCAGGACC-3'

Screening for appropriate pLB vector construction was done through polyacrylamide gel electrophoresis. Constructed plasmid samples were digested for 2 hours using XbaI and XhoI restriction enzymes and run in comparison to the pLB vector backbone, also digested with XbaI/XbaI, on an 8% non-denaturing polyacrylamide gel at 100V for 1 hour. Vector construction was also confirmed by sequencing of the constructed plasmids (Robarts Research Laboratories).

## 2.9: Testing and Expression of shRNA Vectors

### Transfection

Transfections were initiated 24 hours following seeding at a point when cultures had attained approximately 50-70% confluence. Similar methods were used to transfect both the SH-SY5Y and RN33B cell lines using one of three different transfection reagents: Polyethyleneimine (PEI), Lipofectamine LTX (Invitrogen – Product #: 15338-100) or Fugene HD (Promega – Product #: E2311).

PEI transfections were conducted by first preparing 1 mL reactions containing 2-15 µg/mL of plasmid DNA, 10-25 µg/mL of PEI and complete growth media (SH-SY5Y: DMEM; RN33B) DMEM/F12) as needed. Following this, each reaction was allowed to incubate at room temperature for 10 minutes and added drop-wise to cultures grown on either 6 or 10 cm cell culture dishes, resulting in final PEI concentrations between 1.25 and 6.25 µg/mL. Transfection incubation times ranged from 4-48 hrs. Recovery following transfection was typically allowed to

continue for 8 hours, times were varied between 8 – 48 hours to allow for or observe effects on protein expression. Following recovery, transfected cells were harvested for protein extraction via previously outlined means (see section 2.2)

Lipofectamine transfections were performed in accordance with the manufacturer recommendations (Invitrogen). However, transfections were scaled up, from a 24-well plate preparation to a 6 cm dish preparation, in order to provide a protein sample of sufficient concentration for use in subsequent western blot analyses. Transfections were conducted by first diluting 2.5 – 10 µg of DNA in 250 µL of clean serum free media (SH-SY5Y: DMEM; RN33B: DMEM/F12). Following dilution, 2.5 µL of PLUS reagent, diluted in 25 µL of serum-free media, was then added to the DNA mixture and incubated for 5 minutes. After incubation, 6.25 µL of the Lipofectamine LTX reagent, diluted in a further 250 µL of serum-free media, was added then mixed thoroughly with the DNA-PLUS mixture and incubated for 30 minutes to allow formation of DNA-lipid complexes. Once incubated, the reaction mixture was added drop wise to each dish, containing 2 mL of clean serum-free media. Transfections were allowed to continue for 4 – 48 hours. At which time cells were typically allowed to recover for 8 hours, but recovery times were varied between 0 – 48 hours to observe effects on protein expression. Harvesting of transfected cells was subsequently carried out at outlined previously (see section 2.2)

Fugene HD transfections were conducted using various “reagent to DNA” ratios, wherein 6 - 18 µL of the Fugene HD reagent and 1.5 – 6 µg of DNA were added to a sufficient volume of clean, antibiotic-free growth media (SH-SY5Y: DMEM; RN33B: DMEM/F12) to bring the total reaction volume to 3 mL. Once prepared, the mixtures were then vortexed and allowed to incubate for 10 minutes, following which 150 – 300 µL was added to each well of a 6 well plate, containing 3 mL growth media at final volume. The transfected cells were then incubated for 16 or 24 hours and following transfection were allowed to recover for 8 – 24 hours. Following

recovery, transfected cells were harvested for protein extraction via previously outlined means (see section 2.2).

### **Lentiviral Infection**

Lentiviral infections of RN33B and SH-SY5Y cells were conducted / attempted using a number of plasmid vectors, including those constructed for the purposes of this study and some previously constructed or obtained commercially (Table 5). Production of VSV-G pseudotyped lentivirus was carried out through transient transfection of HEK 293 Lenti X cells with the aforementioned plasmids and the packaging plasmids pMDG, pMDL2 and pRSV using polyethyleneimine (PEI) in a 1:3 DNA to PEI ratio. Cells were incubated for 5 hours at 37°C following transfection. Virus collection was carried out 24 hours following the initial transfection and collected virus samples were concentrated for 3 hours at 4°C via ultracentrifugation. Viral titres were determined through transduction of 293T cells and subsequent analysis of eGFP protein expression by flow cytometry 72 hours post-transduction. Titled virus was filter-sterilized and stored at -80°C. Lentiviral samples used possessed a titre of ranging from 1 - 2 x 10<sup>7</sup> TU/mL.

**Table 5: Plasmid Vectors Used in Transfection/Infection Trials**

<b><u>Cell Line / Species</u></b>	<b><u>Plasmid Vector (Origin)</u></b>
<b>SH-SY5Y / Human</b>	<ul style="list-style-type: none"> <li>• pCMV-TSC2 mlu-</li> <li>• pLKO.1-TSC2 (Addgene – Product#: 15478)</li> <li>• pLKO.1-TSC2shRNA v.1 (Constructed)</li> <li>• pLKO.1-TSC2shRNA v.2 (Constructed)</li> <li>• pLKO.1-Scrambled (Porter Lab)</li> </ul>
<b>RN33B / Rat</b>	<ul style="list-style-type: none"> <li>• pLB-TSC2shRNA v.1 (Constructed)</li> <li>• pLB-TSC2shRNA v.2 (Constructed)</li> <li>• pLB-shRNAControl (Constructed)</li> </ul>

For RN33B cells, cells to be infected were seeded on 24 well plates (Sarstedt AG & Co. – Product #: 83.1836)) at a density of  $7 \times 10^4$  cells/well. 24 hours following seeding, when the cells had reached an assumed density of  $3 \times 10^5$  cells/well, they were infected using MOI's of 2, 2.5, 5, or 10. Infections were carried out using growth media composed of a 1:1 mixture of Dulbecco's Modified Eagle's Medium and Ham's Nutrient Mixture F12 (Sigma-Aldrich), supplemented with a 10% concentration of Fetal Bovine Serum (Sigma-Aldrich), but lacking penicillin/streptomycin. Each infection was also supplemented with a 4 mg/mL concentration of polybrene (Santa Cruz – Product #: sc-134220) to enhance infection efficacy. Infected cultures were incubated for 24 hours at 37°C in the presence of the lentivirus, at which time the infection media was exchanged for clean complete growth media. When cells had reached approximately 70% confluence, they were trypsinized and transferred to 60 mm culture dishes and were subsequently allowed to recover for up to 2 weeks to allow sufficient time for population expansion and shRNA expression. Infection efficiency was assessed observationally through visualization of GFP fluorescence and measurement of the approximate proportion of fluorescing cells across several fields of view. Fluorescence imaging was done using an Olympus CKX41 Inverted Microscope (Olympus Canada Inc. – Product #: CKX41). Cultures were viewed at 20x objective magnification using an Olympus 20X UIS lens (Olympus Canada Inc. - Product #: LUCPLFLN20XPH). Image acquisition was conducted using a Q Imaging Micropublisher 3.3 RTV camera (Q Imaging – Product #: MP3.3-RTV-CLR-10). Image processing was conducted using the Q Capture Pro version 6.0 image processing software (Q Imaging).

For SH-SY5Y cells, cells to be infected were seeded on 24 well plates (Sarstedt AG & Co.) most frequently at a density of  $7 \times 10^4$  cell/well. Upon reaching a cell density of  $3 \times 10^5$  cells/well, approximately 48 hours following seeding, the cells were then infected at using Multiplicity of Infection (MOI) ratios of 1, 2, 3, 5 or 10. Infections were carried out using growth media



composed of antibiotic-free Dulbecco's Modified Eagle's Medium (Sigma-Aldrich), supplemented with a 10% concentration of Fetal Bovine Serum (Sigma-Aldrich). Infections were typically supplemented with a 2-4 mg/mL concentration of polybrene (Santa Cruz), however, some infections were conducted in the absence of polybrene (Santa Cruz). Incubation times during infection were variable, ranging from 4 to 24 hours, at 37°C and 4% CO<sub>2</sub>. Following infection, fresh complete growth media added in exchange for the infection media, and all cells observed in suspension were discarded with this media as a precautionary measure to limit contamination of the workspace. Puromycin, to a 1 µg/mL concentration, was subsequently added to the recovering cultures to select for infected cells and was maintained in culture until cell death within the uninfected control cultures was apparent.

## **2.10: Analytical Methods**

### **Densitometric Analyses**

Densitometric analysis was conducted through the use of the FluoroChem HD2 version 6.0.0 (Alpha Innotech) analysis software. TIFF (Tagged Image File Format) images, representing developed PVDF membranes, were captured and examined using the software's Spot Denso feature, to obtain Raw IDV-Average data values for each specified protein. For each protein of interest, these values were corrected against the IDV-Average values obtained for its respective endogenous control (e.g: Target-IDV / Control-IDV). Following this, the values were normalized using Log 10 transformation.

### **Statistical Analyses**

Evaluation of western blot data was conducted using the Log 10 transformed densitometry data. All statistical analyses were conducted using the Microsoft Excel 2007 statistical analysis package. Analysis of changes between individual time points were carried out using paired two sample Student's T-tests. Two-way ANOVA was also used to compare protein

level changes, across full time courses, between selected markers. Linear regression analyses, assessing protein level changes across time, were used to evaluate trend changes across each differentiation / developmental time course. Spearman's correlation analysis was used to compare time course trends between proteins.

## **Chapter 3**

### **3. Results and Analysis**

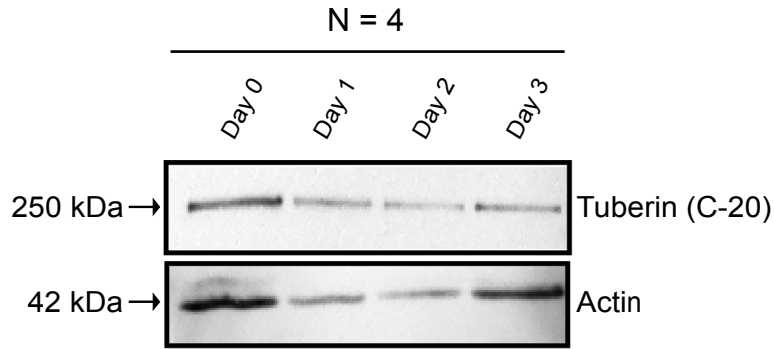
#### **3.1: Tuberin expression levels are regulated during neuronal cell differentiation**

In order to examine the protein expression patterns for Tuberin during neuronal cell differentiation, human SH-SY5Y cells and Rat RN33B cells were stimulated to undergo *in vitro* neuronal differentiation, using exposure to 13-cis-retinoic acid and adjustment of culture temperature of from 33°C to 37°C, respectively. SH-SY5Y and RN33B cells were used for this study, and subsequent other studies, to allow for a more representative observation of Tuberin expression dynamics during mammalian neuronal differentiation, through observation of these dynamics within neuronal progenitor cell types possessing unique species and developmental origins. Immunoblotting analyses for SH-SY5Y protein lysates were conducted across a 3 day differentiation time course, beginning from an undifferentiated state at Day 0 to full differentiation at Day 3 (Figure 4A). RN33B immunoblotting assays were observed over a 6 day time course, beginning from an undifferentiated state at Day 0 to full differentiation at Day 6 (Figure 4C). Neuronal differentiation was determined through neurite to cell soma length ratio measurement (Wright et al. 1997; Soucek et al. 1998, Simpson et al. 2001). SH-SY5Y Tuberin levels displayed a significant and consistent decrease across the 3 day differentiation course, as indicated through regression analysis ( $p = 0.0469$ ;  $\alpha = 0.05$ ) (Figure 4B). RN33B levels, on the other hand, were not found to display any significant changes across the 6 day course (Figure 4D).

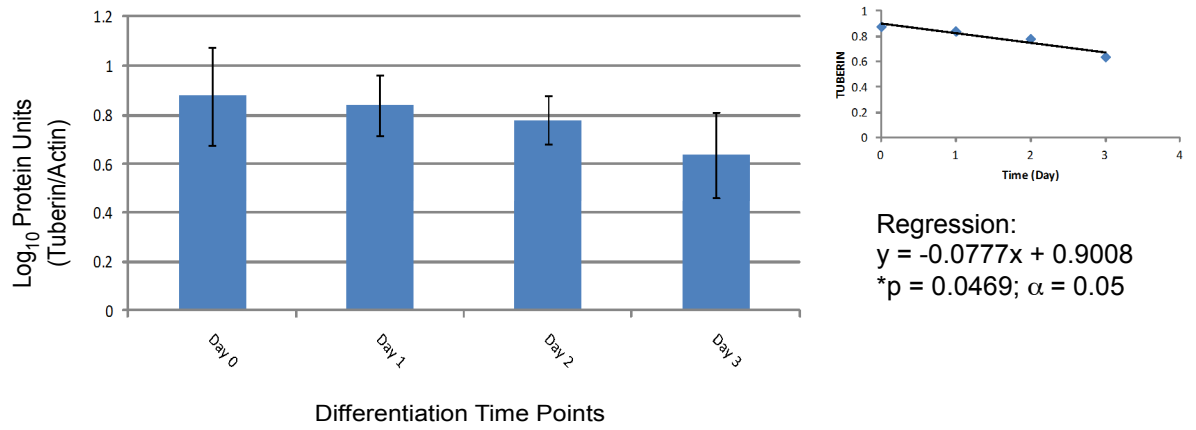
SH-SY5Y Tuberin levels were also measured over a shorter 24 hour differentiation time course, to determine if the previously noted decrease in levels was also apparent on a shorter time scale (Figure 5A – Top). Tuberin levels remained constant through this time course (Figure 5B). mTOR activity, through measurement of p70S6K phosphorylation at the mTORC1-specific

activating phosphorylation site T389, was also assessed as one indicator of Tuberin activity (Figure 5A). Phosphorylation of p70S6K was significantly increased across the 24 hour period, suggesting a potential decrease in Tuberin activity during this time ( $p = 0.00022$ ;  $\alpha = 0.05$ ) (Figure 5C). The differentiation state of these cells was also assessed through measurement of MAP2 protein levels, it was noted that MAP2 levels followed the pattern of Tuberin levels, but did not significantly change during the time course of differentiation (Figure 5D).

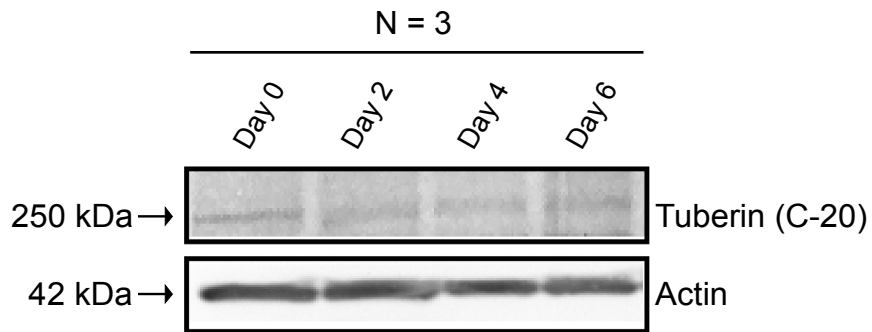
A)



B)



C)



D)

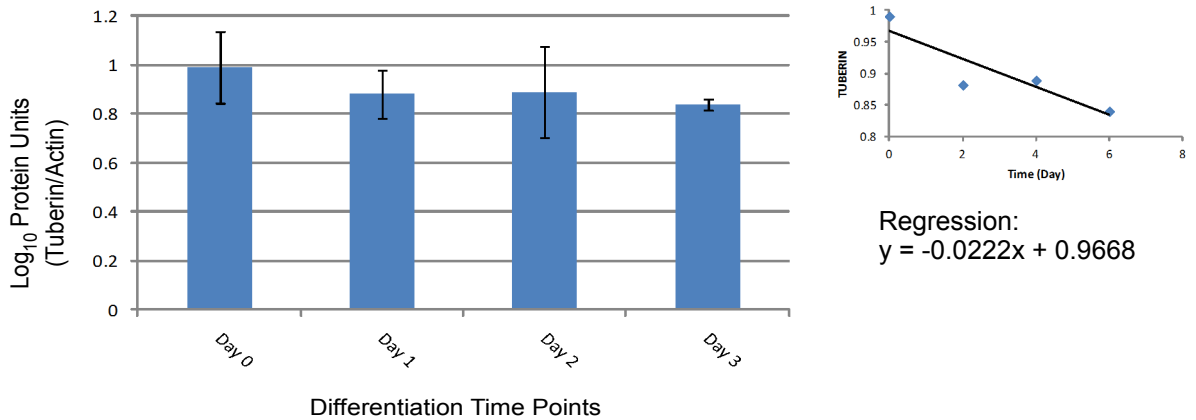


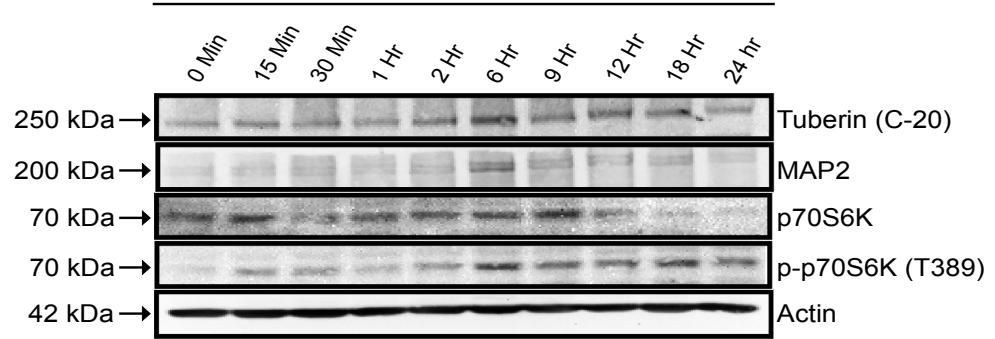
Figure 4 - 55

**Figure 4** *Endogenous levels of Tuberin demonstrate steady down-regulation during induced in vitro neuronal differentiation in human SH-SY5Y cells, but not in rat RN33B cells.*

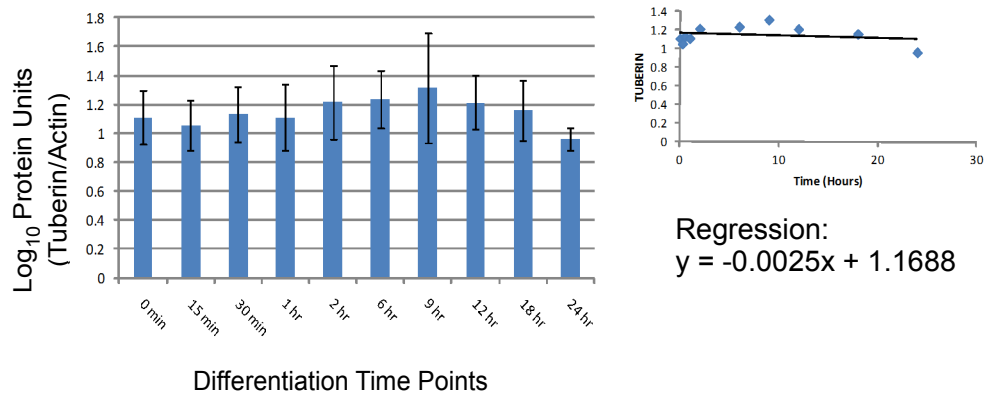
Cultured SH-SY5Y (A & B) and RN33B cells (C & D) were stimulated to differentiate over 3 day and 6 day differentiation time courses, respectively. Protein samples were collected at 0, 1, 2 and 3 days of differentiation for SH-SY5Y cells and 0, 2, 4, and 6 days of differentiation for RN33B cells. Comparison of protein expression between individual time point samples was conducted using spot densitometry analysis. Densitometry values (Y-axis) represent the  $\text{Log}_{10}$  transformed values of corrected Tuberin optical density (OD) values ( $y$ ), where  $y = (\text{Tuberin OD} / \text{Actin OD})$ . **A)** Tuberin levels (250 kDa - Top) were assessed through western blot analysis conducted using 150  $\mu\text{g}$  of protein loaded equally across all lanes. Actin (42 kDa - Bottom) is shown here as a loading control. Proteins were resolved on 7.5% denaturing polyacrylamide gels using SDS-PAGE, (Replicates: N=4). **B)** Graphical representation of densitometry analysis. Statistical analysis was conducted using linear regression of Tuberin level vs. Time ( $R^2 = 0.908$ ;  $p = 0.0469$ ;  $\alpha = 0.05$ ). **C)** Tuberin levels (Top) were assessed through immunoblotting analysis using 200  $\mu\text{g}$  of protein loaded equally across all lanes. Actin (Bottom) is shown here as a loading control. Protein lysates were analyzed through SDS-PAGE, using a 7.5% denaturing polyacrylamide gel (Replicates: N=3). **D)** Graphical representation of densitometry and regression analyses are depicted.

A)

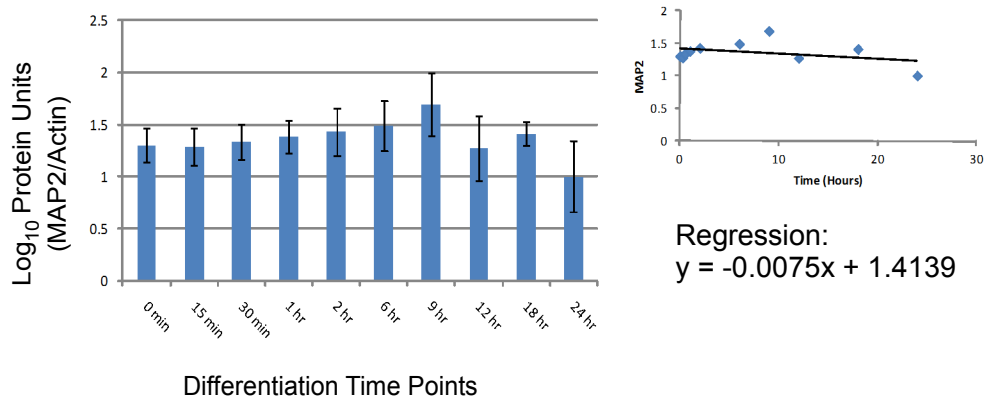
N = 3 (Tuberin, MAP2);  
N = 2 (p70S6K, p-p70S6K)



B)



C)



D)

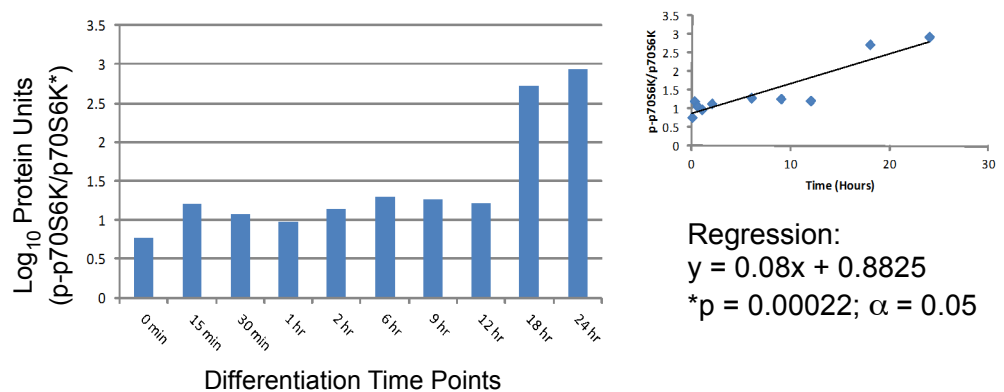


**Figure 5** Regulation of Tuberin activity levels occurs during the first 24 hours of induced *in vitro* neuronal differentiation in human SH-SY5Y cells.

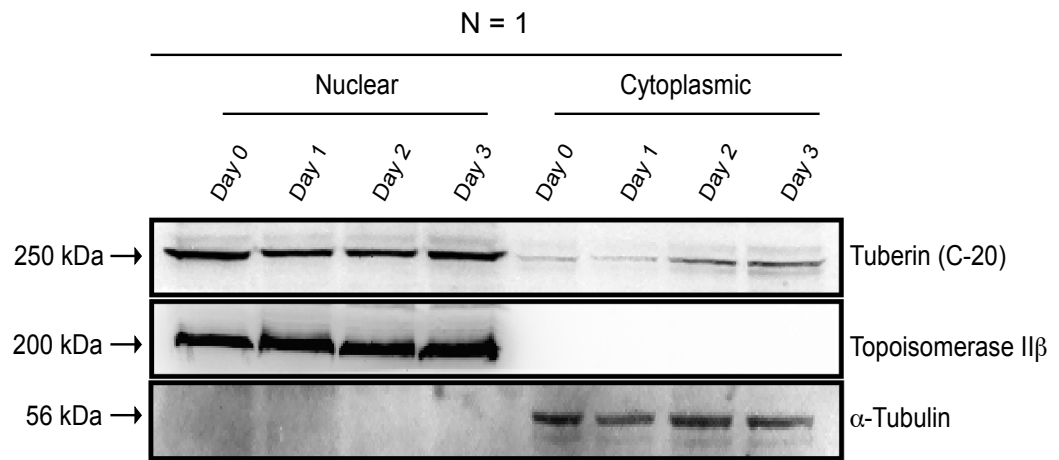
Cultured SH-SY5Y cells were stimulated to differentiate over a 24 hour differentiation time course. Protein samples were collected across a 24 hour period, following the onset of differentiation, at the time points indicated along the X axes. **A)** Immunoblotting for Tuberin, MAP2, and p-p70S6K levels was conducted using 150  $\mu$ g of protein loaded equally across all lanes. p70S6K & Actin are shown here as controls. Proteins were resolved on 7.5% denaturing polyacrylamide gels using SDS-PAGE (Replicates: N=3 - Tuberin, MAP2; N=2 - p-p70S6K). **B-D)** Comparison of protein expression between individual time point samples was conducted using spot densitometry analysis. **B & C)** The densitometry values (Y-axis) for Tuberin and MAP2 represent the  $\text{Log}_{10}$  transformed values of corrected protein optical density values ( $y$ ), where  $y = (\text{Protein OD} / \text{Actin OD})$ . **D)** p-p70S6K densitometry values represent the  $\text{Log}_{10}$  transformed values of corrected p-p70S6K optical density values ( $y$ ), where  $y = ((\text{p-p70S6K OD} / \text{Actin OD}) / (\text{p70S6K OD} / \text{Actin OD}))$ .



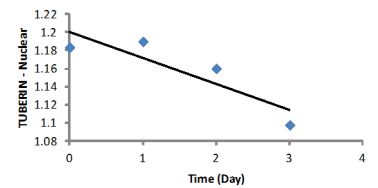
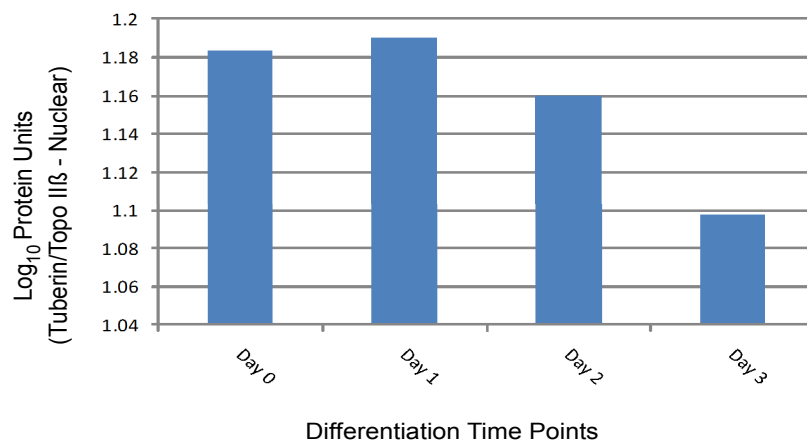
### **3.2: Tuberin levels do not change significantly based on cellular localization during neuronal cell differentiation**

Tuberin protein levels were seen to decline during neuronal differentiation for whole cell protein extracts in SHSY-5Y cells (Figure 4 A & B). To determine whether these differences in expression also influenced the cellular localization of Tuberin, or occur selectively in one cellular compartment during the course of neuronal cell differentiation, cell fractionation was performed and protein levels measured. Retinoic acid treated SH-SY5Y cells were incubated and allowed to differentiate across a 3-day differentiation time course (Figure 6). Interestingly, while repeats are required to determine statistical significance, levels of Tuberin declined uniquely in the nuclear compartment and were in fact increasing in the cytoplasmic compartment. RN33B cells, stimulated to differentiate across a 6 day time course, were also used to investigate the effect of localization (Figure 7). As with whole cell lysates, levels appeared to be relatively stable in both the nuclear and cytoplasmic compartments of this cell line during differentiation (Figure 7C, D). These results support observations that Tuberin is expressed in both the nuclear and cytoplasmic compartments of both cell lines tested during neuronal differentiation; and that levels were only selectively modulated in the nuclear compartment of one of these cell lines.

**A)**

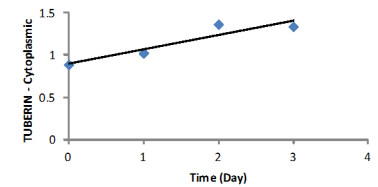
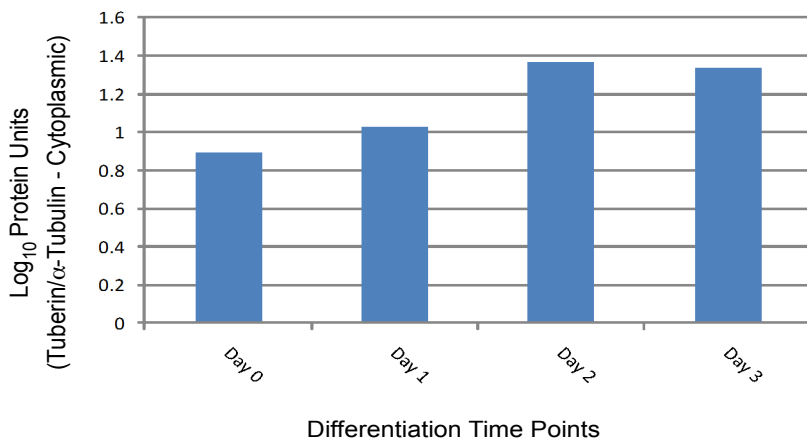


**B)**



Regression:  
 $y = -0.0287x + 1.2007$

**C)**



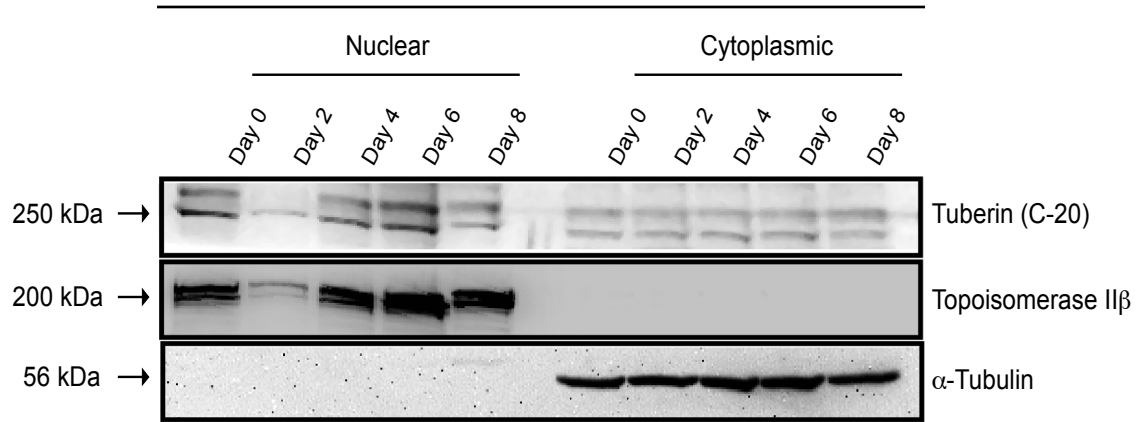
Regression:  
 $y = 0.1686x + 0.902$

**Figure 6** *Reduced levels of Tuberin protein occur in the nuclear compartment of SH-SY5Y cells.*

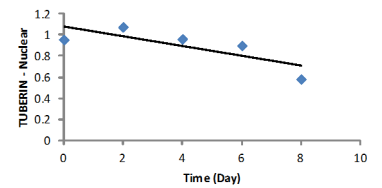
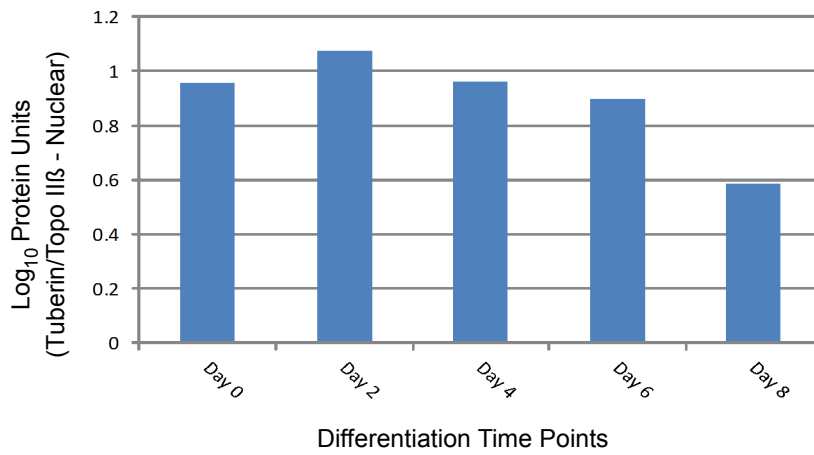
Human SH-SY5Y neuroblastoma cells were cultured in the presence of 13-cis retinoic acid to stimulate neuronal differentiation over a 3 day differentiation time course. Nuclear and cytoplasmic protein fractions were collected from harvested SH-SY5Ys and analysed, via Western blotting, at the following differentiation time points: Day 0, Day 1, Day 2 and Day 3. **A)** Immunoblotting for nuclear (Left) and cytoplasmic Tuberin (right) was conducted using 100 µg of protein loaded equally across all lanes. Topoisomerase IIβ (Topo IIβ) (Panel 2) and α-Tubulin (Panel 3) were used as nuclear and cytoplasmic fractionation controls, respectively. Proteins were resolved on 10% denaturing polyacrylamide gels using SDS-PAGE (Replicates: N=1). **B - C)** Quantitative analyses of Tuberin levels, for both nuclear (B) and cytoplasmic (C), protein fractions were conducted using spot densitometry. Densitometry values (Y-axis) for Tuberin here represent the  $\text{Log}_{10}$  transformed values of corrected protein optical density values ( $y$ ), where  $y_{\text{nuclear}} = (\text{Tuberin OD} / \text{Topoisomerase II}\beta \text{ OD})$  or  $y_{\text{cytoplasmic}} = (\text{Tuberin OD} / \alpha\text{-Tubulin OD})$ . Statistical analysis was conducted using linear regression of Tuberin level vs. Time. Results indicate an  $n=1$ ; repeats are required to determine statistical significance.

**A)**

N = 2 (Nuclear); N = 1 (Cytoplasmic)

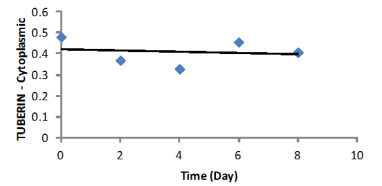
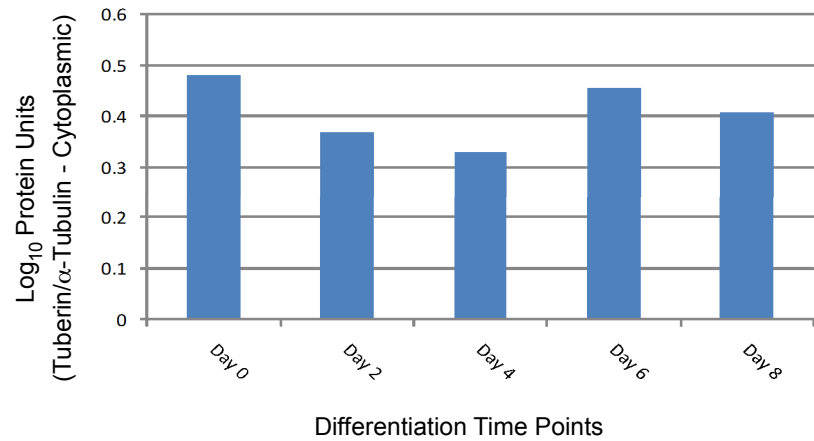


**B)**



Regression:  
 $y = -0.0459x + 1.0784$

**C)**



Regression  
 $y = -0.003x + 0.4202$

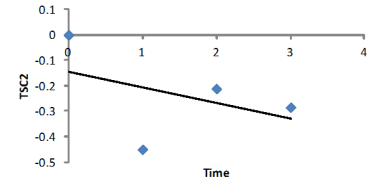
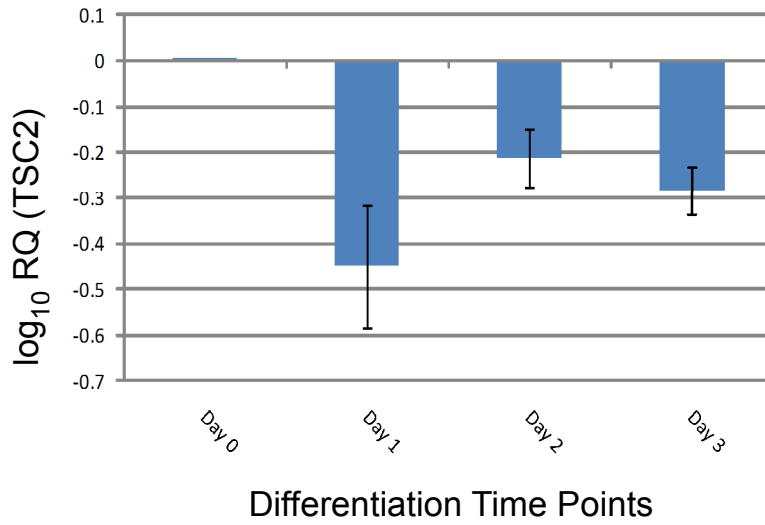
**Figure 7** *Tuberin protein levels are ubiquitous in cellular fractions of RN33B cells during neuronal differentiation.*

Stimulated to differentiate along across an 8 day time course, Rat RN33B cells were harvested for protein analysis at the following time points: Day 0, Day 2, Day 4, Day 6 and Day 8. Protein extracts from the nuclear and cytoplasmic cellular fractions were collected and analysed via Western blotting. **A)** Immunoblotting for nuclear (Left) and cytoplasmic Tuberin (Right) was conducted using 100 µg of protein loaded equally across all lanes. Topoisomerase IIβ (Topo IIβ) (Panel 2) and α-Tubulin (Panel 3) were used here as nuclear and cytoplasmic fractionation controls, respectively. Proteins were resolved through SDS-PAGE, using 10% denaturing polyacrylamide gels. (Replicates: N=2). **B - C)** Quantitative analyses of Tuberin levels, for both nuclear and cytoplasmic, protein fractions were conducted using spot densitometry. Densitometry values (Y-axis) for Tuberin here represent the  $\text{Log}_{10}$  transformed values of corrected protein optical density values ( $y$ ), where  $y_{\text{nuclear}} = (\text{Tuberin OD} / \text{Topoisomerase II}\beta \text{ OD})$  or  $y_{\text{cytoplasmic}} = (\text{Tuberin OD} / \alpha\text{-Tubulin OD})$ . Statistical analysis was conducted using linear regression of Tuberin level vs. Time.

### 3.3: Regulation of TSC2 mRNA levels during neuronal differentiation

With the observation that Tuberin protein levels were undergoing regulation during the course of neuronal differentiation, further investigation was conducted to examine whether regulation in TSC2 expression was also occurring at the mRNA level. QRT-PCR analysis of total TSC2 mRNA levels was conducted for both SH-SY5Y (Figure 8) and RN33B cells (Figure 9) to assess changes during neuronal differentiation. 13-cis retinoic acid stimulated SH-SY5Y cells were differentiated across 3 day and 24 hour time courses. Across the 3 day time course, mean TSC2 mRNA levels failed to demonstrate significant changes in mRNA levels (Figure 8A). Throughout the 24 hour time course, however, mean TSC2 mRNA levels displayed a biphasic pattern of expression, with a significant overall decrease in levels, as indicated through regression analysis ( $R^2 = 0.5711$ ,  $p = 0.0300$ ,  $\alpha = 0.05$ ) (Figure 8B). Temperature-stimulated RN33B cells were also examined across 6 day and 24 hour differentiation time courses (Figure 9). Across the 6 day time course, mean TSC2 mRNA displayed no significant changes (Figure 9A). Similarly, mRNA levels measured across the 24 hour time course also did not demonstrate any significant changes (Figure 9B). Thus, despite the changes observed across the SH-SY5Y 24 hour differentiation course, TSC2 mRNA levels appear to remain relatively stable during differentiation.

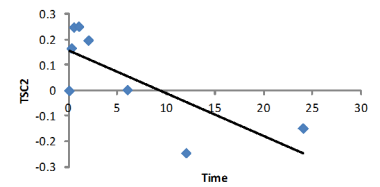
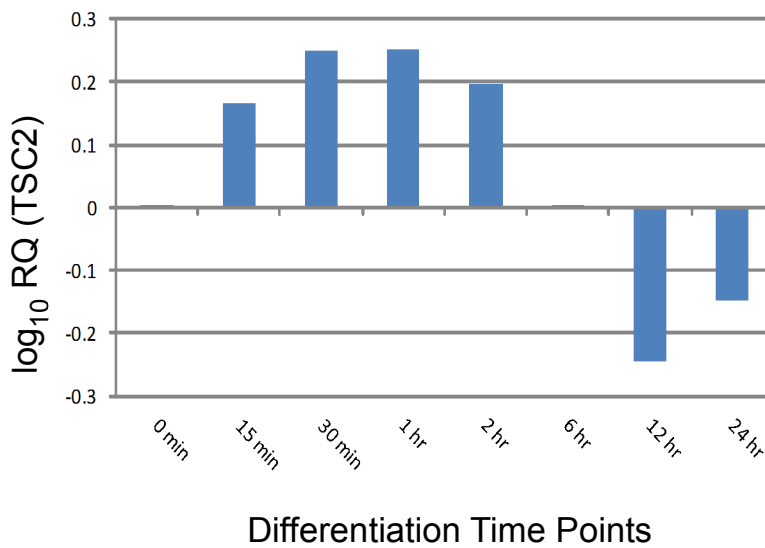
A)



Regression:  
 $y = -0.0615x - 0.1441$

N = 3

B)



Regression:  
 $y = -0.0168x + 0.1553$   
\*p = 0.0301,  $\alpha = 0.05$

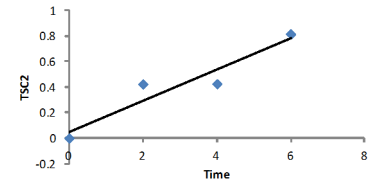
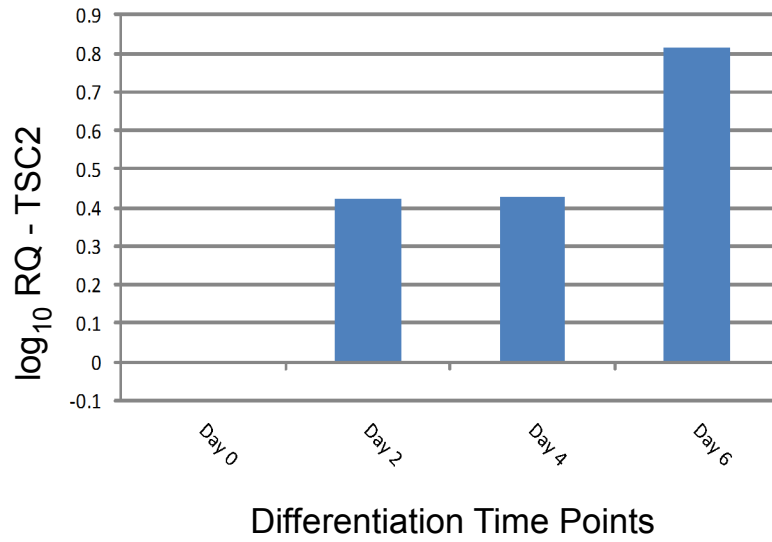
N = 2

**Figure 8** *TSC2 mRNA levels are not regulated across full neuronal differentiation in SH-SY5Y cells*

SH-SY5Y neuroblastoma cells were stimulated with 13-cis retinoic acid to differentiate across 3 day **(A)** and 24 hour **(B)** time courses. Total mRNA was extracted from cell samples collected at the indicated time points and QRT-PCR analysis conducted. mRNA levels are presented as the calculated mean  $\log_{10}$  RQ values for each time point (Y-axis), with error bars indicating the standard error. Target mRNA expression levels were normalized to GAPDH, calibrated using T = 0 (Day 0 or 0 minute) mRNA levels as the internal calibrator and are represented in relation to T = 0 levels. **A)** TSC2 mRNA levels across the 3 day time course (Replicates: N = 3). **B)** TSC2 mRNA levels across the 24 hour time course (Replicates: N = 2). Statistical analysis was conducted using linear regression of TSC2 mRNA level vs. Time ( $R^2=0.571$ ;  $p = 0.0301$ ;  $\alpha = 0.05$ ).



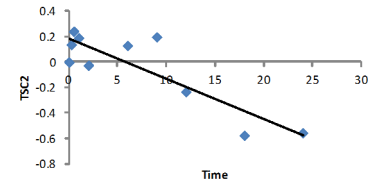
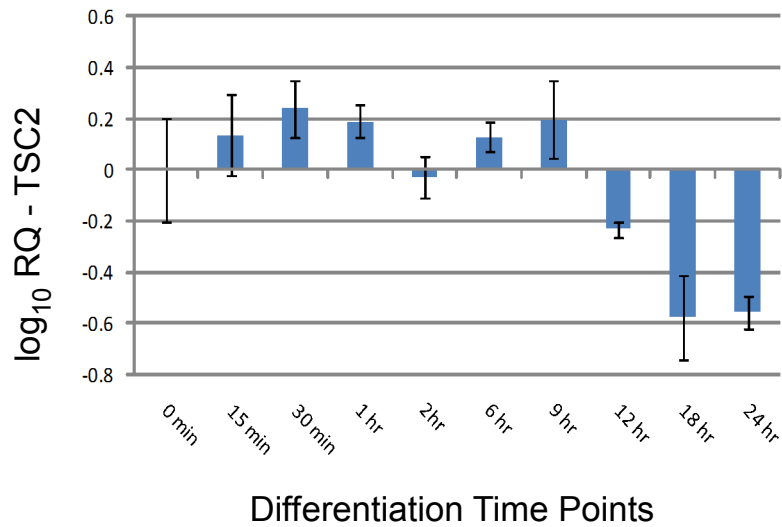
A)



Regression:  
 $y = 0.1227x + 0.048$

N = 2

B)



Regression:  
 $y = -0.0315x + 0.1798$

N = 3

**Figure 9** *TSC2* mRNA levels do not undergo regulation during neuronal differentiation in RN33B cells

RN33B cells were temperature stimulated to differentiate across 6 day **(A)** and 24 hour **(B)** time courses. Total mRNA was extracted from cell samples collected at the indicated time points and QRT-PCR analysis conducted. mRNA levels are presented as the calculated mean  $\log_{10}$  RQ values for each time point (Y-axis), with error bars indicating the standard error. Target mRNA expression levels were normalized to GAPDH, calibrated using T = 0 (Day 0 or 0 minute) mRNA levels as the internal calibrator and are represented in relation to T = 0 levels. **A)** *TSC2* mRNA levels across a 6 day differentiation course (Replicates: N=2). **B)** *TSC2* mRNA levels across the 24 hour time course (Replicates: N=3).

### **3.4: TSC2 mRNA levels show a slight variation between partially committed and stem-like neuronal cell populations**

Though commonly used as representative of neural progenitor populations, the model cell lines employed in the preceding studies were derived from, and consist of, a heterogeneous cell population (Preis et al. 1988; Whittemore & White 1993). Hence these cells exist as a partially committed population comprised of cells at various stages of neural lineage commitment, between neural progenitors and fully differentiated neurons or glial cells. To examine whether Tuberin expression is differentially expressed in the more stem-like cells, we used the neurosphere formation assay, designed by Pacey and associates to select for this population (Pacey et al. 2006).

Neurosphere formation assays were conducted using both SH-SY5Y (Figure 10) and RN33B cells (Figure 11). Stem-like SH-SY5Y cells were stimulated, using culture methods established in Pacey et al. 2006, to form variably sized, roughly spherical clusters of cells, which were subsequently enriched for two passages prior to harvesting (Figure 10A & B). QRT-PCR analysis was used to compare mean TSC2 mRNA levels between neurosphere cultured cells and monolayer culture. To indicate the relative degree of differentiation within the compared cell populations, mean mRNA levels were also examined for the neuronal progenitor/stemness markers Nestin and Octamer-binding Transcription Factor 4 (Oct 4). Upon comparison, mean TSC2 mRNA levels, followed the expression levels of Oct 4. Despite the apparent elevation however, levels were not found to be significantly higher in the neurosphere cultured cells than in the monolayer population (Figure 10C). It is notable that mean Oct 4 (Figure 10D) and mean Nestin mRNA (Figure 10E) levels also displayed no significant changes between the neurosphere and monolayer populations. This indicates that there may have been experimental fluctuation in

the isolation of the stem-like population. Using identical methods to those employed for the SH-SY5Y cells, neurospheres were cultured from native heterogeneous populations of RN33B cells. Following two successive passages, neurospheres, which were generally smaller in size than SH-SY5Y derived neurospheres, were collected and analyzed for TSC2 mRNA levels in comparison to monolayer cultured RN33B cells using QRT-PCR (Figure 11A & B). Nestin and Oct 4 levels were also examined as markers of stemness. Comparative evaluation of mean mRNA levels found, despite apparent elevation, that there were no significant differences in TSC2 mRNA levels between neurosphere and monolayer cultured cell populations (Figure 11C). Both Nestin (Figure 11D) and Oct 4 (Figure 11E) mean levels also showed no significant changes in expression between the two populations. Collectively, given the similarities between TSC2 mRNA levels and those of the stem-ness markers, in both populations, this supports that Tuberin levels may fluctuate based on the sub-set of cells. These data need to be repeated to avoid outlier data and determine statistical relevance.

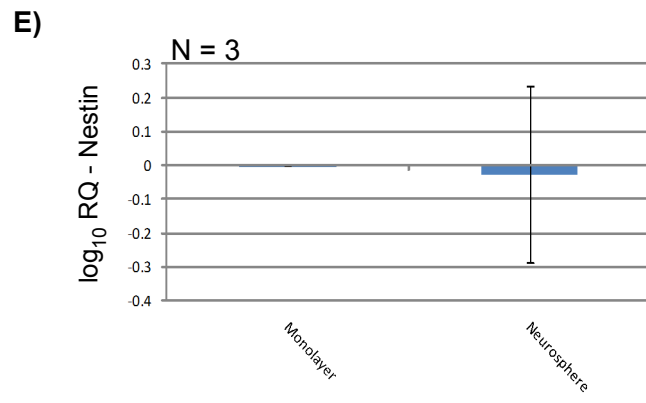
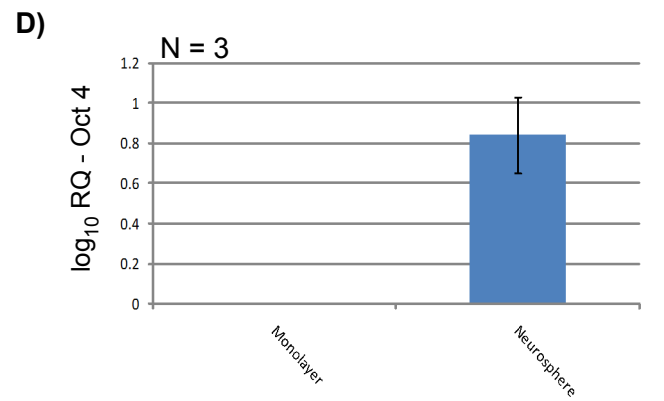
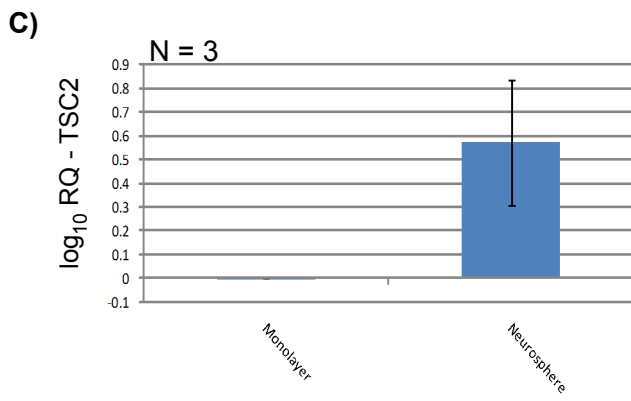
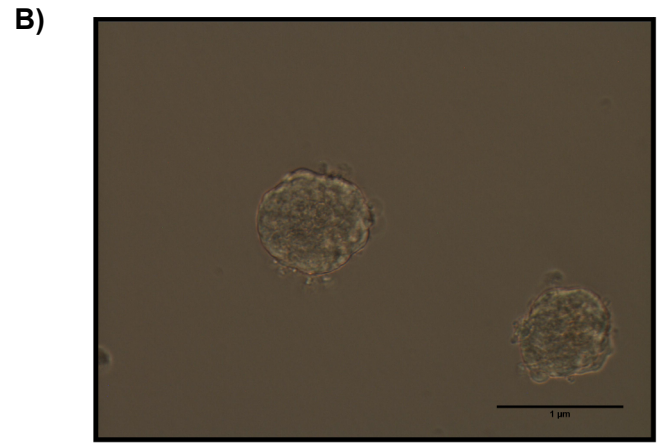
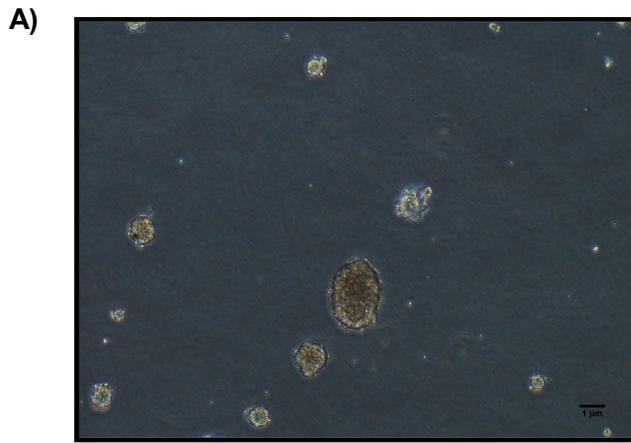


**Figure 10** *TSC2 mRNA levels follow those of Oct4 in neurosphere-cultured SH-SY5Y cells*

SHSY5Y neuroblastoma cells, previously grown under standard prescribed culture conditions, were stimulated to form neurospheres for approximately 2 days, or until suspended spherical structures were observed. **A-B)** Phase contrast micrographs, taken at 4X (**A**) and 20X (**B**) magnification, 2 passages following formation (Scale = 1  $\mu$ m). **C-E)** QRT-PCR analysis was used to compare target mRNA levels between neurosphere-cultured cells (Neurosphere) and monolayer-grown cells (Monolayer), cultured under identical conditions for at least 12 hours prior to analysis. mRNA levels are presented as the calculated mean  $\log_{10}$  RQ values for each sample population (Y-axis), with error bars indicating the standard error. Target mRNA expression levels were normalized to GAPDH, calibrated using monolayer mRNA levels as the internal calibrator and are represented in relation to monolayer levels. N=3.

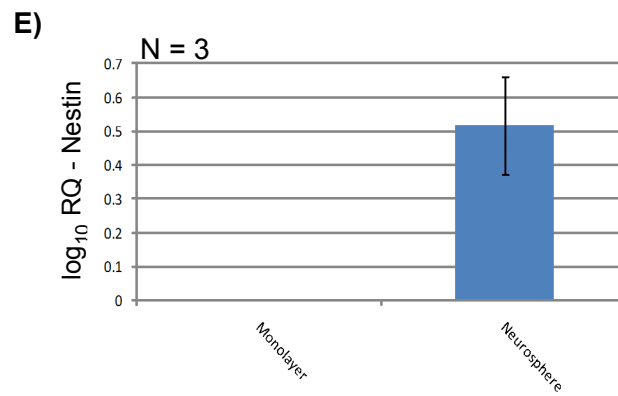
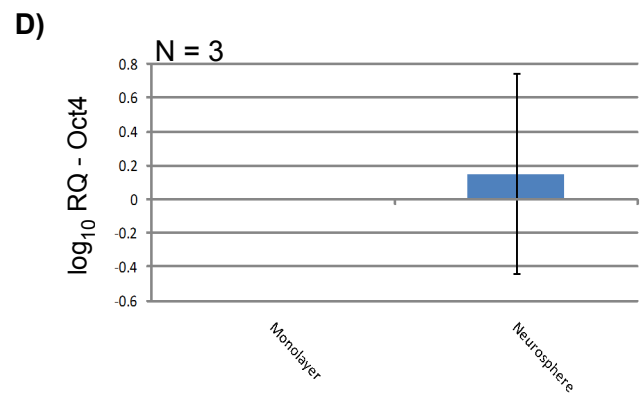
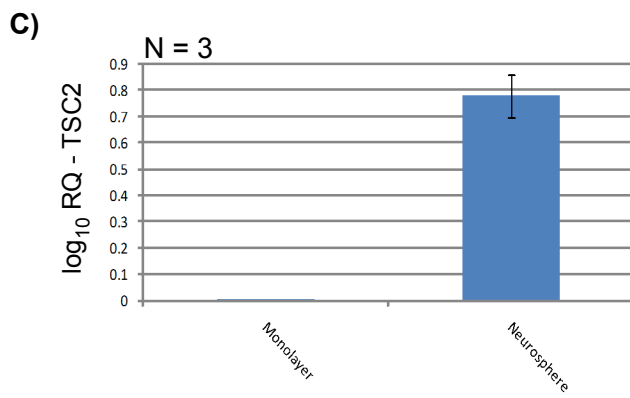
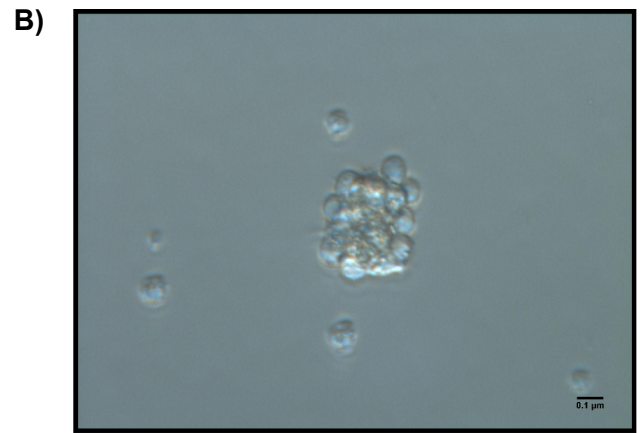
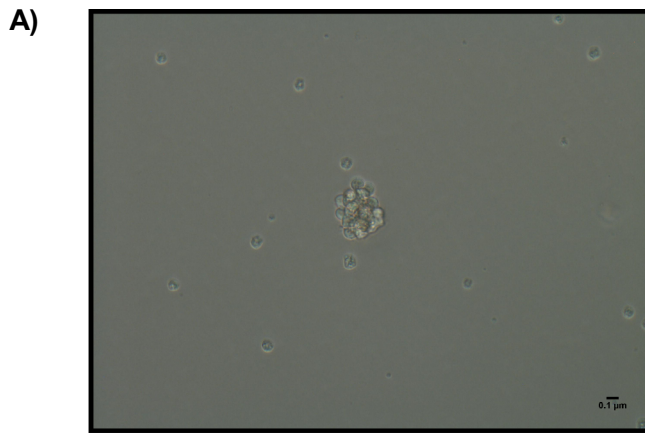


**Figure 11** *TSC2 mRNA levels follow those of Nestin in neurosphere-cultured RN33B cells*

RN33B cells, growth previously under prescribed culture conditions, were stimulated to form neurospheres for approximately 7 days, or until suspended spherical structures were observed. **A-B)** Phase contrast micrographs, taken at 20X (**A**) and 40X (**B**) magnification (Scale = 0.1  $\mu\text{m}$ ). **C-E)** QRT-PCR analysis was used to compare target mRNA levels between neurosphere-cultured cells (Neurosphere) and monolayer-grown cells (Monolayer), cultured under identical conditions for at least 12 hours prior to analysis. mRNA levels are presented as the calculated mean  $\log_{10}$  RQ values for each sample population (Y-axis), with error bars indicating the standard error. Target mRNA expression levels were normalized to GAPDH, calibrated using monolayer mRNA levels as the internal calibrator and are represented in relation to monolayer levels. N=3.



### **3.5: Tuberin expression and activity levels remain relatively consistent during late embryonic and post-natal development**

To examine whether Tuberin levels fluctuate during *in vivo* neural development, neural tissues were harvested from BALB/C mice across a developmental time course extending from embryonic day (E.D) 16 to postnatal day (P.N) 90 (Figures 12-15). Tissues were sectioned to isolate regions of the brain, specifically the hippocampus, olfactory bulbs, cerebral cortex and cerebellum, known to be highly neurogenic during late embryonic/early post-natal development and commonly afflicted with TS-associated lesions (Eriksson et al. 1998, Pagano et al. 2000, Temple 2001, Marcotte & Crino 2006, Ponti et al. 2008). Previous work has demonstrated that Tuberin and Hamartin levels, to be high in the cerebellum at ED13 and the adult brain (Murthy et al. 2001). Western blot analysis was conducted using this expanded time course of extracted tissues to examine Tuberin levels and p70S6K phosphorylation levels, as an indicator of mTOR activity.

Within the hippocampus, Tuberin protein levels (Figure 12A – Panel 1) did not display significant overall changes in levels across the developmental course (Figure 12B). However, there were significant changes in levels between E.D 18 and P.N 2 ( $p = 0.0347$ ,  $\alpha = 0.05$ ). p-p70S6K levels (Figure 12A – Panel 3) similarly did not demonstrate significant overall changes in phosphorylation across the developmental course, but activity was significantly reduced in the aging brain (P.N 21 and P.N 90) as compared to the embryonic brain (E.D. 18) (P.N. 21:  $p = 0.0313$ ,  $\alpha = 0.05$ ; P.N. 90:  $p = 0.0273$ ,  $\alpha = 0.05$ ) (Figure 12C). Comparison of the expression trends for Tuberin and p-p70S6K levels across the developmental course found that they did not differ significantly from each other ( $F(1,5) = 0.0126$ ;  $p = 0.9122$ ;  $\alpha = 0.05$ ) (Figure 12C – Right).

Tuberin and p-p70S6K levels also showed no substantial correlation with each other across the developmental course ( $\rho = 0.2241$ ) (Figure 12C – Right).

Tuberin levels in the olfactory bulbs (Figure 13A – Panel 1) were ubiquitously expressed without significant change in levels across the developmental course (Figure 13B). p-p70S6k levels (Figure 13A – Panel 3) were also not significantly altered across the time course (Figure 13C). The overall trends in Tuberin and p70S6K phosphorylation levels were not observed to differ significantly over the course of development ( $F(1,6) = 0.4180$ ;  $p = 0.5283$ ;  $\alpha = 0.05$ ) and levels were also not found to correlate highly with each other ( $\rho = 0.0356$ ) (Figure 13C - Right).

Cerebral cortex Tuberin levels (Figure 14A – Panel 1) were also ubiquitously expressed and did not display any significant changes in level across the developmental course (Figure 14B). This was similarly reflected in the levels of p-p70S6K (Figure 14A – Panel 3 & Figure 14C). Comparative analysis of Tuberin and p-p70S6K levels found no significant differences in their trends across the developmental course ( $F(1,6) = 0.0074$ ;  $p = 0.9324$ ;  $\alpha = 0.05$ ) and a weak positive correlation between the two within this brain region ( $\rho = 0.3131$ ) (Figure 14C – Right).

In a manner similar to the other regions, Tuberin levels within the cerebellum (Figure 15A – Panel 1) were consistently expressed through development (Figure 15B). There was significance seen in comparing embryonic expression (E.D 18) to post-natal expression levels (P.N 2) ( $p = 0.0347$ ,  $\alpha = 0.05$ ). p-p70S6K levels (Figure 15A – Panel 3), similarly, were found, via regression analysis, to be consistently expressed, but did demonstrate a significant reduction from embryonic stages to P.N 4 (P.N. 4:  $p = 0.0191$ ,  $\alpha = 0.05$ ) (Figure 12C). Comparison here between Tuberin and p70S6K levels indicated their expression trends were not significantly different ( $F(1,6) = 0.07973$ ;  $P = 0.7817$ ;  $\alpha = 0.05$ ) and that observed changes in Tuberin and p-

p70S6K levels showed no substantial correlation with each other across the developmental course ( $p = 0.1170$ ) (Figure 12C – Right).

Overall, Tuberin levels and p70S6K phosphorylation levels appear to be ubiquitous through the developmental time course studied here. Levels of Tuberin, and correlatively p-p70S6K, were found to decrease during post-natal development in both the hippocampus and the cerebellum; potentially supporting a role in the maturation/aging of the adult brain. This data also provides support to *in vitro* findings that Tuberin levels undergo regulation during neuronal cell differentiation and development.

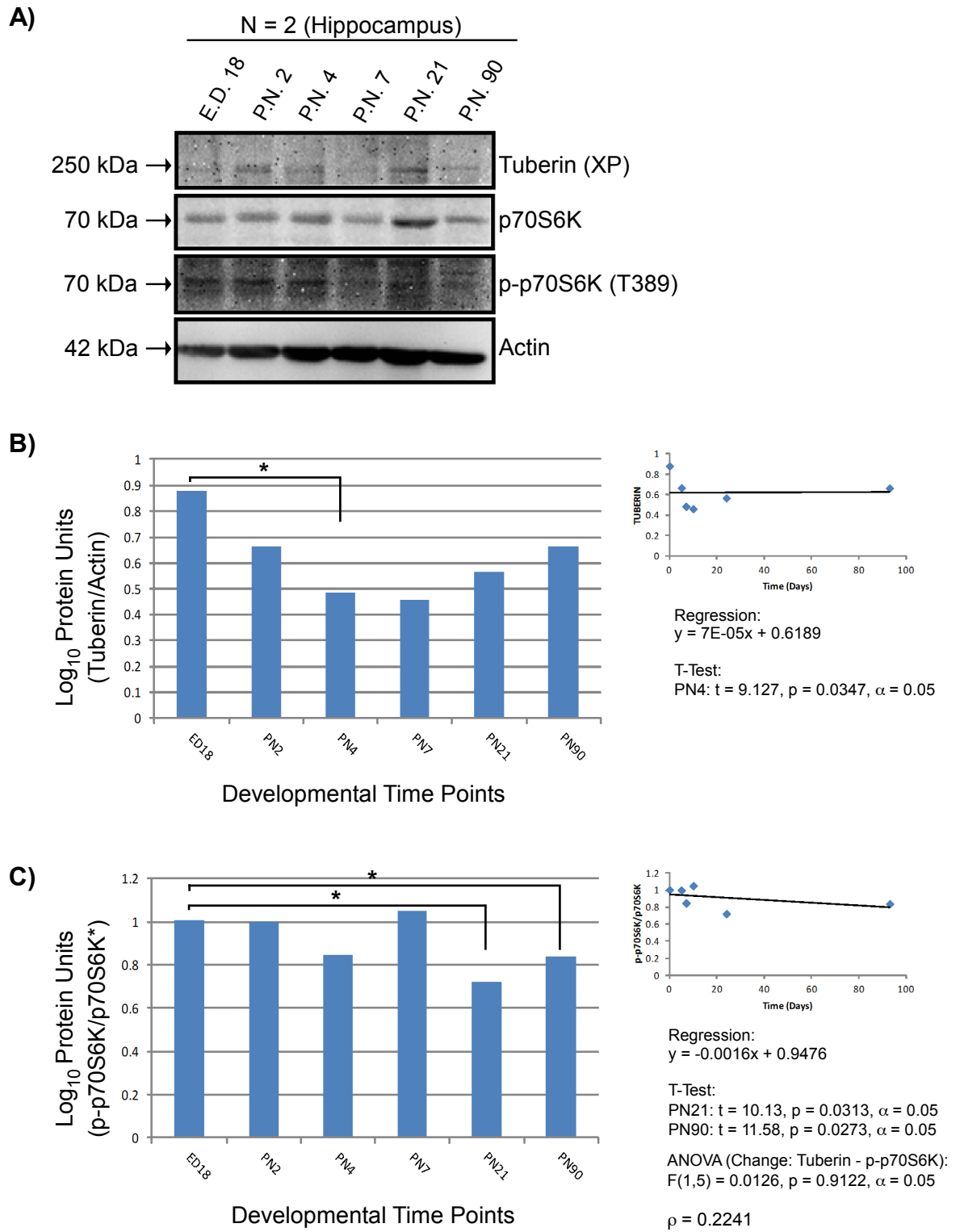
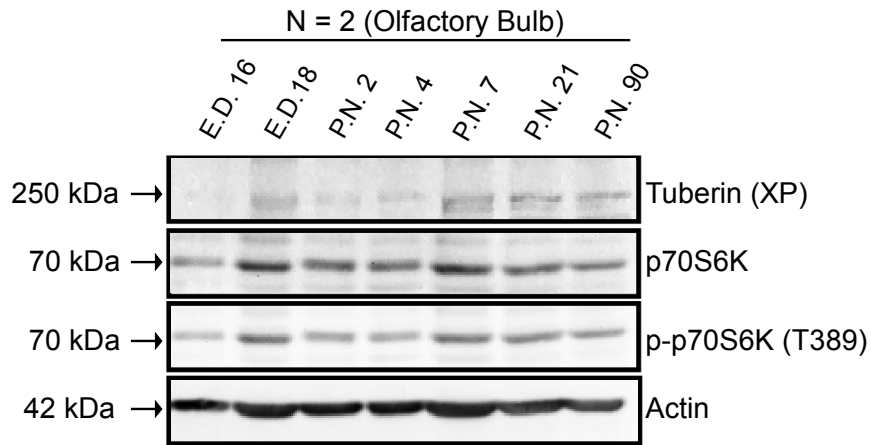


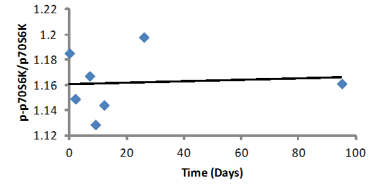
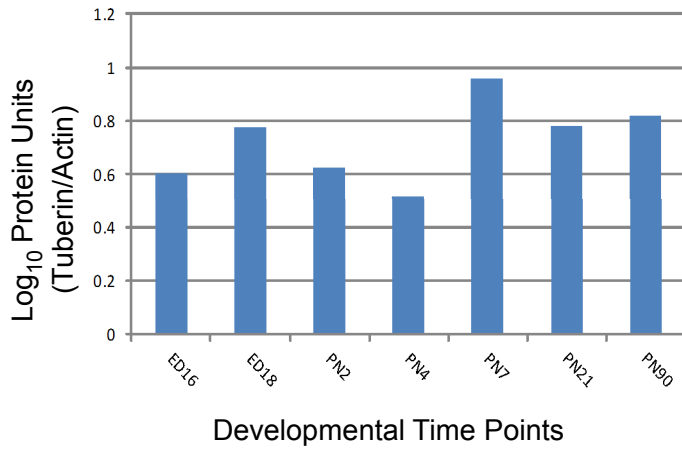
**Figure 12** *Tuberin levels and activity are reduced during post-natal development in the hippocampus*

Protein samples were prepared from Hippocampus tissue extracted from BALB/c mice across a series of time points during late embryonic and postnatal development. **A)** Tuberin (Panel 1) and p-p70S6K (Panel 3) were visualized through western blot analysis conducted using 200  $\mu$ g of protein loaded equally across all lanes. p70S6K (Panel 2) and Actin (Panel 4) are shown as controls. Protein lysates were analyzed using SDS-PAGE, resolved on a 7.5% denaturing polyacrylamide gel (Replicates: N=2). **B-C)** Comparison of protein expression between individual time point samples was conducted using spot densitometry analysis. Densitometry values (Y-axis) for Tuberin represent the  $\text{Log}_{10}$  transformed values of corrected protein optical density values ( $y$ ), where  $y = (\text{Tuberin OD} / \text{Actin OD})$ . p-p70S6K densitometry values represent the  $\text{Log}_{10}$  transformed values of corrected p-p70S6K optical density values ( $y$ ), where  $y = ((\text{p-p70S6K OD} / \text{Actin OD}) / (\text{p70S6K OD} / \text{Actin OD}))$ . Statistical evaluation of Tuberin and p-p70S6K levels were conducted using linear regression, to observe overall changes for each marker across the developmental course, while paired sample t-test (One-sided;  $\alpha = 0.05$ ) was to compare individual changes between time points. Two-way ANOVA was used to compare the level change trends for Tuberin and p-p70S6K across the developmental course ( $\alpha = 0.05$ ). Spearman's Rho analysis was also used to determine the presence of any correlation between Tuberin and p-p70S6K levels.

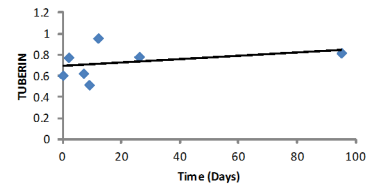
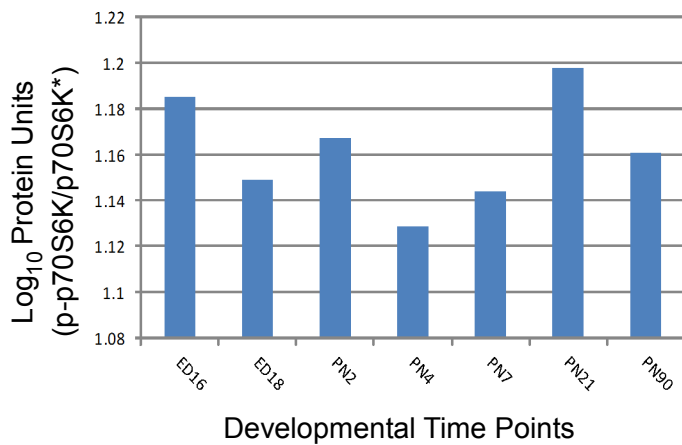
A)



B)



C)

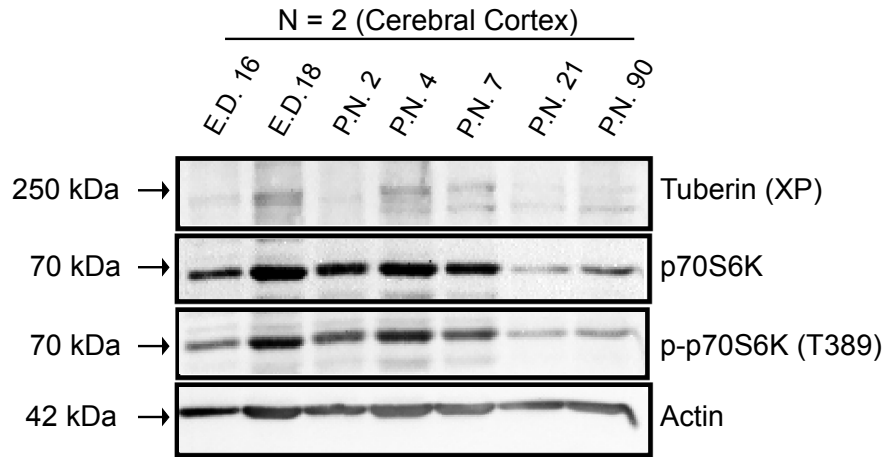


ANOVA (Change: Tuberin - p-p70S6K):  
 $F(1,6) = 0.4180, p = 0.5283, \alpha = 0.05$   
 $\rho = 0.0356$

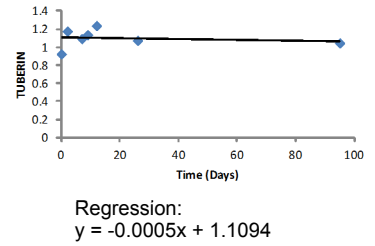
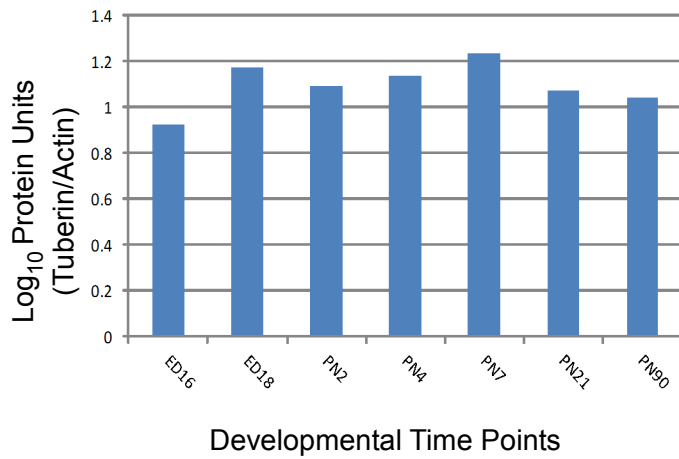
**Figure 13** *Tuberin levels and activity are constant within the olfactory bulb during late embryonic and postnatal development*

Protein samples were prepared from olfactory bulb tissue extracted from BALB/c mice across a series of time points during late embryonic and postnatal development. **A)** Tuberin (Panel 1) and p-p70S6K (Panel 3) were visualized through western blot analysis conducted using 200 µg of protein loaded equally across all lanes. p70S6K (Panel 2) and Actin (Panel 4) are shown as controls. Protein lysates were analyzed using SDS-PAGE, resolved on a 7.5% denaturing polyacrylamide gel (Replicates: N=2). **B-C)** Comparison of protein expression between individual time point samples was conducted using spot densitometry analysis. Densitometry values (Y-axis) for Tuberin represent the  $\text{Log}_{10}$  transformed values of corrected protein optical density values ( $y$ ), where  $y = (\text{Tuberin OD} / \text{Actin OD})$ . p-p70S6K densitometry values represent the  $\text{Log}_{10}$  transformed values of corrected p-p70S6K optical density values ( $y$ ), where  $y = ((\text{p-p70S6K OD} / \text{Actin OD}) / (\text{p70S6K OD} / \text{Actin OD}))$ . Statistical analyses were conducted as described in Figure 12.

A)



B)



C)

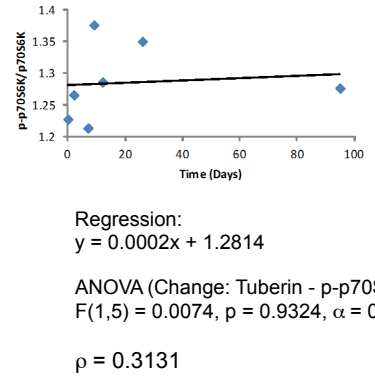
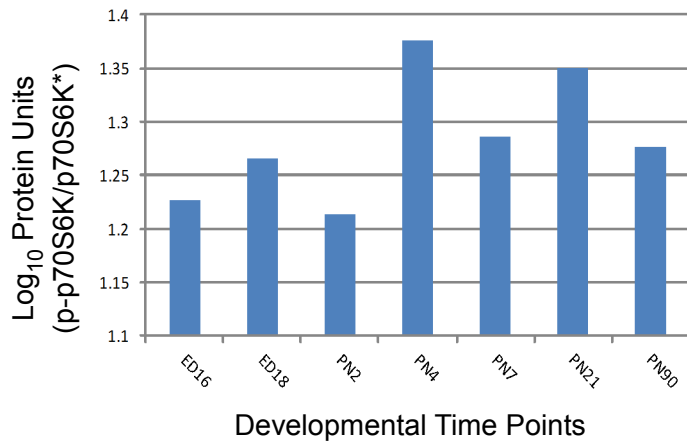
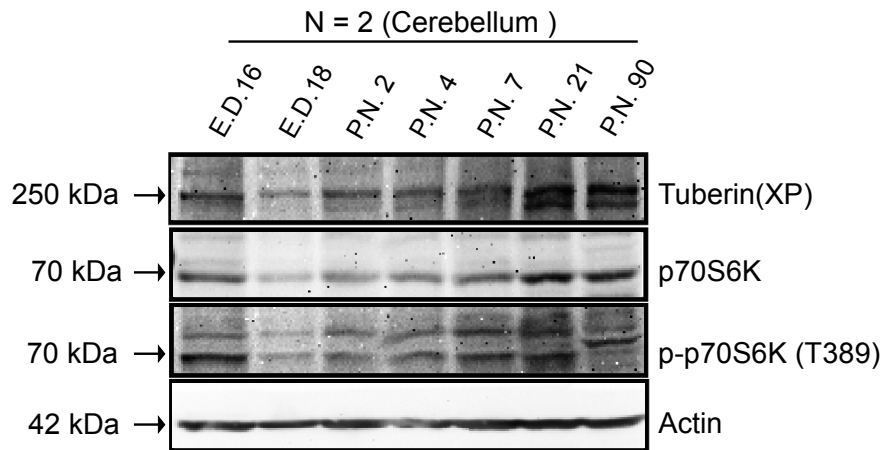




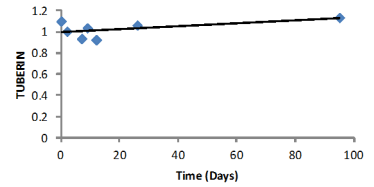
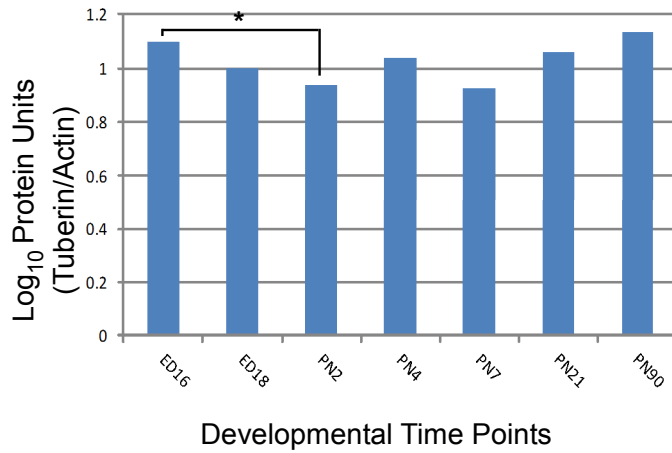
**Figure 14** *Tuberin levels and activity are ubiquitous within the cerebral cortex during late embryonic and postnatal development*

Protein samples were prepared from cerebral cortex tissue extracted from BALB/c mice across a series of time points during late embryonic and postnatal development. **A)** Tuberin (Panel 1) and p-p70S6K (Panel 3) were visualized through western blot analysis conducted using 200  $\mu$ g of protein loaded equally across all lanes. p70S6K (Panel 2) and Actin (Panel 4) are shown as controls. Protein lysates were analyzed using SDS-PAGE, resolved on a 7.5% denaturing polyacrylamide gel (Replicates: N=2). **B-C)** Comparison of protein expression between individual time point samples was conducted using spot densitometry analysis. Densitometry values (Y-axis) for Tuberin represent the  $\text{Log}_{10}$  transformed values of corrected protein optical density values ( $y$ ), where  $y = (\text{Tuberin OD} / \text{Actin OD})$ . p-p70S6K densitometry values represent the  $\text{Log}_{10}$  transformed values of corrected p-p70S6K optical density values ( $y$ ), where  $y = ((\text{p-p70S6K OD} / \text{Actin OD}) / (\text{p70S6K OD} / \text{Actin OD}))$ . Statistical analyses were conducted as described in Figure 12.

A)

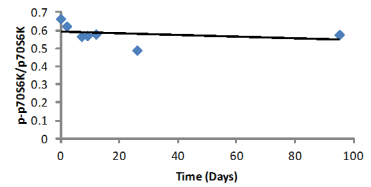
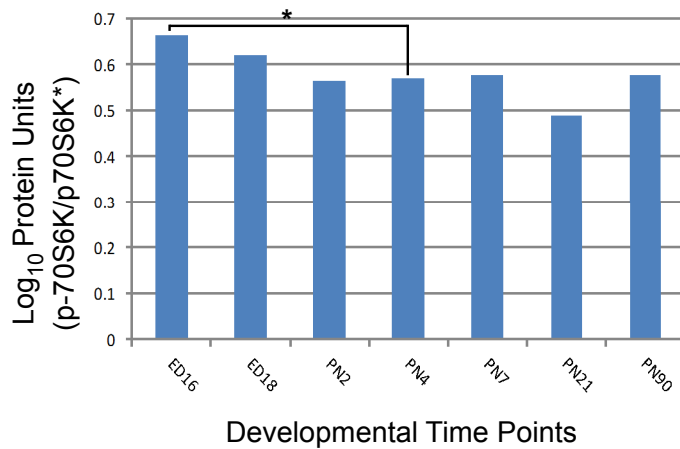


B)



Regression:  
 $y = 0.0013x + 0.9983$   
 T-Test:  
 PN2:  $t = 22.69$ ,  $p = 0.0140$ ,  $\alpha = 0.05$

C)



Regression:  
 $y = -0.0004x + 0.5905$   
 T-Test:  
 PN4:  $t = 16.55$ ,  $p = 0.0191$ ,  $\alpha = 0.05$   
 ANOVA (Change: Tuberin - p-p70S6K):  
 $F(1,5) = 0.0797$ ,  $p = 0.7818$ ,  $\alpha = 0.05$   
 $\rho = 0.1170$

**Figure 15** *Tuberin levels and activity are reduced during post-natal development in the cerebellum*

Protein samples were prepared from cerebellum tissue extracted from BALB/c mice across a series of time points during late embryonic and early postnatal development. **A)** Tuberin (Panel 1) and p-p70S6K (Panel 3) were visualized through western blot analysis conducted using 200 µg of protein loaded equally across all lanes. p70S6K (Panel 2) and Actin (Panel 4) are shown as controls. Protein lysates were analyzed using SDS-PAGE, resolved on a 7.5% denaturing polyacrylamide gel (Replicates: N=2). **B-C)** Comparison of protein expression between individual time point samples was conducted using spot densitometry analysis. Densitometry values (Y-axis) for Tuberin represent the  $\text{Log}_{10}$  transformed values of corrected protein optical density values ( $y$ ), where  $y = (\text{Tuberin OD} / \text{Actin OD})$ . p-p70S6K densitometry values represent the  $\text{Log}_{10}$  transformed values of corrected p-p70S6K optical density values ( $y$ ), where  $y = ((\text{p-p70S6K OD} / \text{Actin OD}) / (\text{p70S6K OD} / \text{Actin OD}))$ . Statistical analyses were conducted as described in Figure 12.

### 3.6: Design and construction of shRNA plasmid vectors for *in vitro* knockdown of TSC2

Our observations demonstrating the regulation of TSC2 levels and activity during neuronal cell development both *in vitro* and *in vivo*, coupled with published evidence outlining the defects in neuronal development and morphology that accompany perturbations in TSC2 expression, suggest that TSC2 could potentially play an important role in neural cell fate decisions (Tavazoie et al. 2005, Floricel et al. 2007, Choi et al. 2008). To concretely address the role for Tuberin in neural differentiation, shRNA plasmid vectors, directed against both human and rat TSC2, were designed and constructed to be used for the purposes of *in vitro* gene knockdown studies. These tools were constructed to elucidate the essentiality of Tuberin protein expression to neural differentiation and cell fate decisions. Constructed utilizing the pLB and pLKO.1 shRNA backbone vectors, these plasmids were designed for introduction into target cells utilizing lentiviral infection systems.

Construction of the pLB based vectors was completed through insertion of shRNA cassette oligonucleotide sequences targeted against multiple regions across isoform 1 of the rat TSC2 transcript (Figure 16A). These oligos were inserted between the HpaI and XhoI restriction sites of the pLB cloning site (Figure 16B). Following ligation, the colonies were screened using polyacrylamide gel electrophoresis examining DNA fragments generated through digestion at the unique restriction enzyme sites XbaI and XhoI (Figure 16C). Upon confirmation of oligonucleotide incorporation through screening, the resultant plasmid vectors, pLB-TSC2shRNA v.1 / v.2 and pLB-shRNAControl, were also sequenced to verify correct insertion of the shRNA cassette sequences into pLB (Figure 16D & E). Lentiviral infection into RN33B cells was then used to confirm vector integrity and expression, as indicated by observation of eGFP fluorescence (Figure 16F).

Construction of the pLKO.1 human lentiviral expression vectors was conducted by inserting shRNA cassette oligonucleotide sequences (Figure 17A), originally designed and validated as part of the RNAi consortium library. Oligos were inserted between the AgeI and EcoRI restriction enzyme sites (Figure 17B). Following ligation of the oligonucleotide sequences into the pLKO.1 cloning site, sequencing of the plasmid vector was used to confirm correct incorporation and orientation of the shRNA cassette sequences. Successful generation of these plasmids will be invaluable tools for the future determination of the essentiality of Tuberin during neural cell fate decisions.

A)

pLB-TSC2shRNA 1

Forward Strand: 5'-AACGCTCCATTACAAGCATGGCTATTTCAAGAGATAGCCATGCTTGTATGGAGCC-3'

Reverse Strand: 5'-TCGAGGCTCCATTACAAGCATGGCTATCTCTTGAATAGCCATGCTTGTATGGAGCGTT-3'

pLB-TSC2shRNA 2

Forward Strand: 5'-AACGGTGAATGCGGCCTCAACAATTTCAAGAGAATTGTTGAGGCCGCATTACCC-3'

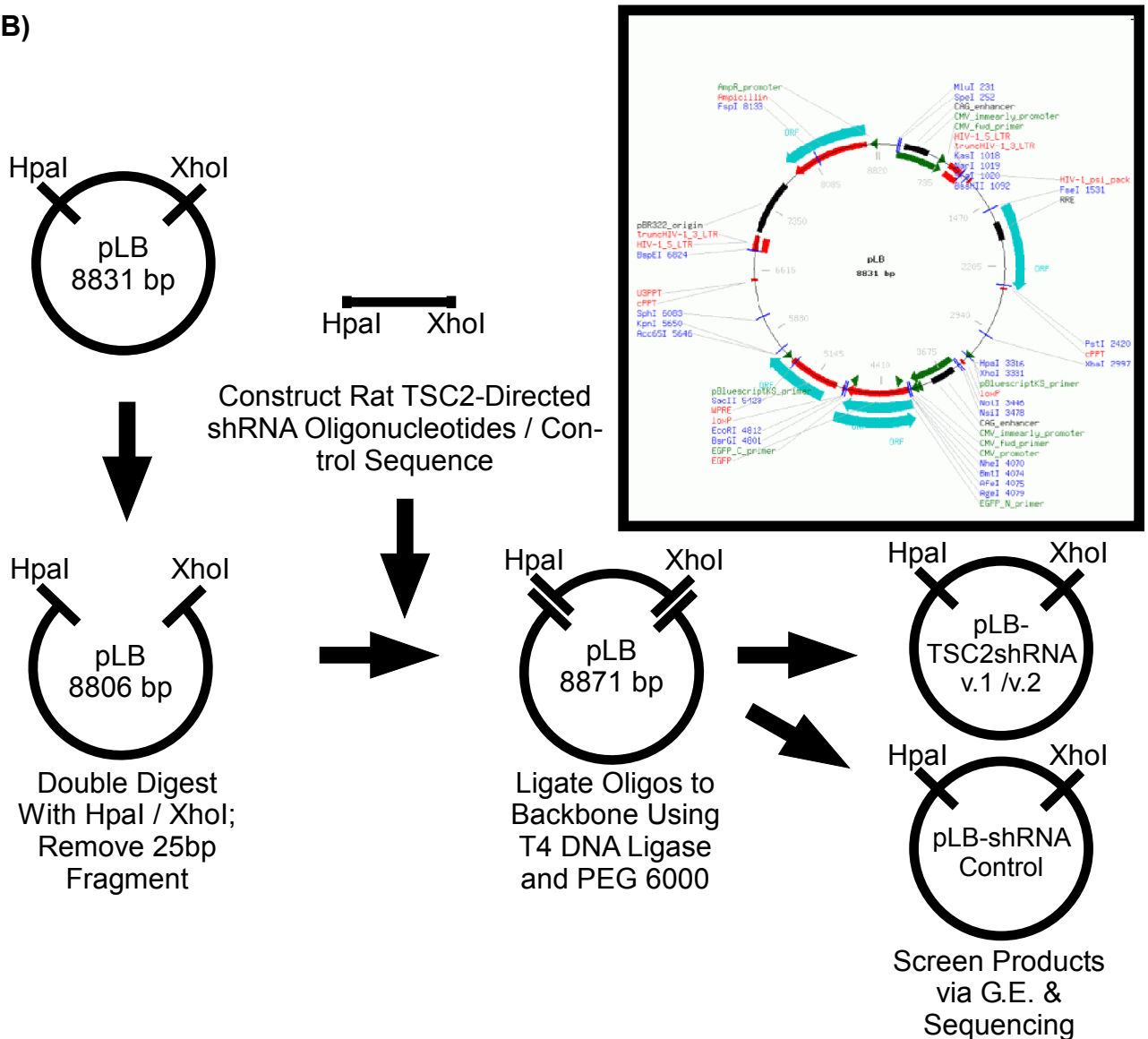
Reverse Strand: 5'-TCGAGGGTGAATGCGGCCTCAACAATCTCTTGAATTGTTGAGGCCGCATTACCGTT-3'

pLB-shRNA Control

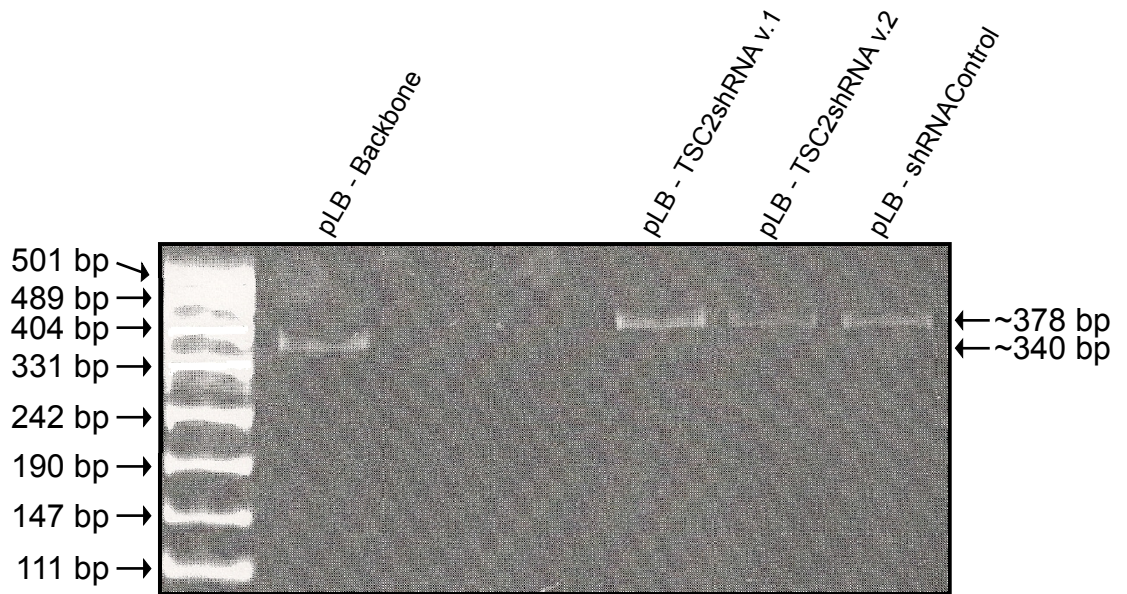
Forward Strand: 5'-AACGTCCTGGAGATGGCCAACATATTTCAAGAGATATGTTGGCCATCTCCAGGACC-3'

Reverse strand: 5'-TCGAGGTCCTGGAGATGGCCAACATATCTCTTGAATATGTTGGCCATCTCCAGGACGTT-3'

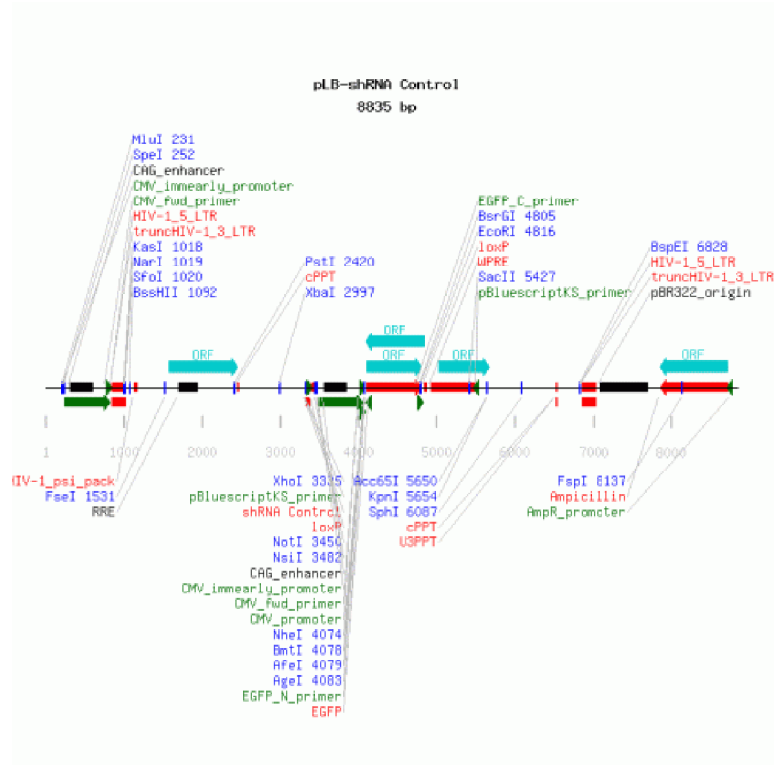
B)



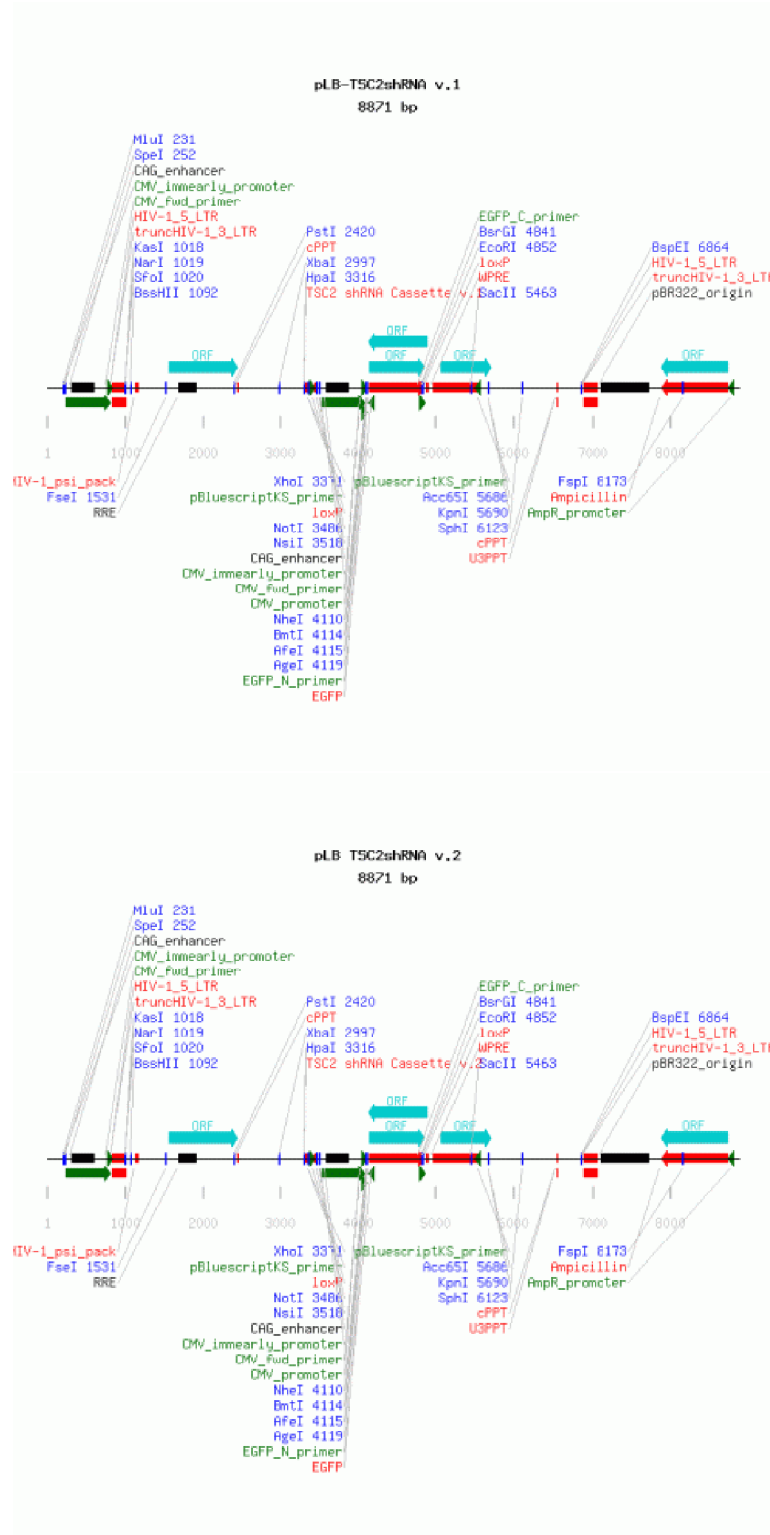
c)



d)

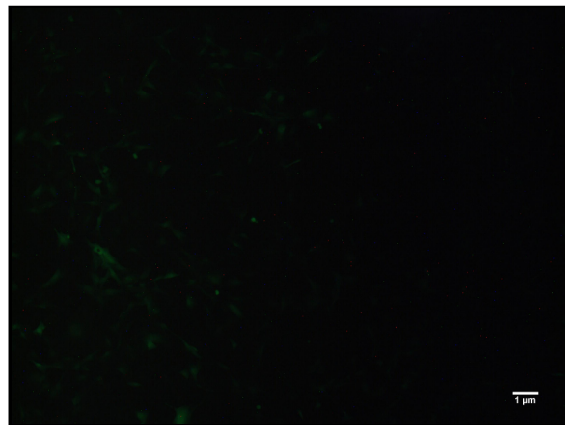
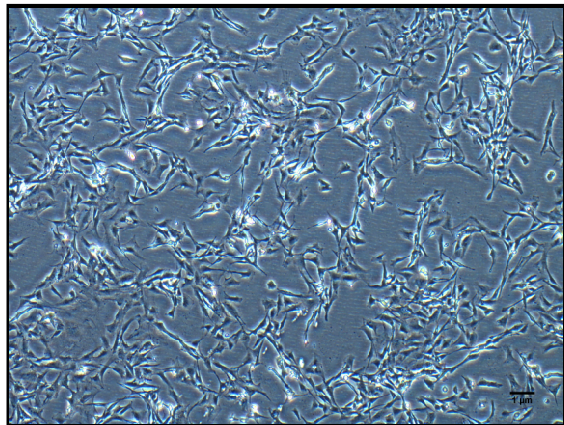


E)





F)



G)

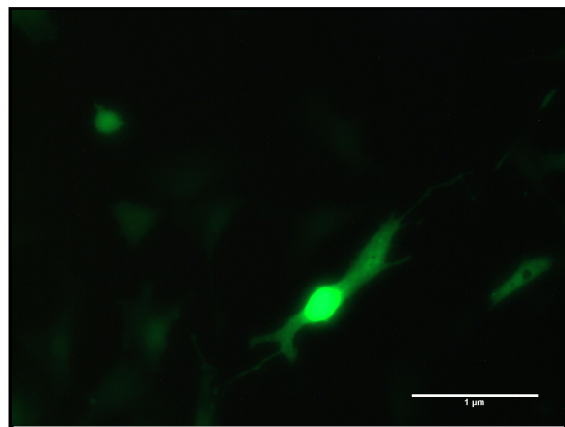
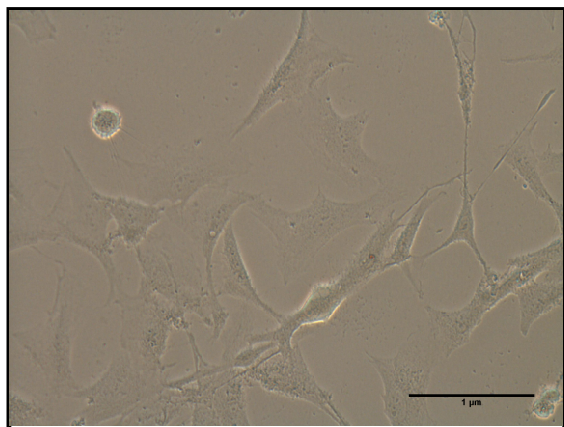


**Figure 16** *Design and cloning of shRNA vectors for knockdown of rat TSC2 in vitro*

Murine shRNA vectors were based on the 8831 bp pLB murine expression backbone, which contains a Green Fluorescent Protein (eGFP) reporter gene under the control of CMV promoter. **A)** pLB-TSC2shRNA v.1 and pLB-TSC2shRNA v.2 were constructed using shRNA cassette oligonucleotide sequences designed against rat TSC2 isoform 1. pLB-shRNAControl was constructed using a nucleotide sequence which does not match to rat TSC2 isoform 1. **B)** Cloning of the pLB vectors was conducted using the outlined strategy. Oligonucleotide sequences were ligated into the pLB backbone, which had previously been digested at its *HpaI* and *XhoI* restriction sites, to produce the completed vectors. **C)** Polyacrylamide gel screening was conducted to confirm incorporation of the designed shRNA cassette oligonucleotides within the pLB cloning site. Successful ligation, observed for pLB-TSC2shRNA v.1/v.2 and pLB-shRNA Control, is indicated by the presence of a DNA fragment of approximately 378bp in size. The native fragment, lacking the insert, from the pLB backbone is pictured as a control. **D)** Vector map of the constructed control plasmid: pLB-shRNA Control. **E)** Vector maps of the constructed plasmids: pLB-TSC2shRNA v.1 and pLB-TSC2shRNA v.1. **F)** Fluorescence micrographs picturing RN33B cells at 4X and **G)** 20X following transfection with pLB-TSC2shRNA v.1. (Scale = 1  $\mu\text{m}$ ).



C)

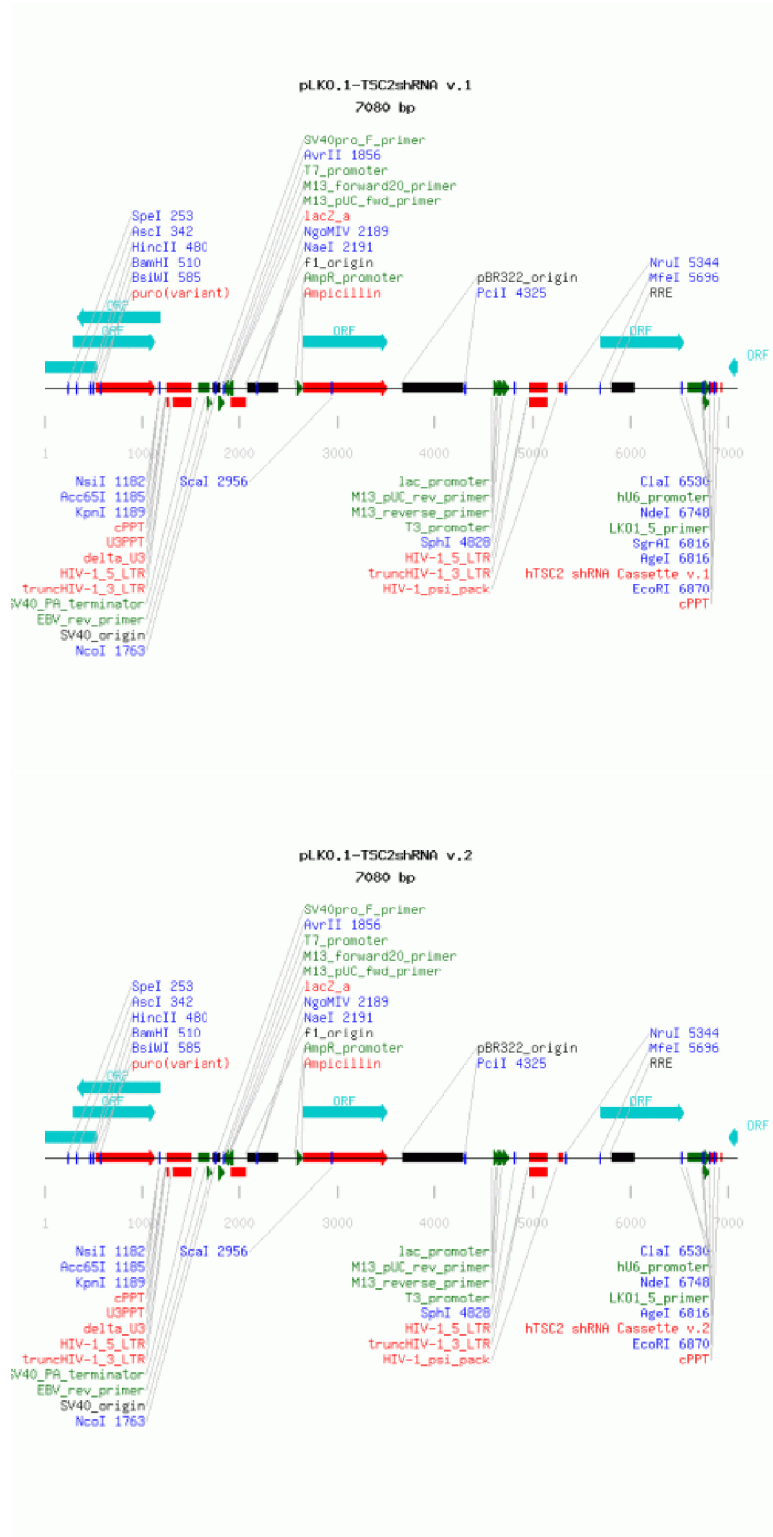


**Figure 17** *Design and cloning of shRNA vectors for in vitro knockdown of human TSC2*

Human shRNA vectors were constructed using the 7085 bp pLKO.1-TSC2 human expression backbone, which contains a Puromycin selection marker gene. **A)** pLKO.1-TSC2shRNA v.1 and pLKO.1-TSC2shRNA v.2 were constructed using shRNA cassette oligonucleotide sequences originally designed by Sigma-Aldrich. **B)** Cloning of the pLB vectors was conducted using the outlined strategy. Oligonucleotide sequences were ligated into the pLKO.1 backbone, which had previously been digested at its *AgeI* and *EcoRI* restriction sites, to remove the original shRNA cassette. **C)** Vector maps of the constructed shRNA and control plasmids.

### **3.7: Testing of constructed TSC2 shRNA plasmid vectors**

To examine the effects of TSC2 knockdown on neural cell fate decisions, testing trials were conducted to verify the integrity and function of the constructed pLB and pLKO.1-based shRNA plasmid vectors. Evaluation of each plasmid's functional TSC2 knockdown were conducted utilizing SH-SY5Y cells, for pLKO.1 based human expression vectors, and RN33B cells, for the pLB-based murine expression vectors (Figure 18).

Initial knockdown trials were attempted using DNA transfection methods (Figure 18A). For these trials, repeated transfections were conducted, individually using one of three transfection reagents: Polyethyleneimine (PEI), Lipofectamine LTX and Fugene HD. Trials were conducted across multiple experiments in which the quantities/concentrations of reagent and DNA, as well as the transfection and post-transfection recovery times, were varied. Additionally, SH-SY5Y transfections were also conducted using the commercially obtained pLKO.1-TSC2 (Addgene) and previously constructed pLKO.1-Scrambled vectors. Western blot analysis, following collection of protein lysates, failed to consistently display significant knockdown in Tuberin levels, when compared to controls prepared from cells grown under normal and serum-starved culture conditions (Figure 18B). For the pLKO.1 vectors, additional attempts were also made to visualize knockdown using serial transfection of SH-SY5Y cells ectopically expressing TSC2, through transfection with the pCMV-TSC2 mlu- mammalian expression vector. However, these attempts were unsuccessful due to cell death, upon serial transfection with pLKO.1-TSC2/pLKO.1-TSC2shRNA v.1/v.2, or loss of overexpression prior to western blotting.

Concurrent with the transfection trials, lentiviral infection trials were also conducted to determine the functional knockdown ability of the designed plasmid vectors (Figure 18A). Infections were carried out, in SH-SY5Y and RN33B cells, using VSV-G pseudotyped lentivirus,

prepared as outlined in Methods and Materials and containing each of the following plasmids: pLKO.1-TSC2, pLKO.1-Scrambled, pLKO.1-TSC2shRNA v.1, pLKO.1-TSC2shRNA v.2 (SH-SY5Y); pLB-TSC2shRNA v.1, pLB-TSC2shRNA v.2, pLB-shRNA Control (RN33B). As in the transfection trials, several experiments were conducted, utilizing variation in the multiplicity of infection (MOI), infection time and post-infection recovery time in order to visualize the knockdown of Tuberin from endogenous levels through western blot analysis (Figure 18A). Within the SH-SY5Y cells, infection trials failed to progress to western blot analysis, as widespread cell death was found to occur during post-infection puromycin selection (Figure 18B). Though few cells were noted, in some cases, to appear viable following puromycin selection, they failed to proliferate and subsequently died. RN33B infections, however, yielded more encouraging results, as the vast majority of cells survived the infection process, yielding an average transfection efficiency of approximately 60%, measured through proportional eGFP fluorescence (Figure 18B). Analysis of protein levels, through immunoblotting, and mRNA levels, through QRT-PCR, however, failed to indicate consistently significant reductions in TSC2 expression.

A)

### Transfection / Infection

Plasmid	Cell Line	Transfection Method	Quantity of DNA/ MOI	Culture Size / Volume	Amount of Reagent Used	Transfection / Recovery Duration	Survival (Post-Transfection)
pLKO-1-TSC2	SH-SY5Y	Polyethylenimine (PEI)	2 - 15 ug	60 mm, 100 mm / 4 mL, 8 mL	10 - 25 ug (1mg/mL)	8 - 48 hours; 0 - 48 hours	Yes
		Lipofectamine LTX	2.5 - 10 ug	60 mm / 4 mL	6.25 uL	16 - 24 hours; 0 - 24 hours	
		Fugene HD	1.5 - 6 ug	6 well / 3 mL	6 - 18 uL	8, 16, 24 hours; N/A	
pLKO-1-TSC2shRNA v.1 pLKO-1-TSC2shRNA v.2 pLKO-1-Scrambled pCMV-TSC2-mil-	SH-SY5Y	Lentiviral Infection	MOI = 1, 2, 3, 5, 10	24 well	Variable (Based on Cell Density)	8 - 48 hours; 0 - 48 hours	Yes
		Polyethylenimine (PEI)	2 - 15 ug	60 mm, 100 mm / 4 mL, 8 mL	10 - 25 ug (1mg/mL)	8 - 48 hours; 0 - 48 hours	
		Lipofectamine LTX	2.5 - 10 ug	60 mm / 4 mL	6.25 uL	16 - 24 hours; 0 - 24 hours	
pL.B-TSC2shRNA v.1 pL.B-TSC2shRNA v.2 pL.B-shRNA Control	RN33B	Fugene HD	1.5 - 6 ug	6 well / 3 mL	6 - 18 uL	24 hours; 2 days - 2 weeks	
		Lentiviral Infection	MOI = 2, 2.5, 5, 10	24 well	Variable (Based on Cell Density)		
		Lentiviral Infection					

B)

### Post-Treatment & Screening

Plasmid	Cell Line	Transfection Method	Evaluation / Selection	Survival (Post-Selection)	Knockdown Evaluation	Western Blotting / Conditions	Knockdown Confirmed
pLKO-1-TSC2	SH-SY5Y	Polyethylenimine (PEI)	Puromycin (24 hours post-infection; continuing until control populations killed)	Yes	Western Blot	Yes, 10% SDS-PAGE Gel, 100V, 3 hours, 22°C	No (Negligible Reduction Observed)
		Lipofectamine LTX					
		Fugene HD					
pLKO-1-TSC2shRNA v.1 pLKO-1-TSC2shRNA v.2	RN33B	Lentiviral Infection	eGFP (Confirmed via Microscopic Analysis)	Yes	Western Blot	Yes, 7.5% SDS-PAGE Gel, 100V, 3 hours, 4°C	No (Negligible Reduction Observed)
		Polyethylenimine (PEI)					
		Lipofectamine LTX					
pL.B-TSC2shRNA v.1 pL.B-TSC2shRNA v.2 pL.B-shRNA Control	RN33B	Fugene HD		Yes	Western Blot, qRT-PCR	Yes, 7.5% SDS-PAGE Gel, 100V, 3 hours, 4°C	No (Negligible Reduction Observed)
		Lipofectamine LTX					
		Lentiviral Infection					

#### Summary

SH-SY5Y - Transfection with PEI, Lipofectamine LTX and Fugene HD failed to produce significant and consistent downregulation of Tuberin levels. Lentiviral infection proceeded well through the initial infection, however few cells survived puromycin selection with the remaining cells failing to thrive.  
 RN33B - eGFP expression was detected following transfection using PEI, Lipofectamine LTX and Lentiviral infection, with lentiviral infection yielding the highest transfection efficiency. Protein and mRNA expression analysis failed to demonstrate a significant reduction in Tuberin mRNA levels.



**Figure 18** *Testing and troubleshooting of pLB and pLKO.1 TSC2 shRNA plasmid vectors*

Testing of pLB and pLKO.1 plasmid vectors was through both standard transfection and lentiviral infection methods. Transfection or infection conditions, including reagent used, DNA amount/MOI, culture size, reagent concentration, and incubation/recovery periods are indicated for each cell line. Results and observations following infection, selection and analysis are also indicated, as are western blotting conditions.

## **Chapter 4**

### **4. Discussion**

It has been well documented that somatic mutations occurring in either the TSC1 or TSC2 genes serve as the principle cause of TS (Jones et al. 1999; Sancak et al. 2005; Niida et al. 1999; van Slegtenhorst et al. 1999). These mutations, which accumulate in a manner consistent with Knudson's hypothesis, typically result in the abrogation of the GTPase function of the TSC, or outright inhibition of TSC formation altogether (Knudson 1971, Jones et al. 1997, Hoogeveen-Westerveld et al. 2010). Consequent inhibition of TSC function abolishes its role as a key regulator of mTOR signaling, leading to misregulation of several of mTOR's downstream signaling effectors (Kumar et al. 2005; Jaworski et al. 2005; Wullschleger et al. 2006; Choi et al. 2008; Han & Sahin 2011). TS gene mutations occur during the embryonic stage of development, leading to pathologies within a range of organ systems. However, of all the involved tissues, the CNS is most frequently affected (Marcotte & Crino 2006). There is evidence to support that the CNS pathologies seen in TS may occur, at least in part, due to defective neural fate decisions (Rennebeck et al. 1998; Crino & Henske 1999; Tavazoie et al. 2005; McNeill et al. 2008; Choi et al. 2008). These observations support the need for further investigation of the functional involvement of the TSC in the regulation of neural cell development and cell fate determination.

Cell fate determination has classically been defined as the process by which a cell proceeds through development to become a differentiated and specialized cell (Cepko et al. 1996). During this process, an immature cell, in response to cues from the environment, undergoes internal changes in gene expression which initiate a program of differentiation, directing the cell towards its terminal fate (Cepko et al. 1996; Livesey & Cepko 2001). Fate determination can be seen to involve two processes: patterning, whereby an immature cell, in response to cues from the environment, undergoes internal changes in gene expression which

induce specification and/or commitment of the cell; and differentiation, where the committed cell responds to external or internal cues which initiate programs of signaling and gene expression which direct the cell to take on the qualities of an end-stage specialized cell (Turner & Cepko 1987; Holt et al. 1988). Cell fate is influenced by factors including the competence of the cell to respond to a given cue, and the potency of the cell to differentiate into a particular range of cell types (Cepko et al. 1996; Ravin et al. 2008; Wexler et al. 2009). Studies conducted by several research groups have identified Tuberin to be mechanistically linked with the signaling of several inter/intracellular regulators of cell specification and differentiation, like Wnt, Notch, MAPK and SHH, and may play an important role in the regulation/mediation of their effects (Artavanis-Tsakonas et al. 1999; Bibel & Barde 2000; Robertson et al. 2004; Karbowiczek & Henske 2005; Bhatia et al. 2009; Ma et al. 2010).

Acknowledging this, the experiments conducted as part of this study were focused at investigating the patterns of Tuberin expression and activity in cells and tissues that are in the process of acquiring a terminal neural fate. Our results demonstrate that Tuberin is expressed throughout neural development and that levels of Tuberin decline during neuronal differentiation in a tissue specific manner. Our data does not reflect a strong correlation in the temporal activation state of the primary downstream effector of Tuberin, mTORC1. These results suggest that the interaction between Tuberin and mTORC1 may be more complex, here in the context of neural fate choice, than characteristic observation of the dynamic between these two proteins might suggest.

***4.1: Regulation of Tuberin Occurs Through the Course of Neuronal Cell Differentiation in vitro, but Does Not Appear to Directly Result in Significant Modulation of p70S6K phosphorylation***

The role of Tuberin, as a regulator of a range of cellular mechanisms, such as cell cycle regulation, gene transcription, protein translation and cell growth, has been extensively investigated over the last two decades. Interestingly, its involvement in neuronal migration, axon guidance and autophagy, have classically been framed in the context of functioning as a regulator of mTOR signaling activity (Wullschleger et al. 2006). It has been observed that Tuberin interacts with a plethora of other signaling pathways which have direct effects on the regulation of cellular differentiation and cell fate in a range of somatic tissue types (Mak 2005; Karbowniczek 2005; Ma et al. 2007; Bhatia et al. 2009; Karbowniczek 2010). An accumulated body of evidence demonstrating Tuberin-linked defects in cell differentiation and recent evidence implicating mTOR signaling as a mediator of cell fate/differentiation, clearly implicate Tuberin as a potentially important player in cell fate and differentiation (Crino & Henske 1999; Tavazoie et al. 2005; McNeill et al. 2008; Choi et al. 2008; Easley et al. 2010). While studies examining Tuberin's regulatory interactions, with kinases like GSK3 $\beta$  and ERK, have accumulated in over the last few decades, attention has recently begun to shift towards examining the functional dynamics of Tuberin during differentiation and fate choices (Ma et al. 2005; Mak et al. 2005; Karbowniczek & Henske 2005; Inoki et al. 2006).

To truly understand these dynamics during neural fate, we first measured Tuberin expression levels during the course of *in vitro* neuronal differentiation using the neural precursor cell lines, SH-SY5Y- human neuroblastoma cells and RN33B rat neuronal precursor cells. Comprised of heterogeneous populations of stem-like progenitors and more committed precursor cells, these oligopotent cell lines possess the ability to assume a neuronal phenotype using chemical (SH-SY5Y) or physical (RN33B) stimulation (Biagotti et al. 2005; Neville et al. 2009; Das et al. 2009). When induced to differentiate, we found significant unidirectional downregulation of Tuberin protein levels in SH-SY5Y cells; however RN33B protein levels

remained largely consistent with only a non-significant decrease in levels (Figure 4). When examined across a shorter differentiation course, SH-SY5Y cells also expressed Tuberin ubiquitously with no significant changes overall in levels (Figure 5B). The previously conducted study by Soucek et al. (1998) showed that Tuberin levels, demonstrate a noticeable upregulation and consistent elevation in levels as early as 6 hours following the onset of differentiation (Soucek et al. 1998). In addition, Floricel et al. (2007) observed an upregulation in Tuberin levels following NGF induced differentiation of PC12 cells, with levels remaining consistent for 72 hours and diminishing thereafter (Floricel et al. 2007). In a process known as terminal differentiation cells eventually withdraw from the cell cycle. Interestingly, Soucek et al. (1997) observed that Tuberin levels were not affected by exit from the cell cycle, indicating the alterations in Tuberin levels resulted directly from the induction of neuronal differentiation (Thiele et al. 1985; Thiele et al. 1989; Soucek et al. 1997; Soucek et al. 1998). On the contrary, in this study we provide results suggesting a progressively decreasing requirement to maintain Tuberin levels as differentiation proceeds. Moreover, this study lends support to work by Wu & Wong (2003) that showed reduced Tuberin levels across a 30-minute time course, following NGF stimulation in PC12 cells. Accordingly, Easley et al. (2010) found that Tuberin levels decline in differentiating H7 hESCs, by comparison to undifferentiated hESCs (Easley et al. 2010). It is possible that these two sets of results are not contrasting, but merely represent a dynamic pattern of protein regulation in response to the situational needs of the cell. While the observations collected by Soucek et al. and Floricel et al. demonstrate increase in Tuberin protein levels following the onset of differentiation, quantification of these levels is not provided. As a consequence, the dynamics of this expression across the measured time frame remained unclear (Soucek et al. 1998; Floricel et al. 2007). The observations collected by Easley et al. are simply end point observations of Tuberin levels and do not make any indication

regarding the regulation of the protein during the process of differentiation (Easley et al. 2010). Also though non-significant, the results I collected for the RN33B full differentiation time courses and the SH-SY5Y 24 hour time courses indicated that Tuberin levels may be elevated or depressed at various points during the process of differentiation, suggesting, when applied to the aforementioned observations, that the regulation of Tuberin during differentiation may be variable, requiring the adjustment of levels to maintain appropriate signaling and facilitate the normal progression of differentiation.

These observations also provide support for the position that due to the observed variability, Tuberin levels may not matter so much, in regards to its regulatory capabilities, as the dynamics of its GAP activity do. To observe the status of Tuberin activity throughout neuronal differentiation, I measured the phosphorylation status of mTORC1's direct downstream target, p70S6K, on the mTORC1 phosphorylation site, T389 (p-p70S6K), over a 24 hour time course in the SH-SY5Y cells. Elevation of p-p70S6K levels have frequently been observed during the course of induced *in vitro* differentiation, in a number of progenitor and stem cell lines, and herein indicates the level of mTOR activation, and in a reciprocal manner, the level of Tuberin activity (Han et al. 2008; Henger et al. 2009; Easley et al. 2010). While phosphorylation levels were found to be highest at 18 and 24 hours, there was a significant overall increase demonstrated across the course. Correlation analysis was performed to compare the mean values for Tuberin and p-p70S6K levels, at each time point, but failed to observe any meaningful positive or negative correlations between the two groups. This suggests that while Tuberin levels may undergo some regulation during differentiation, this regulation may not be directed toward regulating mTOR signaling pathway effectors. Potentially, it could be directed towards regulating the activation of one of its recently identified signaling partners, like p42/p44 MAPK, which are

known to be more closely involved in the process of cell fate determination (Karbowniczek et al. 2005; Iwata & Herver 2009).

During the 24 hour SH-SY5Y time course levels of the microtubule associated protein 2 (MAP2), were also examined, as an indicator of the differentiation status of the cells (Soltani et al. 2005). MAP2 levels were not observed to be significantly elevated across the differentiation course. While MAP2 levels are known to be elevated in differentiated neurons by comparison to progenitor cells, it is not clear whether its levels increase steadily across the full course of differentiation. Observation of neurite outgrowth, as an indicator of differentiation, did confirm that differentiation was successfully occurring within these experiments (data not shown). Experimental reports of MAP2 increases during differentiation of the SHSY-5Y cells tend to use longer differentiation time courses than were used in this study (R. Constantinescu et. al. 2007) and hence the 24 hour time course may be too short to adequately use this marker as a reporter of differentiation. Neural differentiation studies are plagued with the inadequacy of early stage differentiation markers, to ensure that these cells were properly moving along a neuronal course control plates could be left to differentiate long-term to stain with terminal markers such as MAP2 and Tau.

#### ***4.2: Cellular Localization of Tuberin May be Implicated in Cell-Specific Downregulation During Differentiation.***

While most commonly localized to the cytoplasm, Tuberin and the mTOR complex proteins bear the ability to localize to and conduct their functions within both the nucleus and the cytoplasm (Soucek et al. 1998; Nellist et al. 1999; Li et al. 2006; Furuya et al. 2006; Rosner et al. 2007b; Rosner & Hengstschlager 2007). Tuberin, in particular, has been observed to play an important role in the regulation of p27 localization, inhibiting its 14-3-3 mediated cytoplasmic

retention, leading to its nuclear localization through a nuclear localization signal dependent mechanism (Rosner et al. 2007a). Rosner et al. (2007b) demonstrated that Tuberin's ability to localize to the nucleus may be controlled through phosphorylation by Akt at S939 and T1462, which induce cytoplasmic retention/localization of Tuberin (Rosner et al. 2007b). Wu & Wong (2003) also observed that phosphorylation by Akt promoted the degradation of Tuberin by the proteasome (Wu & Wong 2003). Furthermore, nuclear localization of Tuberin has been observed to occur during neuronal differentiation (Soucek et al. 1998). Given Tuberin's ability to move between the nucleus and cytoplasm, we investigated the nuclear and cytoplasmic expression of Tuberin during differentiation. While experimental repeats are required to determine statistical significance and repeatability, we did observe that declines in Tuberin levels were seen in the nuclear compartment for SH-SY5Y cells (Figure 6). Interestingly, cytoplasmic levels of Tuberin appeared to increase through differentiation, a result that would in fact support the observations of Soucek et al. and Floricel et al. (Soucek et al.1998; Floricel et al. 2007). Given that cytoplasmic Tuberin is available for proteasomal degradation, this relocalization may represent a mechanism underlying the decline in overall protein levels seen in the SHSY-5Y cells (Figure 4). Supportive of this, RN33B cells, which express constant levels of Tuberin during differentiation (Figure 4), had constant levels of both nuclear and cytoplasmic Tuberin during differentiation (Figure 7). Further experimentation and replication of these results is definitely needed in order for any conclusions to be drawn from them.

#### ***4.3: Tuberin Protein Levels Do Not Appear to be Transcriptionally Regulated During the Course of Neuronal Differentiation***

Most observations of Tuberin expression and regulation have often neglected to include investigations of the role transcriptional control may play in the regulation of TSC protein



expression, due largely to a general assumption that Tuberin and many of the other TOR proteins are constitutively expressed (Soucek et al. 1997; Miloloza et al. 2000; Schmidt et al. 2010). Soucek et al. (1998) provided support for this view observing that, within SK-N-SH cells, TSC2 mRNA was high in expression prior to and during neuronal differentiation (Soucek et al. 1998). These levels also did not change through the course of differentiation, leading them to conclude that regulation of Tuberin levels occurred primarily in a post-transcriptional manner. Wienecke et al. (1997), however, presented somewhat oppositional evidence to this view, observing that TSC2 mRNA levels were significantly decreased in TS –associated astrocytoma tissues (Wienecke et al. 1997). Studies conducted by Feng et al. (2005), while not demonstrating a direct interaction, also provided support for the presence of transcriptional regulation, finding that p53 activation led to increased TSC2 mRNA levels in MEFs, implicating p53 as a transcriptional regulator of Tuberin expression (Feng et al. 2005). Furthermore, recent studies have identified c-Myc as another potential regulator of Tuberin transcription, as it has been shown to repress the transcription of TSC2 mRNA through binding to an evolutionarily conserved Myc target sequence in the TSC2 promoter (Karbowiczek et al. 2003; Loots et al. 2002; Ravitz et al. 2007). Collectively, these observations, though not in full agreement, indicate that the possibility that Tuberin expression may be, at least in part, regulated at the transcriptional level should be investigated more closely.

To examine expression during differentiation, I utilized QRT-PCR to quantify TSC2 mRNA levels at each time point during differentiation. When measured over a full 3 day differentiation course in the SH-SY5Y cells, TSC2 mRNA levels were expressed consistently with no statistical change (Figure 8A). Across the 24 hour time course, though, mRNA levels did demonstrate a significant overall decrease, presenting with a biphasic pattern of expression, initially increasing

during the first two hours and subsequently decreasing below initial levels thereafter (Figure 8B).

Examination of TSC2 mRNA levels across 6 day and 24 hour time courses using the RN33B cells also demonstrated that TSC2 mRNA expression did not change in any significant manner during differentiation (Figure 9A & B). Ultimately, these results provide support for the conclusion made by Soucek et al. that Tuberin is regulated largely at the protein level (1998). However, the significant change in expression over the 24 hour SH-SY5Y time course, coupled with the apparent, but non-significant, variability observed across all of the other time courses in both the SH-SY5Y and RN33B cells, introduce the probability that TSC2 mRNA levels could in fact be subject to regulation during fate decisions. Across the SH-SY5Y 3-day course, mRNA levels decrease and remain depressed below initial levels in a manner that is reflective of the decreases noted at the protein level. 24 hour levels demonstrate a biphasic pattern, initially increasing then decreasing to below initial levels in a manner that is not only consistent with the Day 1 mRNA results of the 3-day time course, but one that is mimicked during the RN33B 24 hour course and can also be applied to 24 hour time course protein levels. While only observational trends that need to be repeated for more adequate statistical analysis, these data suggest that Tuberin regulation may be temporally shifted due to the kinetics of translation.

The cell lines used in this study are known to be comprised of heterogeneous cell populations containing stem-like progenitor cells and other, more committed precursor cells (Biagotti et al. 2005; Neville 2009). Hence, data obtained from our studies and others can be said to reflect the course of differentiation from an intermediate 'stem-ness' state to a terminal neuronal phenotype. Given the reduction in Tuberin levels through differentiation, I hypothesized that cells in the more stem-like progenitor state should have elevated levels of

Tuberin protein. To test this hypothesis, I cultured neurospheres from normal SH-SY5Y and RN33B cell cultures, to isolate the most stem-like progenitor cells among each culture, and conducted comparative qRT-PCR analysis between the neurospheres and cells from the same original culture, which had been grown in monolayer under normal culture conditions. Comparison of TSC2 mRNA levels between the neurosphere and monolayer populations, however, did not demonstrate any significant differences, for either the SH-SY5Y (Figure 10A & B) or the RN33B cells (Figure 11A & B). Despite this result, it is notable that Tuberin levels mimicked that of the stemness marker Oct4 in SHSY-5Y cells (Figure 10) and the neural stemness marker Nestin in the RN33B cells (Figure 11). It is also important to note that the population of neurosphere cells gathered for both cell types did not demonstrate statistical significance for both stemness markers. In a recent review from the Doetsch lab the benefits and downfalls of the neurosphere assay system, as a mechanism of purifying neural stem cells, is discussed (Pastrana et al 2011). It is possible that due to the high numbers of cells used in this assay, and the lack of clonal passaging, that we did not obtain a pure population of stem cells. Given the similarities in the expression between TSC2 and a subset of stemness markers it is certainly important to follow up these experiments using clonal passaging of small numbers of cells. Should TSC2 mRNA levels remain stable regardless of differentiation status within these precursor cell populations, this would support the observations made by Soucek et al. (1998), indicating that Tuberin mRNA levels are indeed not subject to change as a consequence of differentiation in neuronal cells (Soucek et al. 1998).

#### ***4.4: Tuberin Levels and p70S6K Phosphorylation Are Regulated within Sub-sets of Neural Tissues During Late Embryonic and Postnatal Development***

As development proceeds, the cells that comprise neural tissues become more specialized, differentiating from stem cell populations to produce terminally differentiated neurons and glia (Alberts et al. 2002). Through the use of immunoblotting analyses we demonstrate that within several regions of the BALB/c mouse brain Tuberin protein and p70S6K phosphorylation levels are expressed throughout development. Furthermore, we show that in a tissue specific manner Tuberin levels and p70S6K phosphorylation are downregulated as the brain ages. Observations of Tuberin levels, within the four brain regions sampled (Hippocampus, Olfactory Bulbs, Cerebral Cortex, Cerebellum; Figure 12 – 15), found that overall levels of Tuberin were ubiquitously expressed across the developmental course. Interestingly, in both the hippocampus and cerebellum levels and activity were significantly decreased from embryonic day 18 to early post-natal stages (Figure 12B & 15B). These results provide support for the observations published by Murthy et al. (2001), where they documented Tuberin expression within developing rat tissues and observed that Tuberin levels, representing protein extracted from whole brain tissues, were highly expressed during a developmental time course from E.D. 19 to 12 weeks. Additionally, as part of the same study, Murthy et al. also observed that the Tuberin levels within the cerebellum were high both in fetal and adult Wistar rats. These results provide support for these observations, but also provide a more detailed study of early post-natal days and find an interesting, and potentially important, regulation of Tuberin in the critical first post-natal days. These results suggest that changes in Tuberin levels and activity may be required in the specialization of subsets of cells/tissues of the developing brain. It should be noted however, that while the overall trends in expression demonstrated an effectively consistent pattern of expression, both Tuberin levels and p70S6K phosphorylation, demonstrated a degree of variation during the developmental course. While the limitations on the degree to which these changes can be evaluated exist here, due to the fact that this is an

effect observed across a low number of replicates, this variation did suggest, in concert with the periodic significant changes observed, that the levels of both Tuberin and p70S6K phosphorylation could be undergoing regulation. Additionally, analysis of variance and correlation analyses conducted comparing Tuberin levels to p70S6K phosphorylation levels ultimately failed to demonstrate any significant positive or negative relationships in the patterns of expression displayed by these two markers. Interestingly, the significant downregulation in Tuberin levels occurring in the hippocampus and cerebellum occur just prior to observed changes in p70S6K levels. While the statistical power of the tests conducted to examine this data set is low, this could be indicative of a response in p70S6K phosphorylation that is temporally matched to Tuberin levels. This requires further investigation.

#### ***4.5: Conclusions and Future Directions***

We have demonstrated that the regulation of Tuberin expression and activity at the protein level, and potentially at the mRNA level, are among the cohort of events that mark the process of neural cell differentiation as a component of the process of cell fate determination. However, there is still much that we do not know about the degree and significance of the involvement of Tuberin in this process. Of chief importance is the further clarification of the results obtained as part of this study that have low numbers of repeats, this is essential to obtain full statistical significance of the data. Furthermore, to provide a more complete understanding of Tuberin's role in cell fate, shRNA mediated knockdown of Tuberin expression should be employed using the vectors described in this work. We would expect that loss of Tuberin expression, modeled using the systems employed through these studies, would result in a phenotype indicative of impaired neural differentiation. However, it would be interesting to observe both how this phenotype would develop on a temporal scale and also how loss of

Tuberin would influence signaling, through pathways like MAPK, Wnt and Shh, which are indicative of the process of fate choice. Studies of this type, centered on the functional knockdown of Tuberin expression, would allow for an expansion of this investigation to include the functional consequence of the loss of Tuberin on cell fate. The tools developed during this work make future movement into this area possible.

Further dissecting both the pathways by which Tuberin may be important in regulating neural cell fate, as well as how Tuberin levels are regulated in specific cell types and tissue types are important future avenues for this work. While this study has utilized phosphorylated p70S6K as an indicator of Tuberin activity, there are many other mechanisms by which mTORC1 can be regulated outside of Tuberin, making this an indirect assessment of Tuberin function. Furthermore, there are a great deal of other functions of Tuberin in addition to mTORC1 regulation, and likely many yet to be determined. Interactions between Tuberin and several signaling pathways, such as the Notch and MAPK signaling pathways have been identified, and are likely candidates as mechanisms by which Tuberin may regulate cellular differentiation and fate choice. Investigation into the expression and activity of the prime effector components of these signaling pathways such as Notch1 or ERK1/ERK2, conducted in parallel with further assays of Tuberin expression dynamics would provide significant insight into potential roles of Tuberin in neural development. In addition, future thought into the development of inducible knockdown, or knock-in, mouse models would be an important and valuable direction for addressing the *in vivo* importance of Tuberin during embryonic and early post-natal development. While there is much work to be done, this work contributes toward our understanding of how the protein Tuberin is regulated through neural development. Given the severity of TS, it is important to continue to reveal the basic science behind how this protein is involved in the development of many different organ systems including the CNS. Clearly defining

the roles of Tuberlin during neural development may reveal new perspectives from which to examine the process of cell fate choice and new methods by which to approach the study, diagnosis and treatment of TS.

## References

Aaku-Saraste E, Hellwig A, Huttner WB (1996) Loss of occludin and functional tight junctions, but not ZO-1, during neural tube closure - Remodeling of the neuroepithelium prior to neurogenesis. *Developmental Biology*. 180: 664-679.

Agarwal HL, Taylor WR, Chernov MV, Chernova OB, Stark GR (1998) The p53 network. *Journal of Biological Chemistry*. 273: 1-4.

Alvarez-Medina R, Cayuso J, Okubo T, Takada S, Marti E (2008) Wnt canonical pathway restricts graded shh/gli patterning activity through the regulation of gli3 expression. *Development*. 135:237-247.

Alberts B, Johnson A, Lewis J, Raff M, Roberts K, Walter P (2002) *Molecular biology of the cell*. Garland Science. 4<sup>th</sup> ed.

Artavanis-Tsakonas S, Rand MD, Lake RJ (1999) Notch signaling: Cell fate control and signal integration in development. *Science*. 284:770-776.

Astrinidis A, Henske EP (2005) Tuberous sclerosis complex: linking growth and energy signalling pathways with human disease. *Oncogene*. 24:7475-7481.

Barnes AP, Lilley BN, Pan YA, Plummer LJ, Powell AW, Raines AN, Sanes JR, Polleux F (2007) LKB1 and SAD kinases define a pathway required for the polarization of cortical neurons. *Cell*. 129:549-563.

Barnes EA, Kennerson HL, Mak BC, Yeung RS (2010) The loss of Tuberin promotes cell invasion through the beta-catenin pathway. *American Journal of Respiratory Cell and Molecular Biology*. 43: 617-627.

Benvenuto G, Shaowei L, Brown S, Braverman R, Vass WC, Cheadle JP, Halley DJJ, Sampson JR, Wienecke R, DeClue JE (2000) The tuberous sclerosis-1 (TSC1) gene product hamartin suppresses cell growth and augments the expression of the TSC2 product tuberin by inhibiting its ubiquitination. *Oncogene*. 19: 6306-6316.

Bhatia B, Northcott PA, Hambardzumyan D, Govindarajan B, Brat DJ, Arbiser JL, Holland EC, Taylor MD, Kenney AM (2009) Tuberous sclerosis complex suppression in cerebellar development and medulloblastoma: Separate regulation of mammalian target of rapamycin activity and p27 localization. *Cancer Research*. 69: 7224-7234.

Biagiotti T, D'Amico M, Marzi I, DiGennaro P, Arcangeli A, Wanke E, Olivetto M (2005) Cell renewing in neuroblastoma: electrophysiological and immunocytochemical characterization of stem cells and derivatives. *Stem Cells*. 24: 443-453.

Birchenall-Roberts MC, Fu T, Bang O, Dambach M, Resau JH, Sadowski CL, Betolette DC, Lee HJ, Kim SJ, Ruscetti FW (2004) Tuberous sclerosis complex 2 gene product interacts with human SMAD proteins. A molecular link of two tumor suppressor pathways. *Journal of Biological Chemistry*. 279: 25605-25613.



Boer K, Jansen F, Nellist M, Redeker S, van den Ouweland AM, Spliet WG, van Nieuwenhuizen O, Troost D (2008) Inflammatory processes in cortical tubers and subependymal giant cell tumours of tuberous sclerosis complex. *Epilepsy Research*. 78: 7-21.

Bottenstein JE and Sato GH (1979) Growth of a rat neuroblastoma cell line in serum-free supplemented media. *Proceedings of the National Academy of Sciences USA*. 76: 514-517.

Brown EJ, Albers MW, Shin TB, Ichikawa K, Keith CT, Lane WS, Schreiber SL (1994) A mammalian protein targeted By G1-arresting Rapamycin-receptor complex. *Nature*. 369: 756-758.

Brugarolas JB, Vazquez F, Reddy A, Sellers WR, Kaelin WG (2003) TSC2 regulates VEGF through mTOR-dependent and -independent pathways. *Cancer Cell*. 4: 147-158.

Cadigan KM, Nusse R (1997) Wnt signaling: a common theme in animal development. *Genes & Development*. 11:3286-3305.

Cai SL, Tee AR, Short JD, Bergeron JM, Kim J, Shen J, Guo R, Johnson CL, Kiguchi K, Walker CL (2006) Activity of TSC2 is inhibited by Akt-mediated phosphorylation and membrane partitioning. *Journal of Cell Biology*. 173: 279-289.

Calegari F, Huttner WB (2003) An inhibition of cyclin-dependent kinases that lengthens, but does not arrest, neuroepithelial cell cycle induces premature neurogenesis. *Journal of Cell Science*. 116: 4947-4955.

Calegari F, Haubensak W, Haffner C, Huttner WB (2005) Selective lengthening of the cell cycle in the neurogenic subpopulation of neural progenitor cells during mouse brain development. *Journal of Neuroscience*. 25: 6533-6538.

Campbell K, Gotz M (2002) Radial glia: multi-purpose cells for vertebrate brain development. *Trends in Neurosciences*. 25: 235-238.

Cao Y, Kimoka Y, Yokoi N, Kobayashi T, Hino O, Ondera M, Mochizuki N, Nakae J (2006) Interaction of FoxO1 and TSC2 induces insulin resistance through activation of the mammalian target of rapamycin/p70 S6K pathway. *Journal of Biological Chemistry*. 281: 40242-40251.

Castro AF, Rebhun JF, Clark GJ, Quilliam LA (2003) Rheb binds tuberous sclerosis complex 2 (TSC2) and promotes S6 kinase activation in a rapamycin- and farnesylation-dependent manner. *Journal of Biological Chemistry*. 278: 32493-32496.

Catania MG, Mischel PS, Vinters HV (2007) Hamartin and Tuberin interaction with the G2/M cyclin-dependent kinase CDK1 and its regulatory cyclins A and B. *Journal of Neuropathology and Experimental Neurology*. 60: 711-723.

Cepko CL, Austin CP, Yang X, Aleiades M, Ezzeddine D (1996) Cell fate determination in the vertebrate retina. *Proceedings of the National Academy of Science USA*. 93: 589-595.

- Chiang GG, Abraham RT (2005) Phosphorylation of mammalian target of rapamycin (mTOR) at Ser-2448 is mediated by p70S6 kinase. *Journal of Biological Chemistry*. 280:25485-2590.
- Choi YJ, Di Nardo A, Kramvis I, Meikle L, Kwiatkowski DJ, Sahin M, He X (2008) Tuberous sclerosis complex proteins control axon formation. *Genes and Development*. 22:2485-2495.
- Chong-Kopera H, Inoki K, Li Y, Zhu T, Garcia-Gonzalo FR, Rosa JL, Guan KL (2006) TSC1 stabilizes TSC2 by inhibiting the interaction between TSC2 and the HERC1 ubiquitin ligase. *Journal of Biological Chemistry*. 281:8313-8316.
- Cranenburgh RM (2004) An equation for calculating the volumetric ratios required in a ligation reaction. *Applied Microbiology and Biotechnology*. 65: 200-202.
- Crane JF, Trainor PA (2002) Neural crest stem and progenitor cells. *Annual Review of Cell and Developmental Biology*. 22:267-286.
- Crino PB and Henske EP (1999) New developments in the neurobiology of the tuberous sclerosis complex. *Neurology*. 53:1384-1390.
- Crino PB, Nathanson KL, Henske EP (2006) The tuberous sclerosis complex. *The New England Journal of Medicine*. 355:1345-1358.
- Crino PB, Trojanowski JQ, Dichter MA, Eberwine J (1996) Embryonic neuronal markers in tuberous sclerosis: single-cell molecular pathology. *Proceedings of the National Academy of Sciences USA*. 93: 14152-14157.
- Curatolo P, Cusmai R, Cortesi F, Chiron C, Jambique I, Dulac O (1991) Neuropsychiatric aspects of tuberous sclerosis. *Annals of the New York Academy of Sciences*. 615: 8-16.
- Curatolo P, Bombardieri R (2003) Hamartomatous disorders of cellular lineage: tuberous sclerosis: historical background. *Handbook of Clinical Neurology*. 87:129-130.
- Curatolo P, Bombardieri R, Jozwiak S (2008) Tuberous Sclerosis. *The Lancet* 372: 657-668.
- Curatolo P, Verdecchia M, Bombardieri R (2002) Tuberous sclerosis: a review of neurological aspects. *European Journal of Pediatric Neurology*. 6:15-23.
- D. M. Bourneville (1880) *Sclérose tubéreuse des circonvolution cérébrales: Idiotie et épilepsie hémiplégique*. *Archives de Neurologie*. 1:81-91.
- Dan HC, Sun M, Yang L, Feldman RL, Sui ZM, Chen Ou C, Nellist M, Yeung RS, Halley DJJ, Nicosia SV, Pledger WJ, Cheng JQ (2002) Phosphatidylinositol 3-kinase/Akt pathway regulate tuberous sclerosis tumor suppressor complex by phosphorylation of Tuberin. *Journal of Biological Chemistry*. 277: 35364-35370.
- Das A, Banik N, Ray S (2009) Retinoids induce differentiation and downregulate telomerase activity and N-Myc to increase sensitivity to flavinoids for apoptosis in human malignant neuroblastoma SH-SY5Y. *International Journal of Oncology*. 34: 7575-765.

Dasgupta B, Milbrandt J (2009) AMP-activated protein kinase phosphorylates retinoblastoma protein to control mammalian brain development. *Developmental Cell*. 6: 256-270.

De Robertis EM and Kurdo H (2004) Dorsal-ventral patterning and neural induction in *Xenopus* embryos. *Annual Review of Cell and Developmental Biology*. 20:285-308.

Duester G (2008) Retinoic acid synthesis and signaling during early organogenesis. *Cell*. 134:921-931.

Dufner A, Thomas G (1999) Ribosomal S6 kinase signalling and the control of translation. *Experimental Cell Research*. 253: 100-109.

Durand B, Raff M (2000) A cell-intrinsic timer that operates during oligodendrocyte development. *Bioessays*. 22: 64-71.

Easley IV CA, Ben-Yehudah A, Rediger CJ, Oliver SL, Varum ST, Eisinger VM, Carlisle DL, Donovan PJ, Schatten GP (2010) mTOR-Mediated activation of p70S6K induces differentiation of pluripotent human embryonic stem cells. *Cellular Reprogramming*. 12:263-272.

Englund C, Fink A, Lau C, Pham D, Daza RAM, Bulfone A, Kowalczyk T, Hevner RF (2005) Pax6, Tbr2, and Tbr1 are expressed sequentially by radial glia, intermediate progenitor cells, and postmitotic neurons in developing neocortex. *Journal of Neuroscience*. 25: 247-251.

Eriksson PS, Perfilieva E, Björk-Eriksson T, Alborn AM, Nordborg C, Peterson DA, Gage FH (1998) Neurogenesis in the adult human hippocampus. *Nature Medicine*. 4: 1313–1317.

Feng Z, Zhang H, Levine AJ, Jin S (2005) The coordinate regulation of the p52 and mTOR pathways in cells. *Proceedings of the National Academy of Sciences USA*. 102:8204-8209.

Fidalgo da Silva E, Ansari SB, Maimaiti J, Barnes EA, Kong-Beltran M, Donoghue DJ, Porter LA (2011) The tumor suppressor Tuberin regulates mitotic onset through the cellular localization of cyclin B1. *Cell Cycle*. 10: 3129-3139.

Fingar DC, Blenis J (2004) Target of rapamycin (mTOR): an integrator of nutrient and growth factor signals and coordinator of cell growth and cell cycle progression. *Oncogene*. 23: 3151-3171.

Finlay GA, York B, Karas RH, Fanburg BL, Zhang H, Kwiatkowski DJ, Noonan DJ (2004) Estrogen-induced smooth muscle cell growth is regulated by Tuberin and associated with altered activation of platelet-derived growth factor receptor- $\beta$  and ERK-1/2. *Journal of Biological Chemistry*. 279: 23114-23122.

Florice F, Higaki K, Maki H, Nanba E, Ninomiya H, Ohno K (2007) Antisense suppression of TSC1 gene product, hamartin, enhances neurite outgrowth in NGF-treated PC12h cells. *Brain & Development*. 29: 502-509.

- Fryer AE, Connor JM, Povey S, Yates JRW, Chalmers A, Fraser I, Yates AD, Osborne JP (1987) Evidence that the gene for tuberous sclerosis is on chromosome-9. *Lancet*. 1: 659-661.
- Fisher RP, Morgan DO (1994) A novel cyclin associates with MO15/CDK7 to form the CDK-activating kinase. *Cell*. 78:713-724.
- Furuya F, Hanover JA, Cheng SY (2006) Activation of phosphatidylinositol 3-kinase signaling by a mutant thyroid hormone  $\beta$ -receptor. *Proceedings of the National Academy of Sciences USA*. 103: 1780-1785.
- Gao X, Zhang Y, Arrazola P, Hino O, Kobayashi T, Yeung RS, Ru B, Pan D (2002) TSC tumor suppressor proteins antagonize amino-acid TOR signalling. *Nature: Cell Biology*. 4: 699-704.
- Gaulden J, Reiter JF (2008) Neur-ons and neur-offs: regulators of neural induction in vertebrate embryos and embryonic stem cells. *Human Molecular Genetics*. 17:R60-R66.
- Gingras AC, Raught B, Gygi SP, Niedzwiecka A, Miron M, Burley SK, Polakiewicz RD, Wyslouch-Cieszynska A, Aebersold R, Sonenberg N (2001) Hierarchical phosphorylation of the translation inhibitor 4E-BP1. *Genes & Development*. 15: 2852-2864.
- Gingras AC, Kennedy SG, O'Leary MA, Sonenberg N, Hay N (1998) 4E-BP1, a repressor of mRNA translation, is phosphorylated and inactivated by the Akt(PKB) signaling pathway. *Genes & Development*. 12: 502-513.
- Gotz M, Huttner WB (2005) The cell biology of neurogenesis *Nature Reviews: Molecular Cell Biology*. 6:777-788.
- Green AJ, Smith M, Yates JRW (1994) Loss of heterozygosity on chromosome 16p13.3 in hamartomas from tuberous sclerosis patients. *Nature Genetics*. 6: 193-196.
- Gunther M, Penrose LS (1935) The genetics of epolia. *Journal of Genetics*. 31: 413-430.
- Han JM, Sahin M (2011) TSC1/TSC2 signaling in the CNS. *Federation of European Biochemical Studies (FEBS) Letters*. 585: 973-980.
- Han J, Wang B, Ziao Z, Gao Y, Zhao Y, Zhang J, Chen B, Wang X (2008) Mammalian target of rapamycin (mTOR) is involved in the neuronal differentiation of neural progenitors induced by insulin. *Molecular and Cellular Neuroscience*. 39: 118-124.
- Harris WA (1997) Cellular diversification in the vertebrate retina. *Current Opinions in Genetics & Development*. 7: 651-658.
- Hemmati-Brivanlou A, Kelly OG, Melton DA (1994) Follistatin an antagonist of activin is expressed in the Spemann organizer and displays direct neutralizing activity. *Cell*. 77:283-295.

Henger B, Lange M, Kusch A, Essin K, Sezer O, Schulze-Lohoff E, Luft FC, Gollasch M, Dragun D (2009) mTOR Regulates Vascular Smooth Muscle Cell Differentiation From Human Bone Marrow-Derived Mesenchymal Progenitors. *Arteriosclerosis, Thrombosis, and Vascular Biology*. 29: 232-238.

Hengst L, Reed SI (1998) Inhibitors of the Cip/Kip family. *Current Topics in Microbiology and Immunology*. 227: 25-41.

Henry KW, Yuan X, Koszewski NJ, Onda H, Kwiatkowski DJ, Noonan DJ (1998) Tuberous sclerosis gene 2 product modulates transcription mediated by steroid hormone receptor family members. *Journal of Biological Chemistry*. 273: 20535-20539.

Henske EP (2003) Metastasis of benign tumor cells in tuberous sclerosis complex. *Genes, Chromosomes & Cancer*. 38:376-381.

Hodges AK, Shaowei L, Maynard J, Parry L, Braverman R, Cheadle JP, DeClue JE, Sampson JR (2001) Pathological mutations in TSC1 and TSC2 disrupt the interaction between hamartin and tuberin. *Human Molecular Genetics*. 10: 2899-2905.

Holt CE, Bertsch TW, Ellis HM, Harris WA (1988) Cellular determination in the *Xenopus* retina is independent of lineage and birth date. *Neuron* 1: 15-26.

Hoogeveen-Westerveld M, Exalto C, Maat-Kievit A, van der Ouweland A, Halley D, Nellist M (2010) Analysis of TSC1 truncations defines regions involved in TSC1 stability, aggregation and interaction. *Biochimica et Biophysica Acta – Molecular Basis of Disease*. 1802: 774-781.

Huang J, Manning BD (2008) The TSC1-TSC2 complex: a molecular switchboard controlling cell growth. *Biochemical Journal*. 412:179-190.

Huang J, Manning BD (2009) A complex interplay between Akt, TSC2 and the two mTOR complexes. *Biochemical Society Transactions*. 37:217-222.

Im E, von Lintig FC, Chen J, Zhuang S, Qui W, Chowdhury S, Worley PF, Boss GR, Pilz RB (2002) Rheb is in a high activation state and inhibits B-Raf kinase in mammalian cells. *Oncogene*. 21: 6356-6365.

Inoki K, Zhu T, Guan KL (2003a) TSC2 mediates cellular energy response to control cell growth and survival. *Cell*. 115: 577-590.

Inoki K, Li Y, Xu T, Guan KL (2003b) Rheb GTPase is a direct target of TSC2 GAP activity and regulates mTOR signaling. *Genes & Development*. 17: 1829-1834.

Inoki K, Ouyang H, Zhu T, Lindvall C, Wang Y, Zhang X, Yang Q, Bennett C, Harada Y, Stankunas K, Wang CY, He X, MacDougald OA, You M, Williams BO, Guan KL (2006) TSC2 integrates Wnt and energy signals via a coordinated phosphorylation by AMPK and GSK3 to regulate cell growth. *Cell*. 8: 955-968.

Iwata T, Henver RF (2009) Fibroblast growth factor signaling in development of the cerebral cortex. *Development, Growth & Differentiation*. 51: 299-323.

Jaworski J, Spangler S, Seeburg DP, Hoogenraad CC, Sheng M (2005) Control of dendritic arborisation by the phosphoinositide-3'-kinase-Akt-mammalian target of rapamycin pathway. *Journal of Neuroscience*. 25: 11300-11312.

Joinson C, O'Callaghan FJ, Osborne JP, Martyn C, Harris T, Bolton PF (2003) Learning disability and epilepsy in an epidemiological sample of individuals with tuberous sclerosis complex. *Psychological Medicine*. 33: 335-344.

Jones AC, Daniells CE, Snell RG, Tachataki M, Idziaszczyk SA, Krawczak M, Sampson JR, Cheadle JP (1997) Molecular genetic and phenotypic analysis reveals differences between TSC1 and TSC2 associated familial and sporadic tuberous sclerosis. *Human Molecular Genetics*. 6:2155-2161.

Jones AC, Shymsundar MM, Thomas MW, Maynard J, Idziaszczyk S, Thomkins S, Sampson JR, Cheadle JP (1999) Comprehensive mutation analysis of TSC1 and TSC2 – and phenotypic correlations in 150 families with tuberous sclerosis. *American Journal of Human Genetics*. 64:1305-1315.

Kandt RS, Haines JL, Smith M, Northrup H, Gardner RJ, Short MP, Dumars K, Roach ES, Steingold S, Wall S, Blanton SH, Flodman P, Kwiatkowski DJ, Jewell A, Weber JL, Roses AD, Pericak-Vance MA (1992) Linkage of an important gene locus for tuberous sclerosis to a chromosome 16 marker for polycystic kidney disease. *Nature Genetics*. 2:37-41.

Karbowiczek M (2010) The evolutionarily conserved TSC/Rheb pathway activates Notch in tuberous sclerosis complex and Drosophila external sensory organ development. *Journal of Clinical Investigation*. 120: 93-102.

Karbowiczek M, Cash T, Cheung M, Roberston GP, Astrinidis A, Henske EP (2004) Regulation of B-Raf kinase activity by Tuberin and Rheb is mammalian target of rapamycin (mTOR)-independent. *Journal of Biological Chemistry*. 279: 29930-29937.

Karbowiczek M & Henske EP (2005) The role of Tuberin in cellular differentiation: Are B-raf and MAPK involved. *Annals of the New York Academy of Sciences: Tumor Progression and Therapeutic Resistance*. 1059: 168-173.

Karbowiczek M, Yu J, Henske EP (2003) Renal angiomyolipomas from patients with sporadic lymphangiomyomatosis contain both neoplastic and non-neoplastic vascular structures. *American Journal of Pathology*. 162: 491-500.

King RW, Jackson PK, Kirschner MW, (1994) Mitosis in transition. *Cell*. 45: 563-571.

Knudson AG (1971) Mutation and cancer: statistical study of retinoblastoma. *Proceedings of the National Academy of Science*. 68:820-823.

Krymskaya VP (2003) Tumor suppressors Hamartin and Tuberin: intracellular signalling. *Cellular Signalling*. 15:729-739.

Kumar V, Zhang MX, Swank MW, Kunz J, Wu GY (2005) Regulation of dendritic morphogenesis by Ras-PI3K-Akt-mTOR-and Ras-MAPK signaling pathways. *Journal of Neuroscience*. 25: 11288-11299.

Kwiatkowski DJ, Manning BD (2005) Tuberous sclerosis: a GAP at the crossroads of multiple signaling pathways. *Human Molecular Genetics*. 14: R251-R258.

Kwiatkowska J, Jozwiak S, Hall F, Henske EP, Haines JL, McNamara P, Braiser J, Wigowska-Sowinska J, Kasprzyk-Obara J, Short MP, Kwiatkowski DJ (1998) Comprehensive mutational analysis of the TSC1 gene: observations on frequency of mutation, associated features, and nonpenetrance. *Annals of Human Genetics*. 62: 277-285.

Lamb RF, Roy C, Diefenbach TJ, Vinters HV, Johnson MW, Jay DG, Hall A, (2000) The TSC1 tumor suppressor Hamartin regulates cell adhesion through ERM proteins and the GTPase Rho. *Nature: Cell Biology*. 2: 281-287.

Lang CH, Frost RA (2005) Endotoxin disrupts the leucine-signaling pathway involving phosphorylation of mTOR, 4E-BP1 and S6K1 in skeletal muscle. *Journal of Cellular Physiology*. 203: 144-155.

Latif F, Tory K, Gnarra J, Yao M, Duh FM, Orcutt ML, Stackhouse T, Kuzmin I, Modi W, Geil L, Schmidt L, Zhou F, Li H, Wei MH, Chen F, Glenn G, Choyke P, Walther MM, Weng Y, Duan DSR, Dean M, Glavac D, Richards FM, Crossey PA, Ferguson-Smith MA, LePaslier D, Chumakov I, Cohen D, Chinault AC, Maher ER, Linehan WM, Zbar B, Lerman MI (1993) Identification of the von Hippel-Lindau disease tumor suppressor gene. *Science*. 260: 1317-1320.

Lee DF, Kuo HP, Chen CT, Hsu JM, Chou CK, Wie Y, Sun HL, Li LY, Ping B, Huang WC, He X, Hung JY, Lai CC, Ding Q, Su JL, Yang JY, Sahin AA, Hortobagyi GN, Tsai FJ, Tsai CH, Hung MC (2007) IKK $\beta$  suppression of TSC1 links inflammation and tumorigenesis via the mTOR pathway. *Cell*. 130: 440-445.

Leguis E, Marchuk DA, Collins FS, Glover TW (1993) Somatic deletion of the neurofibromatosis type 1 gene in a neurofibro-sarcoma supports a tumour suppressor gene hypothesis. *Nature Genet*. 3: 122-126.

Levine AJ (1997) p53, the cellular gatekeeper for growth and division. *Cell*. 88: 323-331.

Li J, Meyer AN, Donoghue DJ (1997) Nuclear localization of cyclin B1 mediates its biological activity and is regulated by phosphorylation. *Proceedings of the National Academy of Sciences of the United States of America*. 94: 502-507.

Li H, Tsang CK, Watkins M, Bertram PG, Zheng FS (2006) Nutrient regulates Tor1 nuclear localization and association with rDNA promoter. *Nature*. 442: 1058-1061.

Loots GG, Ovcharenko I (2004) rVISTA 2.0: evolutionary analysis of transcription factor binding sites. *Nucleic Acids Research*. 32: 217-221.

Livesey FJ, Cepko CL (2001) Vertebrate neural cell fate determination: lessons from the retina. *Nature Neuroscience*. 2: 109-118.

Loewith R, Jacinto E, Wullschleger S, Lorberg A, Crespo JL, Bonenfant D, Oppliger W, Jenoe P, Hall MN (2002) Two TOR complexes, only one of which is rapamycin sensitive, have distinct roles in cell growth control. *Molecular Cell*. 10: 457-468.

Lu Z, Hu X, Li Y, Zheng L, Zhou Y, Jiang H, Ning T, Basang Z, Zhang C, Ke Y (2004) Human papillomavirus 16 E6 oncoprotein interferes with insulin signaling pathway by binding to Tuberin. *Journal of Biological Chemistry*. 279: 35664-35670.

Ma L, Chen Z, Erdjument-Bromage H, Tempst P, Pandolfi PP (2005) Phosphorylation and functional inactivation of TSC2 by ERK: implications for tuberous sclerosis and cancer pathogenesis. *Cell*. 121: 179-193.

Ma J, Meng Y, Kwiatkowski DJ, Chen X, Peng H, Sun Q, Zha X, Wang F, Wang Y, Jing Y, Zhang S, Chen R, Wang L, Wu E, Cai G, Malinowska-Kolodziej I, Liao Q, Liu Y, Zhao Y, Sun Q, Xu K, Dai J, Han J, Wu L, Zhao RC, Shen H, Zhang H (2010) Mammalian target of rapamycin regulates murine and human cell differentiation through STAT3/p63/Jagged/Notch cascade. *Journal of Clinical Investigation*. 120: 103-114.

Ma L, Teruya-Feldstein J, Bonner P, Bernardi R, Franz DN, Witte D, Cordon-Cardo C, Pandolfi PP (2007) Identification of S664 TSC2 phosphorylation as a marker for extracellular signal-regulated kinase mediated mTOR activation in tuberous sclerosis and human cancer. *Cancer Research*. 67: 7106-7112.

Maheshwar MM, Cheadle JP, Jones AC, Myring J, Fryer AE, Harris PC, Sampson JR (1997) The GAP-related domain of Tuberin, the product of the TSC2 gene, is a target for missense mutations in tuberous sclerosis. *Human Molecular Genetics*. 6:1991-1996.

Mak BC, Kenerson HL, Aicher LD, Barnes EA, Yeung RS (2005) Abberant beta-catenin signaling in tuberous sclerosis. *American Journal of Pathology*. 167: 107-116.

Mak BC, Takemaru KI, Kenerson HL, Moon RT, Yeung RS (2003) The Tuberin-Hamartin complex negatively regulates  $\beta$ -catenin signaling activity. *Journal of Biological Chemistry*. 278: 5947-5951.

Marchant L, Linker C, Ruiz P, Guerrero N, Mayor R (1998) The inductive properties of mesoderm suggest that the neural crest cells are specified by a BMP gradient. *Developmental Biology*. 198: 319-329.

Marcotte L, Crino PB (2006) The neurobiology of the tuberous sclerosis complex. *Neuromolecular Medicine*. 8:531-546.

Martin J, Han C, Gordon LA, Terry A, Prabhakar S, She X, Xie G, Hellsten U, Chan YM, Altherr M, Couronne O, Aerts A, Bajorek E, Black S, Blumer H, Branscomb E, Brown NC, Bruno WJ, Buckingham JM, Callen DF, Campbell CS, Campbell ML, Campbell EW, Caoile C, Challacombe JF, Chasteen LA, Chertkov O, Chi HC, Christensen M, Clark LM, Cohn JD, Denys M, Detter JC, et al.



(2004) Complete sequencing and characterization of 21,243 full-length human cDNAs. *Nature Genetics*. 36: 40-45.

Mieulet V, Lamb RF (2010) Tuberous sclerosis complex: linking cancer to metabolism. *Trends in Molecular Medicine*. 16: 329-335.

Miloloza A., Rosner M., Nellist M., Halley D., Bernaschek G., Hengstschläger M (2000) The TSC1 gene product, hamartin, negatively regulates cell proliferation. *Human Molecular Genetics*. 9:1721-1727.

Mizuguchi M, Yamanouchi H, Becker LE, Itoh M, Takashima S (2002) Doublecortin immunoreactivity in giant cells of tuberous sclerosis and focal cortical dysplasia. *Acta Neuropathologica*. 104: 418-424.

Murthy V, Han S, Beauchamp RL, Smith N, Haddad LA, Ito N, Ramesh V (2004) Pam and its ortholog Highwire interact with and may negatively regulate the TSC1:TSC2 complex. *Journal of Biological Chemistry*. 279: 1351-1358.

Murthy V, Stemmer-Rachmaninov AO, Haddad LA, Roy JE, Cutone AN, Beauchamp RL, Smith N (2001) Developmental expression of the tuberous sclerosis proteins Tuberin and Hamartin. *Acta Neuropathol*. 101:202-210.

Nakashima A, Yoshino K, Miyamoto T, Eguchi S, Oshiro N, Kikkawa U, Yonezawa K, (2007) Identification of TBC7 having TBC domain as a novel binding protein to TSC1-TSC2 complex. *Biochemical and Biophysical Research Communications*. 361: 218-223.

Nellist M, Goedbloed MA, de Winter C, Verhaaf B, Jankie A, Reuser AJJ, van der Ouweland AMW, van der Sluijs P, Halley DJ (2002) Identification and characterization of the interaction between Tuberin and 14-3-3. *Journal of Biological Chemistry*. 277: 39417-39424.

Nellist M, Janssen B, Brookcarter PT, Hesselgijns ALW, Maheshwar MM, Verhoef S, Vandenouweland AMW, Lindhout D, Eussen B, Cordeiro I, Santos H, Halley DJJ, Sampson JR, Ward CJ, Peral B, Thomas S, Hughes J, Harris PC, Roelfsema JH, Saris JJ, Spruit L, Peters DIM, Dauwerse JG, Breuning MH (The European Chromosome 16 Tuberous Sclerosis Consortium) (1993) Identification and characterization of the tuberous sclerosis gene on chromosome 16. *Cell*. 75:1305-1315.

Nellist M, van Slegtenhorst MA, Goedbloed M, van den Ouweland AMW, Halley DJJ, van der Sluijs P (1999) Characterization of the cytosolic Tuberin-Hamartin complex - Tuberin is a cytosolic chaperone for Hamartin. *Journal of Biological Chemistry*. 274:35647-35652.

Nellist M, Verhaaf B, Goedbloed M, Reuser AJJ, van den Ouweland AMW, Halley DJJ (2001) TSC2 missense mutations inhibit Tuberin phosphorylation and prevent formation of the Tuberin-Hamartin complex. *Human Molecular Genetics*. 10:2889-2899.

Neville CM, Huang AY, Shyu JY (2009) Neural precursor cell lines promote neurite branching. *International Journal of Neuroscience*. 119: 15-39.

Nieto M, Monuki ES, Tang H, Imitola J, Haubst N, Khoury SJ, Cunningham J, Gotz M, Walsh CA (2004) Expression of Cux-1 and Cux-2 in the subventricular zone and upper layers II-IV of the cerebral cortex. *Journal Of Comparative Neurology*. 479: 168-180.

Niida Y, Lawrence-Smith N, Banwell A, Hammer E, Lewis J, Beauchamp RL, Sims K, Ramesh VL, Ozelius L (1999) Analysis of both TCS1 and TSC2 for germline mutations in 126 unrelated patients with tuberous sclerosis. *Human Mutation*. 14: 412-422.

Norbury C, Nurse P (1992) Animal cell cycles and their control. *Annual Review of Biochemistry*. 61:1441-1470.

Ohnuma S, Harris WA (2003) Neurogenesis and the cell cycle. *Neuron*. 40: 199-208.

Ohtsubo M, Theodoras AM, Schumacher J, Roberts JM, Pagano M (1995) Human cyclin E, a nuclear protein essential for the G1-to-S phase transition. *Molecular and Cellular Biology*. 15: 2612-2624.

Pacey LKK, Stead S, Gleave JA, Tomczyk K, Doering LC (2006) Neural stem cell culture: neurosphere generation, microscopical analysis and cryopreservation. *Nature-Protocol Exchange*.

Pagano SF, Impagnatiello F, Girelli M, Cova L, Grioni E, Onofri M, Cavallaro M, Etteri S, Vitello F, Giombini S, Solero CL, Parati EA (2000) Isolation and characterization of neural stem cells from the adult human olfactory bulb. *Stem Cells*. 18: 295-300.

Park SH, Pepkowitz SH, Kerfoot C, De Rosa MJ, Poukens V, Wienecke R, De Clue JE, Vinters HV (1997) Tuberous sclerosis in a 20-week gestation fetus: immunohistochemical study. *Acta Neuropathol*. 94:180-186.

Poehlmann A, Roessner A (2010) Importance of DNA damage checkpoints in the pathogenesis of human cancers. *Pathology - Research and Practice*. 206: 591-601.

Ponti G, Peretto P, Bonfanti L (2008) Genesis of neuronal and glial progenitors in the cerebellar cortex of peripuberal and adult rabbits. *PLoS ONE*. 3: e2366.

Potter CJ, Pedraza LG, Xu T (2002) Akt regulates growth by directly phosphorylating TSC2. *Nature: Cell Biology*. 4: 658-665.

Preis PN, Saya H, Nádasdi L, Hochhaus G, Levin V, Sadée W. (1988) Neuronal cell differentiation of human neuroblastoma cells by retinoic acid plus herbimycin A. *Cancer Research*. 48: 6530-6534.

Ravin R, Hoepfner DJ, Munno DM, Carmel L, Sullivan J, Levitt DL, Miller JL, Athaide C, Panchision DM, McKay RD (2008) Potency and fate specification in CNS stem cell populations in vitro. *Cell - Stem Cell*. 3:670-80.

Ravitz J, Chen L, Lynch M, Schmidt EV (2007) c-myc repression of TSC2 contributes to control of translation initiation and Myc-induced transformation. *Cancer Research*. 67: 11209-11217.

- Roach ES, DiMario FJ, Kandt RS, Nothrup H (1999) Tuberous sclerosis consensus conference: recommendations for diagnostic evaluation. *Journal of Child Neurology*. 14: 401-407.
- Roach ES, Gomez MR, Northrup H (1998) Tuberous sclerosis complex consensus conference: revised clinical diagnostic criteria. *Journal of Child Neurology*. 13: 624-628.
- Robertson CP, Braun MM, Roelink H (2004) Sonic hedgehog patterning in chick neural plate is antagonized by a wnt3-like signal. *Developmental Dynamics*. 229: 510–519.
- Rosner M, Freilinger A, Hanneder M, Fujita N, Lubec G, Tsururo T, Hengstschlager M (2007a) p27<sup>kip1</sup> localization depends on the tumor suppressor protein Tuberin. *Human Molecular Genetics*. 16:1541-1556.
- Rosner M, Freilinger A, Lubec G, Hengstschlager M (2005) The tuberous sclerosis genes, TSC1 and TSC2, trigger different gene expression responses. *International Journal of Oncology*. 27: 1411-1424.
- Rosner M, Freilinger A, Hengstschlager M (2007b) Akt regulates nuclear/cytoplasmic localization of Tuberin. *Oncogene*. 26:521-531.
- Rosner M, Hanneder M, Siegel N, Valli A, Hengstschlager M (2008) The tuberous sclerosis gene products Hamartin and Tuberin are multifunctional proteins with a wide spectrum of interacting partners. *Mutational Research*. 658:234-246.
- Rosner M, Hengstschlager M (2004) Tuberin binds p27 and negatively regulates its interaction with the SCF component Skp2. *Journal of Biological Chemistry*. 279: 48707-48715.
- Rosner M, Hengstschlager M (2007) Cytoplasmic/nuclear localization of Tuberin in different cell lines. *Amino Acids*. 33:575-579.
- Roux PP, Ballif BA, Anjum R, Gygi SP, Blenis J (2004) Tumor-promoting phorbol esters and activated Ras inactivate the tuberous sclerosis tumor suppressor complex via p90 ribosomal S6 kinase. *Proceedings of the National Academy of Science*. 101: 13489-13494.
- Rubinfeld B, Crosier WJ, Albert I, Conroy L, Clark R, McCormick F, Polakis P (1992) Localization of the Rap1gap catalytic domain and sites of phosphorylation by mutational analysis. *Molecular and Cellular Biology*. 12: 4634-4642.
- Rubinfeld B, Munemitsu S, Clark R, Conroy L, Watt K, Crosier WJ, McCormick F, Polakis P (1991) Molecular cloning of a GTPase activating protein-specific for the Krev-1 protein P21rap1. *Cell*. 65: 1033-1042.
- Ruiz i Altaba A, Sanchez P, Dahmane N (2002) Gli and hedgehog in cancer: tumours, embryos and stem cells. *Nature Reviews: Cancer*. 2:361–372.
- Ruvinsky I, Meyuhas O (2006) Ribosomal protein S6 phosphorylation: from protein synthesis to cell size. *Trends in Biochemical Science*. 31: 342-348.

Ruvinsky I, Sharon N, Lerer T, Cohen H, Stolovich-Rain M, Nir T, Dor Y, Zisman P, Meyuhas O (2005) Ribosomal protein S6 phosphorylation is a determinant of cell size and glucose homeostasis. *Genes & Development*. 19: 2199-2211.

Sabatini D (2006) mTOR and cancer: insights into a complex relationship. *Nature Reviews: Cancer*. 6: 729-734.

Sabatini DM, Erdjument-Bromage H, Lui M, Tempest P, Snyder SH. (1994) RAFT1 - a mammalian protein that binds to FKBP12 in a Rapamycin-dependent fashion and is homologous to yeast TORs. *Cell*. 78: 35-43.

Sampson JR (2003) TSC1 and TSC2: genes that are mutated in the human genetic disorder tuberous sclerosis. *Biochemical Society Transactions*. 31:592-596.

Sancak O, Nellist M, Goedloed M, Efferich P, Wouters C, Maat-Kievit A, Zonnenberg B, Verhoef S, Halley D, van de Ouweland A (2005) Mutational analysis of the TSC1 and TSC2 genes in a diagnostic setting: genotype – phenotype correlations and comparison of diagnostic DNA techniques in tuberous sclerosis complex. 13:731-741 .

Sasai Y, Lu B, Steinbeisser H, Geissert D, Gont LK, De Robertis EM (1994) Xenopus chordin: a novel dorsalizing factor activated by organizer-specific homeobox genes. *Cell*. 79:779-790.

Schwartz RA, Fernandez G, Kotulska K, Jozwiak S (2007) Tuberous sclerosis complex: advances in diagnosis, genetics, and management. *Journal of the American Academy of Dermatology*. 57: 189-202.

Sehgal SN (2003) Sirolimus: its discovery, biological properties, and mechanism of action. *Transplant Proceedings*. 35: S7-S14.

Sekimoto T, Fukumoto M, Yoneda Y (2004) 14-3-3 suppresses the nuclear localization of threonine 157-phosphorylated p27Kip1. *EMBO Journal*. 23: 1934–1942.

Shaw RJ, Kosmatka M, Bardeesy N, Hurley RL, Witters LA, DePinho RA, Cantley LC (2004) The tumor suppressor LKB1 kinase directly activates AMP-activated kinase and regulates apoptosis in response to energy stress. *Proceedings of the National Academy of Sciences of the United States of America*. 101: 3329-3335.

Shelley M, Cancedda L, Heilshorn S, Sumbre G, Poo MM (2007) LKB1/STRAD promotes axon initiation during neuronal polarization. *Cell*. 129:565-577.

Sherr CJ (1994) G1 phase progression: cycling on cue. *Cell*. 9: 551-555.

Sherr CJ, Roberts JM (1995) Inhibitors of mammalian G1 cyclin-dependent kinases. *Genes & Development*. 9: 1149-1163.

Shillingford JM, Murcia NS, Larson CYH, Low SH, Hedgepeth R, Brown N, Flask CA, Novick AC, Goldfarb DA, Kramer-Zucker A, Walz G, Piontek KB, Germino GG, Weimbs T (2006) The mTOR pathway is regulated by polycystin-1 and its inhibition reverses renal cytogenesis in polycystic kidney disease. *Proceedings of the National Academy of Science*. 103: 5466-5471.

Simpson PB, Bacha JI, Palfreyman EL, Woollacott AJ, McKeman RM, Kerby J (2001) Retinoic acid-evoked differentiation of neuroblastoma cells predominates over growth factor stimulation: an automated image capture and quantitation approach to neuritogenesis. *Analytical Biochemistry*. 298: 163-169.

Smith M, Handa K, He W, Spear G (1993) Loss of heterozygosity for chromosome 16p 13.3 markers in renal hamartomas from tuberous sclerosis patients. *American Journal of Human Genetics*. 53: 366.

Stevens C, Lin Y, Harrison B, Burch L, Ridgeway RA, Sansom O, Hupp T (2009) Peptide combinatorial libraries identify TSC2 as a death-associated protein kinase (DAPK) death domain-binding protein and reveal a stimulatory role for DAPK in mTORC1 signaling. *Journal of Biological Chemistry*. 284: 334-344.

Soucek T, Holz G, Bernaschek G, Hengstschlager M (1998) A role of the tuberous sclerosis gene-2 product during neuronal differentiation. *Oncogene*. 16:2197-2204.

Soucek T, Pusch O, Wienecke R, DeClue JE, Hengstschlager M (1997) Role of the tuberous sclerosis gene-2 product in cell cycle control - Loss of the tuberous sclerosis gene-2 induces quiescent cells to enter S phase. *Journal of Biological Chemistry*. 272: 29301-29308.

Surpili MJ, Delben TM, Kobarg J (2003) Identification of proteins that interact with the central coiled-coil region of the human protein kinase NEK1. *Biochemistry*. 42: 15369-15376.

Tavazoie SF, Alvarez VA, Ridenour DA, Kwiatkowski DJ, Sabatini BL (2005) Regulation of neuronal morphology and function by tumor suppressors TSC1 and TSC2. *Nature Neuroscience*. 8:1727-1734.

Tee AR, Fingar DC, Manning BD, Kwiatkowski DJ, Cantley LC, Blenis J (2002) Tuberous sclerosis complex-1 and -2 gene products function together to inhibit mammalian target of rapamycin (mTOR)-mediated downstream signalling. *Proceedings of the National Academy of Sciences of the United States of America*. 99: 13571-13576.

Thiele EA (2004) Managing epilepsy in tuberous sclerosis complex. *Journal of Child Neurology*. 19:680-686.

Thiele CJ, Reynolds CP, Israel MA (1985) Decreased expression of n-myc precedes retinoic acid-induced morphological differentiation of human neuro-blastoma. *Nature*. 313: 404-406.

Thiele CJ, Deutsch LA, Israel MA (1988) The expression of multiple proto-oncogenes is differentially regulated during retinoic acid-induced maturation of human neuro-blastoma cell-lines. *Oncogene*. 3: 281-288.

Toman RE, Payne SG, Watterson KR, Maceyka M, Lee NH, Milstein S, Bigbee JW, Spiegel S (2004) Differential transactivation of sphingosine-1-phosphate receptors modulates NGF-induced neurite extension. *Journal of Cell Biology*. 166: 381-392.

Turner DL, Cepko CL (1987) A common progenitor for neurons and glia persists in rat retina late in development. *Nature*. 328: 131-136.

van der Hoeve, J. (1933). Les phakomatoses de Bourneville, de Recklinghausen et de von Hippel-Lindau. *Journal de beige de Neurologie et Psychiatrie*. 33: 752.

van Slegtenhorst M, de Hoogt R, Hermans C, Nellist M, Janssen B, Verhoef S, Lindhout D, van den Ouweland A, Halley D, Young J, Burley M, Jeremiah S, Woodward K, Nahmias J, Fox M, Ekong R, Osborne J, Wolfe J, Povey S, Snell RG, Cheadle JP, Jones AC, Tachataki M, Ravine D, Sampson JR, Reeve MP, Richardson P, Wilmer F, Munro C, Hawkins TL, Sepp T, Ali JB, Ward S, Green AJ, Yates JR, Kwiatkowska J, Henske EP, Short MP, Haines JH, Jozwiak S, Kwiatkowski DJ (1997) Identification of the tuberous sclerosis gene on chromosome 9q34. *Science*. 277:805-808.

van Slegtenhorst M, Verhoef S, Tempelaars A, Bakker L, Wang Q, Wessels M, Bakker R, Nellist M, Lindhout D, Halley D, van den Ouweland A (1999) Mutational spectrum of the TSC1 gene in a cohort of 225 tuberous sclerosis complex patients: no evidence for genotype-phenotype correlation. *Journal of Medical Genetics*. 36: 285-289.

Vermeulen K, Van Bockstaele DR, Berneman Z (2003) The cell cycle: a review of regulation, deregulation and therapeutic targets in cancer. *Cell Proliferation*. 36:131-149.

Vinters HV, Miyata H (2006) Neuropathologic features of tuberous sclerosis. In: McLendon RE, Rosenblum MK, Bigner DD (eds.). *Russel and Rubinsten's Pathology of Tumors of the Nervous System*. 7th ed. Hodder Arnold Publication. London. 955-969.

Wei J, Peng L, Chiriboga L, Mizuguchi M, Yee H, Miller DC, Greco MA (2002) Tuberous Sclerosis in a 19-week fetus: immunohistochemical and molecular study of Hamartin and Tuberin. *Pediatric and Developmental Pathology*. 5:448-464.

Wexler EM, Paucer A, Kornblum HI, Palmer TD, Geschwind DH (2009) Endogenous Wnt signaling maintains neural progenitor cell potency. *Stem Cells*. 27:1130-41.

Wienecke R, Guha A, Maize JC, Heiderman RL, DeClue JE, Gutmann DH (1997) Reduced TSC2 RNA and protein in sporadic astrocytomas and ependymomas. *Annals of Neurology*. 42: 230-235.

Wienecke R, Konig A, DeClue JE (1995) Identification of Tuberin, the tuberous sclerosis-2 product. Tuberin possesses specific Rap1GAP activity. *The Journal of Biological Chemistry*. 270:16409-16414.

Wildonger J, Jan LY, Jan YN (2008) The TSC1-TSC2 complex influences neuronal polarity by modulating TORC1 activity and SAD levels. *Development*. 135:2447-2453.

Wilson L, Maden M (2005) The mechanisms of dorsoventral patterning in the vertebrate neural tube. *Developmental Biology*. 282:1-13.

Wilson PJ, Ramesh V, Kristiansen A, Bove C, Jozwiak S, Kwiatkowski DJ, Short MP, Haines JL (1996) Novel mutations detected in the TSC2 gene from both sporadic and familial TSC patients. *Human Molecular Genetics*. 5:249-256.

White R, Hua Y, Scheithauer B, Lynch DR, Henske EP, and Crino PB (2001) Selective alterations in glutamate and GABA receptor subunit mRNA expression in dysplastic neurons and giant cells of cortical tubers. *Annals of Neurology*. 49: 67–78.

Whittemore SR, White LA (1993) Target regulation of neuronal differentiation in a temperature-sensitive cell line derived from medullary raphe. *Brain Research*. 615: 27-40.

Wright JH, Druceckes P, Bartoe J, Zhao Z, Shen SH, Krebs EG (1997) A role for the SHP-2 tyrosine phosphatase in nerve growth-induced PC12 cell differentiation. *Molecular Biology of the Cell*. 8: 1575-1585.

Wullschleger S, Loewith R, Hall MN (2006) TOR signaling in growth and metabolism. *Cell*. 124: 471-484.

Xiao GH, Shoarinejad F, Jin F, Golemis EA, Yeung RS (1997) The tuberous sclerosis 2 gene product, Tuberin, functions as a Rab5 GTPase activating protein (GAP) in modulating endocytosis. *Journal of Biological Chemistry*. 272:6097-6100.

Xu L, Sterner C, Maheshwar MM, Wilson PJ, Nellist M, Short MP, Haines JL, Sampson JR, Ramesh V (1995) Alternative splicing of the tuberous sclerosis 2 (TSC2) gene in human and mouse tissues. *Genomics*. 27:475-480.

Yasui S, Tsuzaki K, Ninomiya H, Floricel F, Asano Y, Maki H, Takamura A, Nanba E, Higaki K, Ohno K (2007) The TSC1 gene product hamartin interacts with NADE. *Molecular and Cellular Neuroscience*. 35: 100-108.

Yew HH, Hembree M, Prasad K, Preuett B, McFall, C, Benjes C, Crowley A, Sharp S, Tulachan S, Metha S, Tei E, Gittes G (2005) Cross-talk between bone morphogenetic protein and transforming growth factor- $\beta$  signaling is essential for exendin-4-induced insulin-positive differentiation of AR42J cells. *Journal of Biological Chemistry*. 280:32209-32217

Young J, Povey S (1998) The genetic basis of tuberous sclerosis. *Molecular Medicine Today*. 4: 313-319.

Zeng Y, Forbes KC, Wu Z, Moreno S, Piwnica WH, Enoch T (1998) Replication checkpoint requires phosphorylation of the phosphatase Cdc25 by Cds1 or Chk1. *Nature*. 395: 507-510.

Zimmerman LB, De-Jesus-Escobar JM, Harland RM (1996) The spemann organizer signal noggin binds to and activates bone morphogenetic protein. *Cell*. 86:599-606.

**Vita Auctoris**

NAME: Gordon Omar Davis

PLACE OF BIRTH: East York, Toronto, Ontario

YEAR OF BIRTH: 1983

EDUCATION: Courtice Secondary School, Courtice, Ontario  
1990-1995

University of Windsor, Windsor, Ontario  
2003-2008 (B.Sc.)

University of Windsor, Windsor, Ontario  
2008-2011 (M.Sc)